UNIVERSITY OF CALIFORNIA, SAN DIEGO

Discovery and Characterization of the Mechanisms of a Vaccinia Viral Bcl-2 homolog,

F1L, on Inhibition of Caspase-9 and NLRP1

A Dissertation submitted in partial satisfaction of the

requirements for the degree Doctor of Philosophy

in

Molecular Pathology

by

Chi Wang Yu

Committee in Charge:

      Professor Robert C. Liddington, Chair
      Professor John C. Guatelli, Co-Chair
      Professor Partho Ghosh
      Professor Randall S. Johnson
      Professor John C. Reed

2010

UMI Number: 3398745

UMI®

Dissertation Publishing

ProQuest®

The Dissertation of Chi Wang Yu is approved, and it is acceptable in quality and form for

publication on microfilm and electronically:

_____

_____

_____

_____

Co-Chair

_____

Chair

University of California, San Diego

2010

DEDICATION

This dissertation is dedicated to

my parents, my sisters, my brother-in-law, and my nephew

for their love and support.

TABLE OF CONTENTS

Chapter 4
Identification of a novel motif of vaccinia virus Bcl-2-like F1L that is sufficient for

caspase-9 inhibition 90

LIST OF FIGURES

ACKNOWLDEGEMENT

I would like to thank the chair of my thesis committee, Professor Robert C. Liddington, who believed in my abilities, and offered me a chance to pursue my PhD degree in his laboratory. I'd also like to thank other members of my thesis committee, Professors John C. Guatelli, Partho Ghosh, Randall S. Johnson and John C. Reed for their time and helpful discussions.

It would not be possible for me to accomplish my dissertation work without the generous help from others. I would like to express my gratitude to my co-workers and collaborators, especially Dayong Zhai, Yinong Zong, Benjamin Faustin, Motti Gerlic, Naran Gombosuren and Ge Wei. Also, I want to thank Professors John C. Reed and Guy S. Salvesen for their advice. I would also like to thank all the members in Liddington lab for their scientific and non-scientific discussions. I am so grateful to meet all these nice people over the years.

Finally, I'd like to thank my friends and my family, in particular my parents, for their love and support.

Chapter 3, in full, is a reprint of the publication in "Vaccinia virus protein F1L is a caspase-9 inhibitor" Journal of Biological Chemistry, 2010. 285(8):5569-80, by Dayong Zhai*, Eric Yu*, Chaofang Jin, Kate Welsh, Chung-wei Shiau, Lili Chen, Guy S. Salvesen, Robert Liddington, and John C. Reed. The dissertation author was one of two co-primary investigators and authors of this paper (*Equal contribution). Both the dissertation author and Dayong Zhai conceived the project, designed and performed experiments, analyzed data, and wrote the initial draft of the manuscript.

Chapter 4, in part, is a manuscript prepared for publication titled "Identification of a novel motif of vaccinia virus Bcl-2-like F1L that is sufficient for caspase-9 inhibition", by Eric Chi-Wang Yu, Dayong Zhai, Naran Gombosuren, Yinong Zong, Ge Wei, Arnold Satterthwait, John C. Reed Robert C. Liddington. The dissertation author conceived the project, designed and performed experiments, analyzed data, and wrote the initial draft of the manuscript.

Chapter 5, in part, is a manuscript prepared for publication titled "Vaccinia Virus F1L protein inhibits NLRP1 inflammasome activation and promotes virus virulence", by Motti Gerlic*, Benjamin Faustin*, Antonio Postigo, Eric Yu, Naran Gombosuren, Maryla Krajewska, Rachel Flynn, Michael Croft, Michael Way, Arnold Satterthwait, Robert C. Liddington, Shahram Salek-Ardakani, John C. Reed (*Equal contribution). The dissertation author and Benjamin Faustin conceived the project, and designed the initial proof-of-concept experiments. The dissertation author also provided recombinant proteins and DNA constructs for experiments. Motti Gerlic and Benjamin Faustin designed and performed experiments, analyzed data, and wrote the initial draft of the manuscript.

VITA

2002   Bachelor of Science in Biochemistry, Hong Kong University of Science and Technology

2003   Teaching assistant, Department of Biology, Hong Kong University of Science and Technology

2004   Master of Philosophy in Biology, Hong Kong University of Science and Technology

2010   Doctor of Philosophy in Molecular Pathology, University of California, San Diego

PUBLICATIONS

1.   Zhai D*, **Yu EC***, Jin C, Welsh K, Shiau CW, Chen L, Salvesen GS, Liddington RC, and Reed JC. "**Vaccinia virus protein F1L is a caspase-9 inhibitor.**" J Biol Chem (in press). *Contributed equally.

2.   Leone M, **Yu EC**, Liddington RC, Pasquale EB, Pellecchia M. "**The PTB domain of tensin: NMR solution structure and phosphoinositides binding studies.**" Biopolymers. 2008; 89(1):86-92.

3.   Leone M, **Yu EC**, Liddington R, Pellecchia M. "**NMR assignment of the phosphotyrosine binding (PTB) domain of tensin.**" J Biomol NMR. 2006; 36 Suppl 1:40.

ABSTRACT OF THE DISSERTATION

Discovery and Characterization of the Mechanisms of a Vaccinia Viral Bcl-2 homolog,

F1L, on Inhibition of Caspase-9 and NLRP1

by

Chi Wang Yu

Doctor of Philosophy in Molecular Pathology

University of California, San Diego, 2010

Professor Robert C. Liddington, Chair
Professor John C. Guatelli, Co-Chair

The innate immune system detects invading pathogens and provides immediate

response to eliminate pathogens and infected cells, and to trigger secondary immune

response to inhibit infection. Programmed cell death (Apoptosis) and cytokine secretion,

which are mediated by activation of different caspase-family protease cascades, are examples of the numerous mechanisms of our innate immunity against viral infections. Nonetheless, the virus has evolved a variety of strategies to cope with the anti-viral responses of the host. In this dissertation, I discovered that the vaccinia virus (VACV)-encoded Bcl-2 homologue, F1L, directly inhibits caspase-9, the apical caspase in the mitochondrial cell death pathway, and NLRP1 (also known as NALP1), one of the inflammasome proteins that facilitates caspase-1 activation and cytokine secretion.

We provide multiple lines of evidence that F1L directly and selectively binds and suppresses caspase-9 and NLRP1. In cells, F1L specifically represses caspase-9-dependent apoptosis and NLRP1-dependent IL-1β secretion. We identified two conserved motifs at the N-terminus of F1L preceding the Bcl-2-like domain by mutagenesis studies that are responsible for interaction and inhibition of caspase-9 and NLRP1, respectively. I further show that two short peptides derived from these motifs are sufficient to inhibit caspase-9 and NLRP1, respectively. Moreover, F1L is critical for suppression of caspase-1 activation and IL-1β secretion during VACV infection in macrophage cultures. In mice, I show that F1L is a prominent virulence factor that inhibits cytokine secretion upon VACV infection.

In summary, we revealed two novel functions of F1L that are important for the virulence of VACV. F1L is the first caspase-9 inhibitor that is a Bcl-2-like protein, and the first example of viral protein inhibitor of the NLRP family protein.

Chapter 1

Thesis synopsis

Background/Significance

Although we are routinely exposed to potential pathogens, our immune system enables us to resist infections. The innate immune system is the first line of defense against pathogens. A variety of pathogens are recognized by a relatively small group of "pathogen receptors" in cells so that the innate immune system can effectively detect pathogens, and provide immediate response upon infections. Additionally, the innate immune system detects invading pathogens and danger signals from damaged cells, and triggers the adaptive immune response to protect the host from infection.

Being intra-cellular parasites, viruses require resources and protein machineries of the host cell for replication. Therefore, programmed cell death (apoptosis) of infected cells is one of the vital mechanisms of the innate immunity to limit viral propagation in multi-cellular organisms. Apoptosis is mediated by activation of the caspase-family protease cascades. In the mitochondrial pathway, pro-apoptotic signals lead to permeabilization of mitochondrial outer membrane, resulting in the release of cytochrome c into the cytosol. Bound with cytochrome c, apoptotic protease activating factor 1 (Apaf-1) oligomerizes and recruits pro-caspase-9 to form a multi-protein complex, named the apoptosome. Caspase-9 activated by apoptosome then activates downstream effector caspases, and subsequently leads to apoptosis [1-5]. On the other hand, a limited number of receptors called pattern-recognition receptors (PRRs),

1

including Toll-like receptors (TLRs) and Nod-like receptors (NLRs), recognize microbial pathogens and activate inflammatory signaling cascades. In contrast to membrane-bound TLRs that sense microbes on the cell surface or in endosomes, NLRs detect microbial molecules in the cytosol. Upon stimulations, some of the NLRs form large cytoplasmic protein complexes named inflammasomes, which activate inflammatory caspases (mainly caspase-1), and pro-inflammatory cytokines, such as IL-1β [6, 7].

Viruses have evolved a variety of strategies to utilize and modulate the signaling pathways and cellular machineries of the host to facilitate viral replication and infection to neighboring cells [8-10]. Therefore, studying the molecular mechanisms of host-pathogen interactions may give us new insights of not only new drug targets against viral infections, but also how innate immune responses are regulated in cells. Importantly, deregulations of the apoptotic and innate inflammatory pathways have been implicated in various human diseases, including cancer, degenerative and auto-inflammatory diseases [11-14]. Understanding the molecular mechanisms of how viral proteins modulate the signaling pathways of host cells may lead us to discovery of novel therapeutic strategy to treat human diseases.

F1L is a Bcl-2 homologue encoded in different poxviruses' genomes, including vaccinia virus (VACV), and variola virus (VARV) which causes smallpox. Similar to cellular anti-apoptotic Bcl-2 proteins, F1L has been shown to inhibit apoptosis during infection by interacting with pro-apoptotic proteins, such as Bak and Bim [15-18]. Although controversial, it has been shown that Bcl-XL might directly inhibit apoptosome, and thus the mitochondrial apoptotic pathway [19-22]. In addition, it has been shown that the NLRP1 (one of the NLRs) inflammasome is inhibited by Bcl-2

family proteins, Bcl-2 and Bcl-XL, linking the apoptotic pathway to innate immunity [23].

Hypothesis

Being a viral Bcl-2 homologue, F1L may also possess novel functions that are related to the apoptosome- or inflammasome-dependent pathways. In addition to interaction with pro-apoptotic Bcl-2 family proteins, Bcl-2 and Bcl-XL also interfere with both the apoptosome and NLRP1 inflammasome. Therefore, I hypothesized that F1L might suppress apoptosis by inhibiting apoptosome, and inflammation by inhibiting NLRP1 inflammasome.

Specific aims

1. Determine if F1L can inhibit apoptosome-dependent apoptosis, and characterize the underlying mechanism of this inhibition.
2. Determine if F1L can inhibit NLRP1 inflammasome, and characterize the underlying mechanism of this inhibition.
3. Investigate the role of F1L during vaccinia virus infection *in vivo*.

Brief summary of data chapters

During my dissertation research, we discovered that F1L directly inhibits both caspase-9 and NLRP1. There are two main parts of this work: (i) Characterization of

F1L-mediated caspase-9 inhibition is presented in Chapter 3 and 4; (ii) Characterization of NLRP1 inflammasome inhibition by F1L and study of the role of F1L during vaccinia virus infection in mouse model are presented in Chapter 5. Chapter 2 is a literature review of caspase activation pathways and viral Bcl-2 proteins. Chapter 6 is a general discussion of the results presented in this dissertation, and the possible future directions arisen from the discoveries in this project. The key ideas and results of the data chapters (Chapter 3-5) are briefly summarized below.

Chapter 3

The novel interaction between the vaccinia viral Bcl-2 homologue, F1L, and the apical protease in the mitochondrial cell death pathway, caspase-9, is described in Chapter 3. We show by *in vitro* and cell-based assays that F1L selectively binds and inhibits caspase-9, but not other caspases. A point mutation within the N-terminal region of F1L preceding the Bcl-2-like domain disrupts caspase-9 inhibition and significantly reduces anti-apoptotic activity of F1L. We further show that a mutant F1L, which does not bind the pro-apoptotic Bcl-2 family protein, Bak, is able to bind and inhibit caspase-9. F1L thus provides the first example of caspase inhibition by a viral Bcl-2 protein, which inhibits two sequential steps in the mitochondrial cell death pathway.

Chapter 4

Chapter 4 describes the identification of a novel motif within the F1L N-terminus that is required and sufficient for the interaction and inhibition of caspase-9. We further show that the F1L N-terminal motif binds only to active caspase-9 protease, suggesting that the motif directly blocks to the catalytic site of the protease. In addition, the Bcl-2-

like domain of F1L is able to bind to both pro- and active caspase-9, implying this domain might also possesses a caspase-9 binding site supplementary to the N-terminal motif of F1L. Our evidence suggests a distinct mechanism of caspase-9 inhibition by F1L that the N-terminal motif of F1L inhibits active caspase-9, while the Bcl-2-like domain may inhibit the recruitment and activation of pro-caspase-9 by the apoptosome.

Chapter 5

Chapter 5 illustrates that F1L is a NLRP1 inflammasome inhibitor, thus defining the first example of a viral Bcl-2 protein that interferes with the inflammasome, which is reminiscent of the mechanism employed by cellular Bcl-2 and Bcl-XL. A second motif within the N-terminal region of F1L directly and selectively binds and inhibits NLRP1, and thus caspase-1 activation mediated by the NLRP1 inflammasome. Infections of macrophages in culture with VACVΔF1L causes elevated caspase-1 activation and IL-1β secretion, when compared to wild type virus. Moreover, we show that F1L is an important virulence factor *in vivo*. VACVΔF1L was attenuated in its virulence in mouse model, resulting in increase proteolytic processing of caspase-1 without affecting virus replication.

References

1.   Liu, X., et al., *Induction of apoptotic program in cell-free extracts: requirement for dATP and cytochrome c.* Cell, 1996. **86**(1): p. 147-57.

2.   Zou, H., et al., *Apaf-1, a human protein homologous to C. elegans CED-4, participates in cytochrome c-dependent activation of caspase-3.* Cell, 1997. **90**(3): p. 405-13.

3. Li, P., et al., *Cytochrome c and dATP-dependent formation of Apaf-1/caspase-9 complex initiates an apoptotic protease cascade.* Cell, 1997. **91**(4): p. 479-89.

4. Du, C., et al., *Smac, a mitochondrial protein that promotes cytochrome c-dependent caspase activation by eliminating IAP inhibition.* Cell, 2000. **102**(1): p. 33-42.

5. Verhagen, A.M., et al., *Identification of DIABLO, a mammalian protein that promotes apoptosis by binding to and antagonizing IAP proteins.* Cell, 2000. **102**(1): p. 43-53.

6. Martinon, F., K. Burns, and J. Tschopp, *The inflammasome: a molecular platform triggering activation of inflammatory caspases and processing of proIL-beta.* Mol Cell, 2002. **10**(2): p. 417-26.

7. Agostini, L., et al., *NALP3 forms an IL-1beta-processing inflammasome with increased activity in Muckle-Wells autoinflammatory disorder.* Immunity, 2004. **20**(3): p. 319-25.

8. Benedict, C.A., P.S. Norris, and C.F. Ware, *To kill or be killed: viral evasion of apoptosis.* Nat Immunol, 2002. **3**(11): p. 1013-8.

9. Best, S.M., *Viral subversion of apoptotic enzymes: escape from death row.* Annu Rev Microbiol, 2008. **62**: p. 171-92.

10. Postigo, A. and P.E. Ferrer, *Viral inhibitors reveal overlapping themes in regulation of cell death and innate immunity.* Microbes Infect, 2009. **11**(13): p. 1071-8.

11. McDermott, M.F. and J. Tschopp, *From inflammasomes to fevers, crystals and hypertension: how basic research explains inflammatory diseases.* Trends Mol Med, 2007. **13**(9): p. 381-8.

12. Tschopp, J., F. Martinon, and K. Burns, *NALPs: a novel protein family involved in inflammation.* Nat Rev Mol Cell Biol, 2003. **4**(2): p. 95-104.

13. Martinon, F., A. Mayor, and J. Tschopp, *The inflammasomes: guardians of the body.* Annu Rev Immunol, 2009. **27**: p. 229-65.

14. MacFarlane, M. and A.C. Williams, *Apoptosis and disease: a life or death decision.* EMBO Rep, 2004. **5**(7): p. 674-8.

15. Wasilenko, S.T., et al., *The vaccinia virus F1L protein interacts with the proapoptotic protein Bak and inhibits Bak activation.* J Virol, 2005. **79**(22): p. 14031-43.

16. Taylor, J.M., et al., *The vaccinia virus protein F1L interacts with Bim and inhibits activation of the pro-apoptotic protein Bax.* J Biol Chem, 2006. **281**(51): p. 39728-39.

17. Campbell, S., et al., *Vaccinia virus F1L interacts with Bak using highly divergent BCL-2 homology domains and replaces the function of Mcl-1.* J Biol Chem, 2009.

18. Postigo, A., et al., *Interaction of F1L with the BH3 domain of Bak is responsible for inhibiting vaccinia-induced apoptosis.* Cell Death Differ, 2006. **13**(10): p. 1651-62.

19. Yajima, H. and F. Suzuki, *Identification of a Bcl-XL binding region within the ATPase domain of Apaf-1.* Biochem Biophys Res Commun, 2003. **309**(3): p. 520-7.

20. Pan, G., K. O'Rourke, and V.M. Dixit, *Caspase-9, Bcl-XL, and Apaf-1 form a ternary complex.* J Biol Chem, 1998. **273**(10): p. 5841-5.

21. Hu, Y., et al., *Bcl-XL interacts with Apaf-1 and inhibits Apaf-1-dependent caspase-9 activation.* Proc Natl Acad Sci U S A, 1998. **95**(8): p. 4386-91.

22. Chinnaiyan, A.M., et al., *Interaction of CED-4 with CED-3 and CED-9: a molecular framework for cell death.* Science, 1997. **275**(5303): p. 1122-6.

23. Bruey, J.M., et al., *Bcl-2 and Bcl-XL regulate proinflammatory caspase-1 activation by interaction with NALP1.* Cell, 2007. **129**(1): p. 45-56.

Chapter 2

Introduction

Through the process of host-pathogen co-evolution, the host has developed a variety of defense mechanisms to cope with viral infection. Our innate immune system detects invaders and provokes "alarm signals" that promote the immune response. Since viruses are intracellular parasites, programmed cell death (or apoptosis) of infected cells is one of the key defense mechanisms to suppress viral replication in multi-cellular organisms. Moreover, cytokine secreted from infected cells plays an important role in our immunity by triggering additional immune response, such as immune cell infiltrations. Therefore, viruses must subvert host cell's apoptosis and immune response in order to replicate effectively. Activation of a highly conserved protease family, known as cysteine-dependent aspartate-specific proteases (caspases), has been implicated in apoptosis and inflammatory cytokine production. To prolong host cell viability for replication and prevent cytokine secretion, viruses are equipped with various viral proteins to target the apoptotic and inflammatory machineries of the host. In this chapter, I briefly review the mechanisms of activation and inhibition of different caspases.

Vaccinia virus

Although its origin is not clear, vaccinia virus (VACV) is the virus used in the vaccine of variola virus (VARV), which is the causative agent of smallpox. Apart from being used as vaccine, VACV has been used as the model of poxvirus biology. VACV

belongs to the *Orthopoxvirus* subfamily of the *Poxviridae* family. Poxviruses are the largest known animal viruses, which contain about 200 genes in their relatively large DNA genomes (130-300 kb). In the life cycle of VACV, upon entry and uncoating, transcription of early viral genes is carried out by a set of transcription factors that is contained in the viral particle. Since poxviruses replicate entirely in the cytoplasm, their genomes encode proteins that carry out all the essential functions for viral replication independent of the nucleus of the host cell. Essentially, other viral gene products utilize and modulate the signaling pathways and cellular machineries of the host to facilitate viral replication and infection to neighboring cells [1-3].

Viral Bcl-2 proteins

Despite the role of apoptosis in host defense is not clearly understood, the large repertoire of anti-apoptotic proteins encoded by viruses underscores the importance of the cell death process in limiting viral replication in host cells. Cellular anti-apoptotic Bcl-2 proteins (Bcl-2, Bcl-XL, Bcl-w, Mcl-1 and A1), which are mainly localized on the mitochondrial outer membrane, function as apoptosis regulator by suppressing the release of pro-apoptotic signaling factors, such as cytochrome c, from mitochondria. These factors promote activation of caspase-family cascades, and eventually cause apoptosis (**Figure 2-4** & see text below). DNA viruses encode an array of viral homologues of cellular anti-apoptotic Bcl-2 proteins, called viral Bcl-2 (vBcl-2) proteins [3-5]. Intriguingly, all the vBcl-2 proteins share extremely weak sequence similarity with their mammalian homologues. However, most, if not all, of these vBcl-2 proteins adopt a Bcl-

2-like conformation [6-12]. Moreover, domain organization of most vBcl-2 proteins is thought to resemble their cellular Bcl-2 homologues, which possess four Bcl-2 homology (BH) domains (BH1-4). In fact, vBcl-2 proteins employ similar mechanisms to inhibit apoptosis by binding pro-apoptotic Bcl-2 family proteins, including Bax, Bak and Bim [3-5]. To date, there are four proteins (A52R, B14R, F1L, N1L) that have Bcl-2-like structure found in VACV [6, 7, 10, 13]. Interestingly, while F1L and N1L have been shown to be anti-apoptotic, A52R, B14R and N1L have been implicated in the inhibition of the NFκ-B activation [13, 14].

VACV F1L protein was found to be responsible for inhibition of mitochondrion-dependent apoptosis [15]. F1L is localized on the mitochondrial outer membrane via its C-terminal hydrophobic region (**Figure 2-1**) [15, 16]. Cells infected by F1L-deficient virus were more susceptible to apoptosis [15-20]. Further, overexpression of Bcl-2 could rescue cells infected with VACV without F1L [20]. Recent studies have shown that F1L suppresses apoptosis by directly interacting with Bak and Bim [17-21]. Upon interaction with Bak and Bim, cytochrome c release and subsequent apoptosis are inhibited (see text below). Even though F1L and its cellular Bcl-2 homologues possess similar anti-apoptotic activities, their primary sequences share less than 20% identity. Contrary to other Bcl-2 proteins, F1L exists as dimer in solution, but the crystal structure and sequence analysis show that F1L adopts a Bcl-2-like fold containing all 4 putative BH domains (BH1-4) (**Figure 2-1**) [18, 21]. Notably, F1L has an unusual N-terminal extension preceding its C-terminal Bcl-2-like domain. While the Bcl-2-like domain of F1L is highly conserved among all the orthologues (>95% identity), this N-terminal extension is variable in length and sequence. In addition, it has been shown that this N-

terminal extension is not required for the interaction of F1L with the pro-apoptotic Bcl-2 family proteins, such as Bak [18].

```
F1L      MLSMFMCNNIVDYVDDIDNGIVQDIEDEASNNVDHDYVYPLPENMVYRFDKSTNILDYLS 60
Bcl-XL   ------------------------------------------------------------


F1L      TERDHVMMAVRYYMSKQRLDDLYRQLP--------------------------------- 87
BcL-XL   -MSQSNRELVVDFLSYKLSQKGYSWSQFSDVEENRTEAPEGTESEMETPSAINGNPSWHL 59
              BH4

F1L      --------------------TKTRSYIDIINIYCDKVS-NDYNRDMNIMYD--MASTKS 123
Bcl-XL   ADSPAVNGATAHSSSLDAREVIPMAAVKQALREAGDEFEL-RYRRAFSDLTSQLHITP-G 117
                                    BH3

F1L      FTVYDINNEVNTILMDNKGLGVRLATISFITELGRRC--M---NPVETIKMFTLLSHTI- 177
Bcl-XL   TAYQSFEQVVNELFRDGVNWGRIVAFFSFGGALCVES--VDKEMQVLVSRIAAWMATYLN 175
                     BH1

F1L      --C--DDYF-VDYITDISPPDNTIPNTSTR---EYLKLIGITAIMFATYKTLKYMIG-- 226
Bcl-XL   DHLEPWIQENGGWDTFVELYGNNAAAESRKGQERFNRWF-LTGMTVAGVVLLGSLFSRK 233
              BH2
```

Figure 2-1. Sequence alignment of F1L and Bcl-XL based on secondary structure. F1L from vaccinia virus strain Western Reserve (VACV-WR) and Bcl-XL from human were aligned based on their secondary structure. Colored boxes depict the BH1-4 domains in Bcl-XL. Mitochondrial-targeting hydrophobic regions are underlined.

Caspases

Caspases are cysteine proteases, which have been implicated in the apoptotic and inflammatory pathways. They are encoded in the genomes from C. elegans to humans. Among the 14 caspases identified in mammals, two homologues (caspase-11 and -12) are unique to murines [22, 23]. Caspase-1 was the first member in the family identified as interleukin-1β converting enzyme (ICE), which converts pro-interleukin-1β (pro-IL-1β) to its mature form [24-27]. This protease family was later brought into the field of cell death research by the discovery that the CED-3 protein, which was found to be required

for developmental apoptosis in C. elegan, is closely related to the mammalian ICE (now named caspase-1) [28]. This discovery led to identification of a large family of caspases. The caspase family, in general, can be categorized into two subgroups: (i) inflammatory caspases (caspase-1 and -5) which cleave and activate pro-inflammatory cytokines, and (ii) apoptosis-related proteases (caspase-2, -3, -6, -7, -8, -9 and -10). During apoptosis, the initiator caspases (caspase-2, -8, -9 and -10) propagate and amplify pro-apoptotic signals by activating the downstream effector caspases (caspase-3, -6 and -7), which ultimately execute apoptosis by cleaving a variety of proteins in cells.

Caspases are similar in amino acid sequence, structure and substrate specificity. They always cleave the peptide bond C-terminal to aspartic acid residues on their substrates. At least four amino acids N-terminal to the cleavage site are necessary for caspase recognition and cleavage. All caspases consist of a N-terminal pro-domain and a C-terminal catalytic domain. Similar to other protease families, caspases are expressed as single-chain zymogens. Activation of these proteases is regulated by their pro-domains that are variable in sequence and size. The initiator caspases (caspase-1, -2, -8, -9 and -10), which are responsible for initiating caspase cascades, contain different N-terminal pro-domains (**Figure 2-2**). The pro-domains facilitate the interactions between these caspases and their specific adaptor protein complexes (see text below). The activation of caspase-1, -2, -8 and -9 in mammalian cells depends on the inflammasome, the PIDDosome, the death-inducing signaling complex (DISC) and the apoptosome, respectively (**Figure 2-3**). The initiator caspases exist as monomers. Upon interaction with their adaptor protein complexes, they are brought to close proximity and activated by proximity-driven dimerization. Contrary to the initiator caspases, the downstream

effector caspases (caspase-3, -6 and -7) have short or no pro-domains, and exist as dimers (**Figure 2-3**). Activity of these effector caspases is induced by internal cleavage within the catalytic domain. Although it is not necessary for the catalytic activity of caspase-9 [29, 30], all caspases are proteolytically cleaved at the internal aspartic acid residues within their catalytic domains upon activation, resulting in a large and a small subunit. The cleavage allows re-arrangement of the loop regions of the caspase to form the active site. Furthermore, the presence of internal protease (or caspase) cleavage sites indicates that caspases can be activated through autocatalysis, or cleavage by upstream caspases or proteases that possess similar specificity to aspartic acid residue [22, 23, 31].
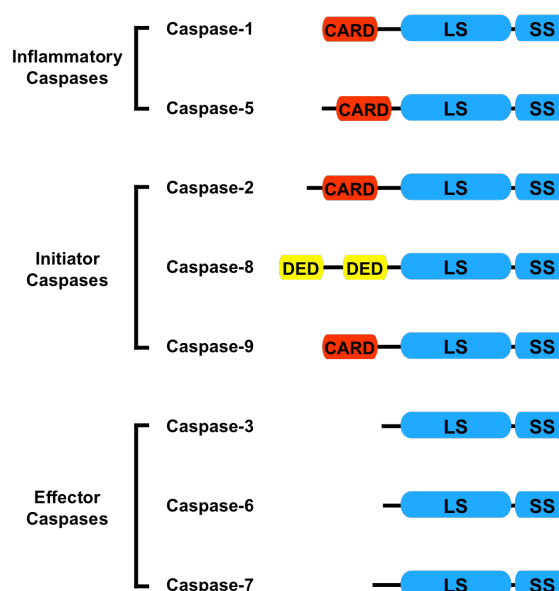
Figure 2-2. Domain architecture of caspases discussed in this chapter. All caspases contain a catalytic domain, which consists of large (LS) and small (SS) subunits. Upon activation, pro-caspase is cleaved between the large and small subunits. The inflammatory and initiator caspases possess different N-terminal pro-domains, such as CARD and DED, for homotypic interactions with their adaptor proteins. Except caspase-9, other caspases are cleaved between the pro-domain and catalytic domain upon full activation.

Caspase Activation Pathways

Apoptosis and innate immune response are orchestrated by specialized machineries that activate different caspase cascades that are highly regulated. Signaling pathways leading to apoptosis are generally known as either (i) the mitochondrial-dependent/intrinsic pathway, (ii) the death receptor-dependent/extrinsic pathway, (iii) granzyme B-dependent pathway, or (iv) PIDDosome-dependent pathway [1, 32]. Activation of caspase-1 during inflammation depends on formation of the inflammasomes [32].

Mitochondrial-dependent pathway

The "intrinsic" apoptotic pathway is triggered by cellular stress signals, such as DNA damage, cytotoxic drugs and heat shock. Pro-apoptotic signals of the "intrinsic" pathway converge to mitochondria, resulting in permeabilization of its outer membrane. Subsequently, cytochrome c and other pro-apoptotic proteins, such as second mitochondria-derived activator of caspase (SMAC), are released into the cytosol [33-35]. The release of cytochrome c is regulated by the Bcl-2 family proteins. Pro-apoptotic signals are propagated to the mitochondria by the BH3-only members of the Bcl-2 protein family, such as Bid and Bim. The BH3-only proteins induce oligomerization of the pro-apoptotic Bcl-2 family proteins on the outer mitochondrial membrane, such as Bak and Bax, leading to cytochrome c release, while other Bcl-2 family proteins, such as Bcl-2 and Bcl-XL, repress this event (reviewed in [32, 36, 37]). Bound with cytochrome c, apoptotic protease activating factor 1 (Apaf-1) utilizes ATP/dATP to oligomerizes together with pro-caspase-9 to form a multi-protein complex, named apoptosome. After

forming apoptosome with Apaf-1, pro-caspase-9 is processed and activated. Active caspase-9 then converts downstream pro-caspase-3 and -7 into their active forms, and subsequently leads to apoptosis [33, 38, 39] (**Figure 2-4**).

Both Apaf-1 and pro-caspase-9 exist as monomers in the cytosol. Apaf-1 possesses three distinct domains: a N-terminal caspase recruitment domain (CARD), a central nucleotide-binding domain (NBD) and 12-13 WD40 repeats at its C-terminus. Without stimulation, Apaf-1 is "locked" in an inactive conformation by its auto-inhibitory WD40 repeats. Upon stimulations, cytochrome c released into the cytosol binds to the WD40 repeats and activates Apaf-1. Using ATP/dATP as the co-factor, the NBD facilitates oligomerization of Apaf-1, forming a wheel-shaped heptameric structure, with the CARD and NBD clustering at the center region [29, 40]. The exposed CARD of Apaf-1 recruits pro-caspase-9 to this complex through interaction with the pro-domain (CARD) of the caspase [39, 41] (**Figure 2-3A**). Emerging evidence suggests that recruitment of pro-caspase-9 monomers to the multi-protein complex brings them into close proximity and promotes dimerization of the monomers [42-44]. Consequently, pro-caspase-9 is activated and auto-catalytically cleaved at the linker region between the large and small subunit of its catalytic domain.

Death receptor-dependent pathway

The "extrinsic" pathway starts with stimulation of the tumor necrosis factor (TNF) superfamily of death receptors by extracellular ligands, such as FS-7-associated surface antigen ligand (FasL; also know as APO-1 or CD95 ligand) [45] and TNF receptor-related apoptosis-inducing ligand (TRAIL) [46]. Upon binding of ligands, death

receptors recruit cytosolic adaptor proteins, such as Fas-associated death domain-containing protein (FADD) [47, 48], and initiator caspases (caspase-8 and -10) [49-51], to form a protein complex called death-inducing signaling complex (DISC) [47]. Consequently, the initiator caspases are activated. Active caspase-8 or -10 processes and stimulates downstream effector caspases, such as caspase-3. Caspase-8 also links the "extrinsic" and "intrinsic" apoptotic pathways through proteolytic cleavage of the BH3-only member of the Bcl-2 protein family, Bid, which is converted into truncated Bid (tBid) upon cleavage. tBid translocates to mitochrondria, triggering the "intrinsic" apoptotic pathway [52, 53] (**Figure 2-4**).

Activated death receptor ligands are homo-trimeric, thus death receptors are thought to be oligomerized in response to ligand binding [54]. The death receptor, Fas, contains a death domain (DD) at its cytoplasmic region. Its adaptor protein, FADD, contains a death effector domain (DED) at its N-terminus and a DD at its C-terminus. Upon ligand binding, oligmerized Fas recruits FADD through DD-DD interaction, leading to clustering of FADD [55]. FADD cluster activates pro-caspase-8 by recruiting the protease to the complex through homotypic interactions with the two N-terminal DEDs of caspase-8 (**Figure 2-3D**). Active caspase-8 is then auto-catalytically processed in two regions. The first region is between the large and the small subunits of the catalytic domain, while the second one occurs between the pro-domain and the catalytic domain, resulting in removal of the two DEDs from active caspase-8 (**Figure 2-4**) [51, 56]. Recently, E3 ubiquitin ligase CUL3 was identified as a component of the DISC complex. Polyubiquitination of caspase-8 by CUL3 promotes aggregation and stabilization of the activated caspase-8 dimers, and thus subsequent apoptosis [57].

Granzyme B-dependent pathway

To eliminate transformed or virally infected cells, cytotoxic T lymphocytes (CTLs) and natural killer (NK) cells deliver cytolytic granules containing proteins, such as granzyme B, which can induce apoptosis, to their target cells. Granzyme B has been shown to be able to cleave caspase-3 and -8 to provoke apoptosis [58-60]. Granzyme B can also cleave Bid. Similar to tBid, the fragment produced by granzyme B-mediated processing, named gtBid, translocates to mitochondria to promote cytochrome c release and subsequent apoptosome assembly [61-64]. Since there is a battery of viral proteins that specifically inhibit different caspases, targeting various proteins in the apoptotic signaling cascades by granzyme B is one of the countermeasures against infections developed by the host during the process of co-evolution.

PIDDosome-dependent pathway

Caspase-2 has been implicated in stress-induced apoptosis [65]. Although the underlying mechanism is not clear, p53 is required for activation of caspase-2 mediated by PIDDosome in response to DNA damage [66, 67]. In addition, caspase-2 can be cleaved and activated by other caspases, such as caspase-1 and -3 [68], implying that caspase-2 can be stimulated through other apoptotic pathways. Active caspase-2 in the cytosol causes apoptosis by directly inducing permeabilization of the mitochondrial outer membrane [69, 70] or through cleavage of Bid (**Figure 2-4**) [69, 71]. In the cytosol, p53-induced protein with a death domain (PIDD) oligomerizes and recruits the adaptor protein of caspase-2, RIP-associated ICH-1/CED-3 homologous protein with a death domain (RAIDD) [72], to form a protein complex, named PIDDosome (**Figure 2-3B**)

[66]. Upon binding to PIDDosome, caspase-2 is auto-catalytically processed and activated. Apart from the cytosol, caspase-2 can be found in the nucleus [73-75]. It has been shown that caspase-2 can somehow provoke cytochrome c relesase from the nucleus [76]. Recently, nuclear caspase-2 was found to be phosphorylated by the nuclear serine/threonine protein kinase, DNA-PKcs. Caspase-2, DNA-PKcs, together with PIDD form a protein complex, named DNA-PKcs-PIDDosome, leading to activation of caspase-2 in the nucleus (**Figure 2-3C**) [77]. Although there is no evidence that links the DNA-PKcs-PIDDosome to apoptosis, this finding raises the possibility of distinct apoptotic pathway induced by this protein complex from the nucleus. However, the molecular mechanism of apoptosis induced by nuclear caspase-2 activity is yet to be elucidated.

PIDD contains seven leucine-rich repeats (LRRs) at its N-terminal region, two central ZU-5 domains, followed by a C-terminal DD. PIDD in cells is always auto-proteolytically processed between the two ZU-5 domains resulting in two fragments, named PIDD-N and PIDD-C [66, 78]. Further auto-proteolysis on PIDD-C after the second ZU-5 domain produces a fragment containing only the DD, named PIDD-CC. RAIDD and caspase-2 are recruited by PIDD-CC to form the PIDDosome [78]. RAIDD, which contains a CARD at its N-terminus and a DD at its C-terminus, acts as an adaptor protein linking caspase-2 to PIDD through homotyptic interactions (**Figure 2-3B**). Similar to caspase-9, caspase-2 contains a N-terminal CARD as its pro-domain and the catalytic domain at its C-terminus. Recently, a crystal structure showed that five PIDD DDs together with seven RAIDD DDs assemble into an oligomeric complex, providing a model of how the PIDD-CC and RAIDD function as a core platform for caspase-2

recruitment and activation [79]. On the other hand, nuclear PIDD recruits caspase-2 through DNA-PKcs, forming the DNA-PKcs-PIDDosome [77]. DNA-PKcs interacts with PIDD DD by its N-terminal HEAT repeats, and with caspase-2 CARD by its C-terminal catalytic PI-3 kinase (PI3K) domain (**Figure 2-3C**) [77]. At present, the stoichiometry of the complex of these three proteins remains unknown. Similar to caspase-8, pro-caspase-2 is auto-catalytically processed in two regions upon activation. The first region is between the large and the small subunits of the catalytic domain, while the second one occurs between the pro-domain and the catalytic domain, resulting in removal of the CARD from active caspase-2.

Inflammasome-dependent pathway

Caspase-1 (was named ICE) was the first member in the caspase family. It has been shown that caspase-1 activity is required for maturation and secretion of IL-1β and IL-18 [24-27, 80, 81]. Moreover, caspase-1 facilitates secretion of IL-1α and other proteins by an unknown mechanism even though these proteins are not substrates of caspase-1 [80-82]. Caspase-1 activation and subsequent cytokine (IL-1β and IL-18) secretion from macrophages/monocytes are essential for immune response against bacterial and viral pathogens (reviewed in [83, 84]). Additionally, caspase-1 is implicated in a cell-death pathway that is activated by pathogens, named pyroptosis [85-87]. This cell-death process exhibits distinct features different from apoptosis and necrosis, and is not dependent on the apoptotic caspases, such as caspase-3. Consistent to the activation mechanisms of caspase-2 and -9, a multi-protein complex, named inflammasome, was found to be responsible for caspase-1 activation in macrophages (**Figure 2-3**) [88]. The

inflammasomes are composed of nucleotide-binding domain and leucine-rich repeat containing protein (NLR) family members, apoptosis-associated speck-like protein containing a CARD (ASC) and caspase-1. One important property of the inflammasome family is the ability to detect a variety of conserved structures called pathogen-associated molecular patterns (PAMPs), such as peptidoglycan, lipopolysaccharide (LPS), flagellin, microbial RNA and double strained DNA, from the pathogens [83, 89]. The sensing of PAMPs is achieved by the diversity of the NLR protein family. To date, there are 22 members in the NLR family in the human genome [90]. The NLR protein family can be divided into five sub-families based on their N-terminal protein-protein interaction domains: (i) NLRA, possesses an acidic trans-activation domain, (ii) NLRB, has baculoviral inhibitory repeat (BIR)-like domains, (iii) NLRC, has CARD, (iv) NLRP, has a pyrin domain (PYD), and (v) NLRX, has a domain with no strong homology to the N-terminal domain of any other NLR family members. Essentially, all the NLR family members contain a NACHT (domain present in NAIP, CIITA, HET-E, and TP-1) domain that is though to be analogous to the NBD of Apaf-1, and a leucine-rich repeat (LRR) domain at their C-termini. Recently, four inflammasomes (NLRP1, NLRP3, NLRC4 and AIM2) have been partially characterized (reviewed in [89, 91]). In these inflammasomes, NLRP1, NLRP3, NLRC4 and absent in melanoma 2 (AIM2) function as pattern-recognition receptors (PRRs), which oligomerize upon stimulations, while ASC acts as the adaptor protein that links the PPR to caspase-1. Similar to other initiator caspases, caspase-1 were brought in close proximity and activated by this multi-protein platform. Among these PRRs, NLRC4 is the only protein without a PYD, but instead possesses a CARD at its N-terminus. Therefore, it is possible that NLRC4 can directly bind and

activate caspase-1 through CARD-CARD interaction. However, it has been demonstrated that ASC is somehow critical for NLRC4-mediated caspase-1 activation in macrophages and mice [92, 93]. The role of ASC in the NLRC4 inflammasome remains elusive.

Since all the NLR proteins contain a NACHT domain that is thought to be analogous to the NBD of Apaf-1, it is plausible that the NACHT facilitates oligomerization of NLR proteins using ATP as co-factor similar to the NBD of Apaf-1 [88, 94-96]. In the case of NLRP1 inflammasome, NLRP1 oligomerizes upon stimulation by microbial ligand, such as muramyl-dipeptide (MDP) [94, 95]. Similar to Apaf-1, NLRP1 is "locked" in an inactive form by its auto-inhibitory LRR domain [88]. Presumably, MDP binds the LRR domain of NLRP1, and thus stimulates NLRP1 oligomerization, forming a wheel-shaped structure [94]. The adaptor protein, ASC contains a PYD at its N-terminus and a CARD at its C-terminus. Casapse-1 is recruited to the NLRP1 complex by ASC through homotypic interactions. In addition to caspase-1, NLRP1 recruits and activates caspase-5 by the CARD at its C-terminus (**Figure 2-3E**) [88]. Apart from NLR inflammasomes, AIM2 has been identified as a new member of the inflammasome protein family, which recognizes cytosolic double-strained DNA [87, 97-99]. AIM2 possesses a N-terminal PYD and a C-terminal HIN200 (hematopoietic interferon-inducible nuclear proteins with a 200-amino-acid repeat) domain. Double-strained DNA binds the HIN200 domain and activates AIM2. Active AIM2 then induces caspase-1 activity by recruiting ASC as the adaptor like other inflammasomes (**Figure 2-3G**) [87, 97-99]. Intriguingly, the lack of NACHT domain on AIM2 suggests a distinct mechanism of caspase-1 activation from other NLR inflammasomes that remains unknown.
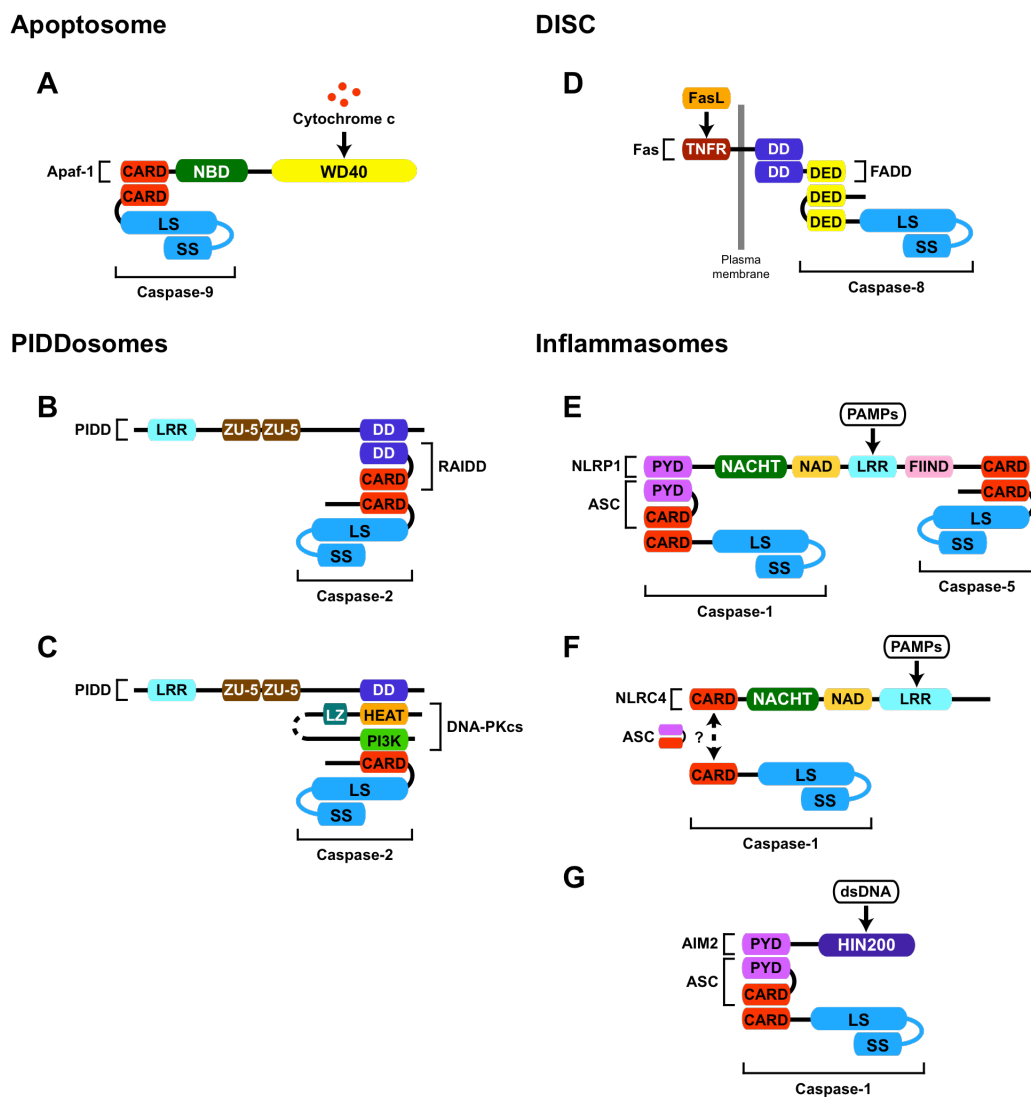
Figure 2-3. Caspase-activating protein complexes. (**A**) Cytochrome c induces assembly of the apoptosome to activate caspase-9. (**B, C**) Unknown ligands induce assembly of the PIDDosome to activate caspase-2. (**D**) FasL binds Fas to induce assembly of the DISC to activate caspase-8. (**E, F**) Bacterial ligands (PAMPs) induce assembly of the inflammasomes to activate caspase-1 and/or -5. (**G**) Double stranded DNA (dsDNA) induced AIM2 to activate caspase-1. See text for details. LZ, lucine zipper; PI3K, PI-3 kinase domain; TNFR, TNF receptor domain; NAD, NACHT-associated domain; FIIND, F-interacting domain.

Figure 2-4. Caspase cascades leading to cell death. Three major apoptotic and two inflammatory caspase activation pathways are depicted. In the death receptor-dependent pathway, caspase-8 (or caspase-10) is activated through formation of the DISC, which includes FADD upon binding of a ligand to a cell death receptor, for example FasL to Fas. Although the molecular pathway of genotoxicity-induced PIDDosome formation remains elusive, caspase-2 is activated by the PIDDosome, which is composed of PIDD and RAIDD. Active caspase-8 and -2 cleaves and activates downstream effector caspases, such as caspase-3, and the BH3-only protein, Bid. Truncated Bid (tBid) and other BH3-only proteins induce the mitochondrial-dependent apoptotic pathway by triggering oligomerization of pro-apoptotic proteins, such as Bak and Bax, leading to cytochrome c release from the inter-membrane space of the mitochondria to the cytosol, while anti-apoptotic Bcl-2 family proteins, such as Bcl-2 and Bcl-XL, inhibit release of cytochrome c. Binding of cytochrome c induces oligomerization of Apaf-1, which recruits and activates caspase-9 through assembly of the apoptosome, leading to activation of effector caspases and apoptosis. Caspase-1 is activated through formation of the inflammasomes, which include ASC, upon binding of bacterial or viral ligands to various inflammasome proteins, such as NLRP1 and AIM2. Active caspase-1 facilitates secretion of cytokines, such as IL-1β and IL-18, leading to inflammation. In addition, caspase-1 can induce the cell death process called pyroptosis.
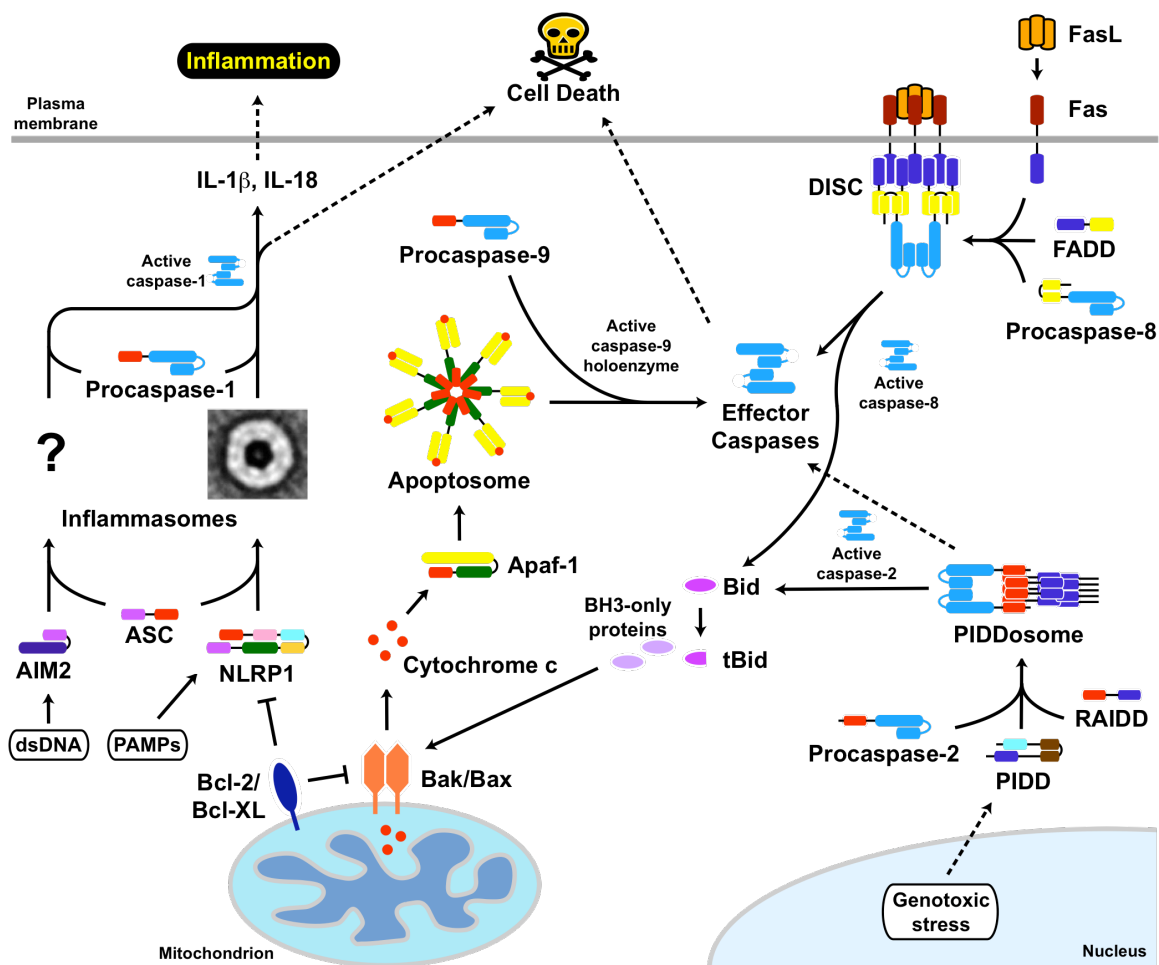
Figure 2-4. Caspase cascades leading to cell death.

Regulation of Caspase Activation

Apoptosis plays crucial roles in cell homeostasis, development and diseases. Although the activation mechanism mediated by multi-protein complex described above provides good measures of caspase activity regulation, there are additional layers of controls to fine-tune their activities. Emerging evidence suggests that caspases are regulated by post-translational modifications, such as phosporylation and ubiquitination

[57, 100, 101]. In addition, a collection of viral and cellular proteins has been identified to suppress caspase activation and/or activity by directly binding to caspases, or to their adaptor proteins. In the following paragraphs, I focus on these caspase binding partners, and discuss about how these proteins interfere with caspase activities.

Caspase-like decoy proteins

The caspase-like decoy proteins resemble the structures of caspases, but possess no catalytic activity. For example, viral-FLICE-like inhibitory protein (v-FLIP) and its two cellular homologues, c-FLIP$_L$ and c-FLIP$_S$, which contain the tandem DEDs at their N-termini, have been shown to have inhibitory effects on the DISC-dependent apoptosis pathway by interacting with caspase-8 [51].

There are proteins that contain either a CARD or a PYD only. These CARD-only proteins (COPs) and PYD-only proteins (POPs) function as decoy proteins in cells that prevent caspases to interact with their adaptor proteins. The COPs, such as Iceberg, COP1 (also know as Pseudo-ICE) and inhibitory CARD (INCA), sequester caspase-1 from inflammasome through CARD-CARD interaction [102, 103]. The single nucleotide polymorphisms (SNPs) found in the human caspase-12 gene result in expression of either a CARD-only version (caspase-12-S) or a catalytically inactive caspase [104]. Indeed, human caspase-12 has been shown to suppress inflammatory response by binding and inhibiting caspase-1 [105, 106]. Therefore, it is believed that caspase-12 and caspase-12-S function as negative regulators of caspase-1 activation like the FLIPs and COPs, respectively. Similar to caspase-12, there is a short variant of nucleotide-binding

oligomerization domain containing 2 (NOD2) protein (a NLR family protein), named NOD2-S, which possesses only the first CARD of NOD2. Contrary to other COPs, NOD2-S does not interact with caspase-1 but with its adaptor, receptor-interacting protein kinase 2 (RIP2), and NOD2 through CARD-CARD interaction. NOD2-S binds to both NOD2 and RIP2, and interferes with oligomerization of NOD2, thus inhibiting NOD2/RIP2-dependent caspase-1 activation [107]. Apart from COPs, inflammasome-dependent caspase-1 activation is inhibited by the POP family proteins. POP1 (also known as ASC2) and POP2, interact with ASC and NLRPs, respectively through PYD-PYD interaction. Binding of POP1 and POP2 to ASC and NLRPs prevents ASC recruitment to NLRPs, thus inhibiting subsequent activation of caspaes-1 by the inflammasome (reviewed in [102]). Additional to cellular POPs, viral homologues of these proteins were identified. Myxoma virus-encoded M13L and Shope fibroma virus-encoded vPOP have been shown to interact with ASC to modulate caspase-1 activity during infection [108, 109].

Other caspase inhibitors

In addition to caspase-like decoy proteins, there are other proteins that directly bind and inhibit different caspases. The most studied caspase inhibitors include cytokine response modifier A (CrmA) from poxvirus, p35 from baculovirus, and X-linked inhibitor of apoptosis (XIAP) from mammals [110]. The molecular basis of caspase inhibition mediated by CrmA, p35 and XIAP have been extensively studied. Intriguingly, they employ various strategies to inhibit caspases.

CrmA was first found to inhibit IL-1β maturation via caspase-1 suppression [111]. It was later discovered that CrmA also prevents apoptosis induced by TNF or FasL treatment, probably through inhibition of caspase-8 [112-116]. In the context of structure and reaction mechanism, CrmA belongs to the serpin superfamily except that CrmA cross-reacts with both cysteine proteases and serine proteases. CrmA acts as a suicide substrate that the P_1 Asp residue in the reactive site loop (RSL) of CrmA is attacked by the caspase active site. Once the RSL is cleaved, caspase is trapped in a kinetically stable intermediate complex with CrmA so that the protease is no longer active [117].

p35 was the second caspase inhibitor identified. Although it is encoded by baculovirus that infects insect cells, p35 has been shown to inhibit a broad range of mammalian caspases, including caspase-1, -3, -6, -7, -8 and -10 [118]. The crystal structures of the native p35 and its inhibitory complex with caspase-8 have elucidated the mechanism of caspase inhibition mediated by p35 [119-121]. Similar to CrmA, p35 also acts as a suicide substrate of caspases. The key mechanism of inhibition by p35 is the formation of the protected covalent thiol ester linkage between the cleaved polypeptide of p35 and the cysteine residue at the catalytic center of the caspase, thus blocking caspase activities. In addition, cleavage of the p35 RSL results in structural rearrangement of the protease [121].

IAP was first discovered in baculovirus that can rescue the loss of p35 during infection [122]. Sequence analysis identified other viral and cellular homologues of IAP, which bear one to three baculoviral IAP repeats (BIRs). Among the IAP protein family, XIAP is the most thoroughly studied mammalian member. Previous studies showed that XIAP is capable to inhibit caspase-3, -7 and -9. Unlike CrmA and p35, cleavage of XIAP

is not required for caspase inhibition. XIAP contains three BIRs. The second BIR domain (BIR2) of XIAP has been shown to be sufficient and necessary for inhibition of caspase-3 and -7 [123-125]. Interestingly, the linker region between BIR1 and BIR2 domains is also required for inhibition [125]. Crystallographic studies demonstrated that the peptide fragment N terminal to BIR2 docks into the active site of the caspases in a reverse orientation compared to substrate binding, and thus blocks their activities (**Figure 2-5C & D**) [126, 127]. In contrast to effector caspases, the initiator caspase, caspase-9 exists as an inactive monomer. Dimerization of caspase-9 is required for its activity [42]. XIAP BIR3 employs an unconventional strategy to inhibit caspase-9 by sequestering processed caspase-9 in its inactive, monomeric state [128] (**Figure 2-5A & B**).

Inhibition of NLRP1 inflammasome by Bcl-2 and Bcl-XL

Recently, it has been shown that the NLRP1 inflammasome is inhibited by Bcl-2 family proteins, Bcl-2 and Bcl-XL, linking the apoptotic pathway to the innate immunity [96]. The "loop" region between the BH4 (α-helix-1) and BH3 (α-helix-2) motifs of Bcl-2 and Bcl-XL directly binds to NLRP1, suppressing NLRP1 inflammasome and subsequent caspase-1 activation [94-96].

In conclusion, caspases play crucial roles in the apoptotic and inflammatory pathways. Therefore, activation of caspases is highly regulated by endogenous proteins in cells. In addition, pathogens have evolved various strategies to target the apoptotic and inflammatory machineries of the host in order to infect and replicate in the host. Therefore, studying the mechanisms of how pathogens subvert the immunity of the host

will help us to understand the regulation of the apoptotic and inflammatory pathways in humans, which may inspire us to develop new therapeutic approaches for human diseases.
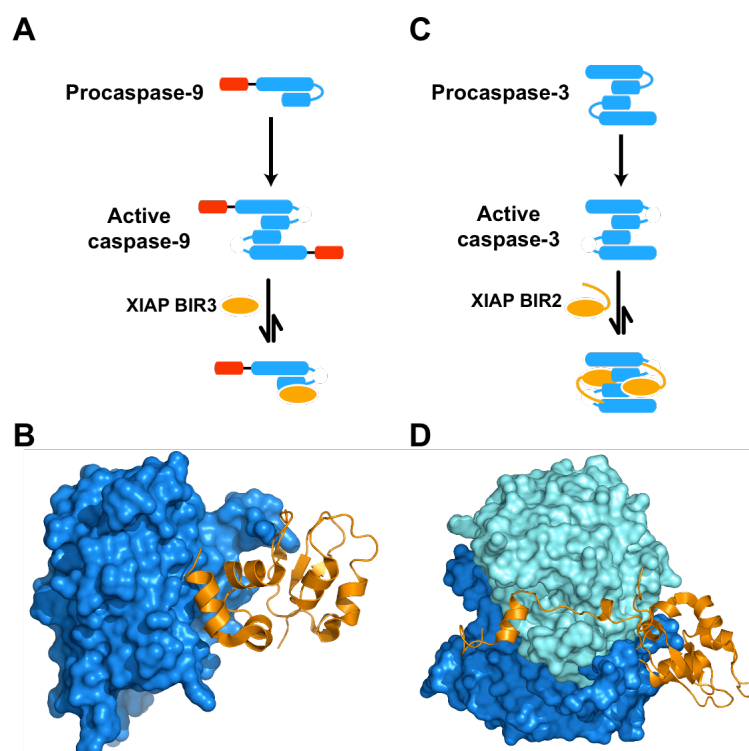
Figure 2-5. Mechanisms of caspase inhibition by XIAP. (A) Schematic illustration of caspase-9 inhibition mediated by XIAP BIR3 domain. XIAP BIR3 binds to the dimerization interface of cleaved caspse-9, trapping the caspase in the inactive monomeric state. **(C)** Schematic illustration of caspase-3 inhibition mediated by XIAP BIR2 domain. XIAP BIR2 binds to an active caspase-3 (or caspase-7), and the flanking peptide N-terminal to the BIR2 domain directly binds to the active site of caspase-3 or -7. Other substrate caspase inhibitors, such as CrmA and p35, utilize similar mechanism, of which CrmA and p35 anchor to the caspase and their RSLs directly target the active sites (see text for details). **(B, D)** Structure of caspase-9 in complex with XIAP BIR3 (PDB 1NW9) (B), and caspae-3 in complex with XIAP BIR2 (PDB 1I3O) (D). The caspase is in surface representation (blue and cyan). The XIAP BIR domain and its flanking region are in orange cartoon representation. In (D), only one BIR2 domain bound on caspase-3 is shown for clarity.

References

1. Benedict, C.A., P.S. Norris, and C.F. Ware, *To kill or be killed: viral evasion of apoptosis.* Nat Immunol, 2002. **3**(11): p. 1013-8.

2. Best, S.M., *Viral subversion of apoptotic enzymes: escape from death row.* Annu Rev Microbiol, 2008. **62**: p. 171-92.

3. Postigo, A. and P.E. Ferrer, *Viral inhibitors reveal overlapping themes in regulation of cell death and innate immunity.* Microbes Infect, 2009. **11**(13): p. 1071-8.

4. Galluzzi, L., et al., *Viral control of mitochondrial apoptosis.* PLoS Pathog, 2008. **4**(5): p. e1000018.

5. Cuconati, A. and E. White, *Viral homologs of BCL-2: role of apoptosis in the regulation of virus infection.* Genes Dev, 2002. **16**(19): p. 2465-78.

6. Kvansakul, M., et al., *Vaccinia virus anti-apoptotic F1L is a novel Bcl-2-like domain-swapped dimer that binds a highly selective subset of BH3-containing death ligands.* Cell Death Differ, 2008. **15**(10): p. 1564-71.

7. Aoyagi, M., et al., *Vaccinia virus N1L protein resembles a B cell lymphoma-2 (Bcl-2) family protein.* Protein Sci, 2007. **16**(1): p. 118-24.

8. Douglas, A.E., et al., *Structure of M11L: A myxoma virus structural homolog of the apoptosis inhibitor, Bcl-2.* Protein Sci, 2007. **16**(4): p. 695-703.

9. Kvansakul, M., et al., *A structural viral mimic of prosurvival Bcl-2: a pivotal role for sequestering proapoptotic Bax and Bak.* Mol Cell, 2007. **25**(6): p. 933-42.

10. Cooray, S., et al., *Functional and structural studies of the vaccinia virus virulence factor N1 reveal a Bcl-2-like anti-apoptotic protein.* J Gen Virol, 2007. **88**(Pt 6): p. 1656-66.

11. Huang, Q., et al., *Solution structure of the BHRF1 protein from Epstein-Barr virus, a homolog of human Bcl-2.* J Mol Biol, 2003. **332**(5): p. 1123-30.

12. Huang, Q., et al., *Solution structure of a Bcl-2 homolog from Kaposi sarcoma virus.* Proc Natl Acad Sci U S A, 2002. **99**(6): p. 3428-33.

13. Graham, S.C., et al., *Vaccinia virus proteins A52 and B14 Share a Bcl-2-like fold but have evolved to inhibit NF-kappaB rather than apoptosis.* PLoS Pathog, 2008. **4**(8): p. e1000128.

14. DiPerna, G., et al., *Poxvirus protein N1L targets the I-kappaB kinase complex, inhibits signaling to NF-kappaB by the tumor necrosis factor superfamily of*

receptors, and inhibits NF-kappaB and IRF3 signaling by toll-like receptors. J Biol Chem, 2004. **279**(35): p. 36570-8.

15. Wasilenko, S.T., et al., *Vaccinia virus encodes a previously uncharacterized mitochondrial-associated inhibitor of apoptosis.* Proc Natl Acad Sci U S A, 2003. **100**(24): p. 14345-50.

16. Stewart, T.L., S.T. Wasilenko, and M. Barry, *Vaccinia virus F1L protein is a tail-anchored protein that functions at the mitochondria to inhibit apoptosis.* J Virol, 2005. **79**(2): p. 1084-98.

17. Fischer, S.F., et al., *Modified vaccinia virus Ankara protein F1L is a novel BH3-domain-binding protein and acts together with the early viral protein E3L to block virus-associated apoptosis.* Cell Death Differ, 2006. **13**(1): p. 109-18.

18. Postigo, A., et al., *Interaction of F1L with the BH3 domain of Bak is responsible for inhibiting vaccinia-induced apoptosis.* Cell Death Differ, 2006. **13**(10): p. 1651-62.

19. Taylor, J.M., et al., *The vaccinia virus protein F1L interacts with Bim and inhibits activation of the pro-apoptotic protein Bax.* J Biol Chem, 2006. **281**(51): p. 39728-39.

20. Wasilenko, S.T., et al., *The vaccinia virus F1L protein interacts with the proapoptotic protein Bak and inhibits Bak activation.* J Virol, 2005. **79**(22): p. 14031-43.

21. Campbell, S., et al., *Vaccinia virus F1L interacts with Bak using highly divergent BCL-2 homology domains and replaces the function of Mcl-1.* J Biol Chem, 2009.

22. Rupinder, S.K., A.K. Gurpreet, and S. Manjeet, *Cell suicide and caspases.* Vascul Pharmacol, 2007. **46**(6): p. 383-93.

23. Thornberry, N.A. and Y. Lazebnik, *Caspases: enemies within.* Science, 1998. **281**(5381): p. 1312-6.

24. Thornberry, N.A., et al., *A novel heterodimeric cysteine protease is required for interleukin-1 beta processing in monocytes.* Nature, 1992. **356**(6372): p. 768-74.

25. Cerretti, D.P., et al., *Molecular cloning of the interleukin-1 beta converting enzyme.* Science, 1992. **256**(5053): p. 97-100.

26. Kostura, M.J., et al., *Identification of a monocyte specific pre-interleukin 1 beta convertase activity.* Proc Natl Acad Sci U S A, 1989. **86**(14): p. 5227-31.

27. Black, R.A., et al., *A pre-aspartate-specific protease from human leukocytes that cleaves pro-interleukin-1 beta.* J Biol Chem, 1989. **264**(10): p. 5323-6.

28.   Yuan, J., et al., *The C. elegans cell death gene ced-3 encodes a protein similar to mammalian interleukin-1 beta-converting enzyme.* Cell, 1993. **75**(4): p. 641-52.

29.   Acehan, D., et al., *Three-dimensional structure of the apoptosome: implications for assembly, procaspase-9 binding, and activation.* Mol Cell, 2002. **9**(2): p. 423-32.

30.   Stennicke, H.R., et al., *Caspase-9 can be activated without proteolytic processing.* J Biol Chem, 1999. **274**(13): p. 8359-62.

31.   Bao, Q. and Y. Shi, *Apoptosome: a platform for the activation of initiator caspases.* Cell Death Differ, 2007. **14**(1): p. 56-65.

32.   Creagh, E.M., H. Conroy, and S.J. Martin, *Caspase-activation pathways in apoptosis and immunity.* Immunol Rev, 2003. **193**: p. 10-21.

33.   Liu, X., et al., *Induction of apoptotic program in cell-free extracts: requirement for dATP and cytochrome c.* Cell, 1996. **86**(1): p. 147-57.

34.   Du, C., et al., *Smac, a mitochondrial protein that promotes cytochrome c-dependent caspase activation by eliminating IAP inhibition.* Cell, 2000. **102**(1): p. 33-42.

35.   Verhagen, A.M., et al., *Identification of DIABLO, a mammalian protein that promotes apoptosis by binding to and antagonizing IAP proteins.* Cell, 2000. **102**(1): p. 43-53.

36.   Youle, R.J. and A. Strasser, *The BCL-2 protein family: opposing activities that mediate cell death.* Nat Rev Mol Cell Biol, 2008. **9**(1): p. 47-59.

37.   Kroemer, G., L. Galluzzi, and C. Brenner, *Mitochondrial membrane permeabilization in cell death.* Physiol Rev, 2007. **87**(1): p. 99-163.

38.   Zou, H., et al., *Apaf-1, a human protein homologous to C. elegans CED-4, participates in cytochrome c-dependent activation of caspase-3.* Cell, 1997. **90**(3): p. 405-13.

39.   Li, P., et al., *Cytochrome c and dATP-dependent formation of Apaf-1/caspase-9 complex initiates an apoptotic protease cascade.* Cell, 1997. **91**(4): p. 479-89.

40.   Yu, X., et al., *A structure of the human apoptosome at 12.8 A resolution provides insights into this cell death platform.* Structure, 2005. **13**(11): p. 1725-35.

41.   Qin, H., et al., *Structural basis of procaspase-9 recruitment by the apoptotic protease-activating factor 1.* Nature, 1999. **399**(6736): p. 549-57.

42.   Pop, C., et al., *The apoptosome activates caspase-9 by dimerization.* Mol Cell, 2006. **22**(2): p. 269-75.

43.   Yin, Q., et al., *Caspase-9 holoenzyme is a specific and optimal procaspase-3 processing machine.* Mol Cell, 2006. **22**(2): p. 259-68.

44.   Renatus, M., et al., *Dimer formation drives the activation of the cell death protease caspase 9.* Proc Natl Acad Sci U S A, 2001. **98**(25): p. 14250-5.

45.   Suda, T., et al., *Molecular cloning and expression of the Fas ligand, a novel member of the tumor necrosis factor family.* Cell, 1993. **75**(6): p. 1169-78.

46.   Pan, G., et al., *The receptor for the cytotoxic ligand TRAIL.* Science, 1997. **276**(5309): p. 111-3.

47.   Kischkel, F.C., et al., *Cytotoxicity-dependent APO-1 (Fas/CD95)-associated proteins form a death-inducing signaling complex (DISC) with the receptor.* EMBO J, 1995. **14**(22): p. 5579-88.

48.   Chinnaiyan, A.M., et al., *FADD/MORT1 is a common mediator of CD95 (Fas/APO-1) and tumor necrosis factor receptor-induced apoptosis.* J Biol Chem, 1996. **271**(9): p. 4961-5.

49.   Boldin, M.P., et al., *Involvement of MACH, a novel MORT1/FADD-interacting protease, in Fas/APO-1- and TNF receptor-induced cell death.* Cell, 1996. **85**(6): p. 803-15.

50.   Muzio, M., et al., *FLICE, a novel FADD-homologous ICE/CED-3-like protease, is recruited to the CD95 (Fas/APO-1) death--inducing signaling complex.* Cell, 1996. **85**(6): p. 817-27.

51.   Peter, M.E. and P.H. Krammer, *The CD95(APO-1/Fas) DISC and beyond.* Cell Death Differ, 2003. **10**(1): p. 26-35.

52.   Luo, X., et al., *Bid, a Bcl2 interacting protein, mediates cytochrome c release from mitochondria in response to activation of cell surface death receptors.* Cell, 1998. **94**(4): p. 481-90.

53.   Li, H., et al., *Cleavage of BID by caspase 8 mediates the mitochondrial damage in the Fas pathway of apoptosis.* Cell, 1998. **94**(4): p. 491-501.

54.   Yan, N. and Y. Shi, *Mechanisms of apoptosis through structural biology.* Annu Rev Cell Dev Biol, 2005. **21**: p. 35-56.

55.   Scott, F.L., et al., *The Fas-FADD death domain complex structure unravels signalling by receptor clustering.* Nature, 2009. **457**(7232): p. 1019-22.

56.	Ashkenazi, A. and V.M. Dixit, *Apoptosis control by death and decoy receptors.* Curr Opin Cell Biol, 1999. **11**(2): p. 255-60.

57.	Jin, Z., et al., *Cullin3-based polyubiquitination and p62-dependent aggregation of caspase-8 mediate extrinsic apoptosis signaling.* Cell, 2009. **137**(4): p. 721-35.

58.	Van de Craen, M., et al., *Cleavage of caspase family members by granzyme B: a comparative study in vitro.* Eur J Immunol, 1997. **27**(5): p. 1296-9.

59.	Medema, J.P., et al., *Cleavage of FLICE (caspase-8) by granzyme B during cytotoxic T lymphocyte-induced apoptosis.* Eur J Immunol, 1997. **27**(12): p. 3492-8.

60.	Atkinson, E.A., et al., *Cytotoxic T lymphocyte-assisted suicide. Caspase 3 activation is primarily the result of the direct action of granzyme B.* J Biol Chem, 1998. **273**(33): p. 21261-6.

61.	Pinkoski, M.J., et al., *Granzyme B-mediated apoptosis proceeds predominantly through a Bcl-2-inhibitable mitochondrial pathway.* J Biol Chem, 2001. **276**(15): p. 12060-7.

62.	Barry, M., et al., *Granzyme B short-circuits the need for caspase 8 activity during granule-mediated cytotoxic T-lymphocyte killing by directly cleaving Bid.* Mol Cell Biol, 2000. **20**(11): p. 3781-94.

63.	Heibein, J.A., et al., *Granzyme B-mediated cytochrome c release is regulated by the Bcl-2 family members bid and Bax.* J Exp Med, 2000. **192**(10): p. 1391-402.

64.	Sutton, V.R., et al., *Initiation of apoptosis by granzyme B requires direct cleavage of bid, but not direct granzyme B-mediated caspase activation.* J Exp Med, 2000. **192**(10): p. 1403-14.

65.	Lassus, P., X. Opitz-Araya, and Y. Lazebnik, *Requirement for caspase-2 in stress-induced apoptosis before mitochondrial permeabilization.* Science, 2002. **297**(5585): p. 1352-4.

66.	Tinel, A. and J. Tschopp, *The PIDDosome, a protein complex implicated in activation of caspase-2 in response to genotoxic stress.* Science, 2004. **304**(5672): p. 843-6.

67.	Vakifahmetoglu, H., et al., *Functional connection between p53 and caspase-2 is essential for apoptosis induced by DNA damage.* Oncogene, 2006. **25**(41): p. 5683-92.

68.	Harvey, N.L., et al., *Processing of the Nedd2 precursor by ICE-like proteases and granzyme B.* Genes Cells, 1996. **1**(7): p. 673-85.

69.   Guo, Y., et al., *Caspase-2 induces apoptosis by releasing proapoptotic proteins from mitochondria.* J Biol Chem, 2002. **277**(16): p. 13430-7.

70.   Robertson, J.D., et al., *Caspase-2 acts upstream of mitochondria to promote cytochrome c release during etoposide-induced apoptosis.* J Biol Chem, 2002. **277**(33): p. 29803-9.

71.   Gao, Z., Y. Shao, and X. Jiang, *Essential roles of the Bcl-2 family of proteins in caspase-2-induced apoptosis.* J Biol Chem, 2005. **280**(46): p. 38271-5.

72.   Duan, H. and V.M. Dixit, *RAIDD is a new 'death' adaptor molecule.* Nature, 1997. **385**(6611): p. 86-9.

73.   Colussi, P.A., N.L. Harvey, and S. Kumar, *Prodomain-dependent nuclear localization of the caspase-2 (Nedd2) precursor. A novel function for a caspase prodomain.* J Biol Chem, 1998. **273**(38): p. 24535-42.

74.   Zhivotovsky, B., et al., *Caspases: their intracellular localization and translocation during apoptosis.* Cell Death Differ, 1999. **6**(7): p. 644-51.

75.   O'Reilly, L.A., et al., *Caspase-2 is not required for thymocyte or neuronal apoptosis even though cleavage of caspase-2 is dependent on both Apaf-1 and caspase-9.* Cell Death Differ, 2002. **9**(8): p. 832-41.

76.   Paroni, G., et al., *Caspase-2 can trigger cytochrome C release and apoptosis from the nucleus.* J Biol Chem, 2002. **277**(17): p. 15147-61.

77.   Shi, M., et al., *DNA-PKcs-PIDDosome: a nuclear caspase-2-activating complex with role in G2/M checkpoint maintenance.* Cell, 2009. **136**(3): p. 508-20.

78.   Tinel, A., et al., *Autoproteolysis of PIDD marks the bifurcation between pro-death caspase-2 and pro-survival NF-kappaB pathway.* EMBO J, 2007. **26**(1): p. 197-208.

79.   Park, H.H., et al., *Death domain assembly mechanism revealed by crystal structure of the oligomeric PIDDosome core complex.* Cell, 2007. **128**(3): p. 533-46.

80.   Kuida, K., et al., *Altered cytokine export and apoptosis in mice deficient in interleukin-1 beta converting enzyme.* Science, 1995. **267**(5206): p. 2000-3.

81.   Li, P., et al., *Mice deficient in IL-1 beta-converting enzyme are defective in production of mature IL-1 beta and resistant to endotoxic shock.* Cell, 1995. **80**(3): p. 401-11.

82.   Keller, M., et al., *Active caspase-1 is a regulator of unconventional protein secretion.* Cell, 2008. **132**(5): p. 818-31.

83. Johnston, J.B., M.M. Rahman, and G. McFadden, *Strategies that modulate inflammasomes: insights from host-pathogen interactions.* Semin Immunopathol, 2007. **29**(3): p. 261-74.

84. McIntire, C.R., G. Yeretssian, and M. Saleh, *Inflammasomes in infection and inflammation.* Apoptosis, 2009. **14**(4): p. 522-35.

85. Brennan, M.A. and B.T. Cookson, *Salmonella induces macrophage death by caspase-1-dependent necrosis.* Mol Microbiol, 2000. **38**(1): p. 31-40.

86. Cervantes, J., et al., *Intracytosolic Listeria monocytogenes induces cell death through caspase-1 activation in murine macrophages.* Cell Microbiol, 2008. **10**(1): p. 41-52.

87. Hornung, V., et al., *AIM2 recognizes cytosolic dsDNA and forms a caspase-1-activating inflammasome with ASC.* Nature, 2009. **458**(7237): p. 514-8.

88. Martinon, F., K. Burns, and J. Tschopp, *The inflammasome: a molecular platform triggering activation of inflammatory caspases and processing of proIL-beta.* Mol Cell, 2002. **10**(2): p. 417-26.

89. Schroder, K., D.A. Muruve, and J. Tschopp, *Innate immunity: cytoplasmic DNA sensing by the AIM2 inflammasome.* Curr Biol, 2009. **19**(6): p. R262-5.

90. Ting, J.P., et al., *The NLR gene family: a standard nomenclature.* Immunity, 2008. **28**(3): p. 285-7.

91. Franchi, L., et al., *The inflammasome: a caspase-1-activation platform that regulates immune responses and disease pathogenesis.* Nat Immunol, 2009. **10**(3): p. 241-7.

92. Franchi, L., et al., *Cytosolic flagellin requires Ipaf for activation of caspase-1 and interleukin 1beta in salmonella-infected macrophages.* Nat Immunol, 2006. **7**(6): p. 576-82.

93. Mariathasan, S., et al., *Differential activation of the inflammasome by caspase-1 adaptors ASC and Ipaf.* Nature, 2004. **430**(6996): p. 213-8.

94. Faustin, B., et al., *Reconstituted NALP1 inflammasome reveals two-step mechanism of caspase-1 activation.* Mol Cell, 2007. **25**(5): p. 713-24.

95. Faustin, B., et al., *Mechanism of Bcl-2 and Bcl-X(L) inhibition of NLRP1 inflammasome: loop domain-dependent suppression of ATP binding and oligomerization.* Proc Natl Acad Sci U S A, 2009. **106**(10): p. 3935-40.

96. Bruey, J.M., et al., *Bcl-2 and Bcl-XL regulate proinflammatory caspase-1 activation by interaction with NALP1.* Cell, 2007. **129**(1): p. 45-56.

97.   Fernandes-Alnemri, T., et al., *AIM2 activates the inflammasome and cell death in response to cytoplasmic DNA.* Nature, 2009. **458**(7237): p. 509-13.

98.   Burckstummer, T., et al., *An orthogonal proteomic-genomic screen identifies AIM2 as a cytoplasmic DNA sensor for the inflammasome.* Nat Immunol, 2009. **10**(3): p. 266-72.

99.   Roberts, T.L., et al., *HIN-200 proteins regulate caspase activation in response to foreign cytoplasmic DNA.* Science, 2009. **323**(5917): p. 1057-60.

100.   Yang, Y. and X. Yu, *Regulation of apoptosis: the ubiquitous way.* FASEB J, 2003. **17**(8): p. 790-9.

101.   Kurokawa, M. and S. Kornbluth, *Caspases and kinases in a death grip.* Cell, 2009. **138**(5): p. 838-54.

102.   Stehlik, C. and A. Dorfleutner, *COPs and POPs: modulators of inflammasome activity.* J Immunol, 2007. **179**(12): p. 7993-8.

103.   Lamkanfi, M., et al., *Caspases in cell survival, proliferation and differentiation.* Cell Death Differ, 2007. **14**(1): p. 44-55.

104.   Fischer, H., et al., *Human caspase 12 has acquired deleterious mutations.* Biochem Biophys Res Commun, 2002. **293**(2): p. 722-6.

105.   Saleh, M., et al., *Enhanced bacterial clearance and sepsis resistance in caspase-12-deficient mice.* Nature, 2006. **440**(7087): p. 1064-8.

106.   Saleh, M., et al., *Differential modulation of endotoxin responsiveness by human caspase-12 polymorphisms.* Nature, 2004. **429**(6987): p. 75-9.

107.   Rosenstiel, P., et al., *A short isoform of NOD2/CARD15, NOD2-S, is an endogenous inhibitor of NOD2/receptor-interacting protein kinase 2-induced signaling pathways.* Proc Natl Acad Sci U S A, 2006. **103**(9): p. 3280-5.

108.   Johnston, J.B., et al., *A poxvirus-encoded pyrin domain protein interacts with ASC-1 to inhibit host inflammatory and apoptotic responses to infection.* Immunity, 2005. **23**(6): p. 587-98.

109.   Dorfleutner, A., et al., *A Shope Fibroma virus PYRIN-only protein modulates the host immune response.* Virus Genes, 2007. **35**(3): p. 685-94.

110.   Callus, B.A. and D.L. Vaux, *Caspase inhibitors: viral, cellular and chemical.* Cell Death Differ, 2007. **14**(1): p. 73-8.

111. Ray, C.A., et al., *Viral inhibition of inflammation: cowpox virus encodes an inhibitor of the interleukin-1 beta converting enzyme.* Cell, 1992. **69**(4): p. 597-604.

112. Zhou, Q., et al., *Target protease specificity of the viral serpin CrmA. Analysis of five caspases.* J Biol Chem, 1997. **272**(12): p. 7797-800.

113. Tewari, M. and V.M. Dixit, *Fas- and tumor necrosis factor-induced apoptosis is inhibited by the poxvirus crmA gene product.* J Biol Chem, 1995. **270**(7): p. 3255-60.

114. Talley, A.K., et al., *Tumor necrosis factor alpha-induced apoptosis in human neuronal cells: protection by the antioxidant N-acetylcysteine and the genes bcl-2 and crmA.* Mol Cell Biol, 1995. **15**(5): p. 2359-66.

115. Enari, M., H. Hug, and S. Nagata, *Involvement of an ICE-like protease in Fas-mediated apoptosis.* Nature, 1995. **375**(6526): p. 78-81.

116. Los, M., et al., *Requirement of an ICE/CED-3 protease for Fas/APO-1-mediated apoptosis.* Nature, 1995. **375**(6526): p. 81-3.

117. Komiyama, T., et al., *Inhibition of interleukin-1 beta converting enzyme by the cowpox virus serpin CrmA. An example of cross-class inhibition.* J Biol Chem, 1994. **269**(30): p. 19331-7.

118. Zhou, Q., et al., *Interaction of the baculovirus anti-apoptotic protein p35 with caspases. Specificity, kinetics, and characterization of the caspase/p35 complex.* Biochemistry, 1998. **37**(30): p. 10757-65.

119. dela Cruz, W.P., P.D. Friesen, and A.J. Fisher, *Crystal structure of baculovirus P35 reveals a novel conformational change in the reactive site loop after caspase cleavage.* J Biol Chem, 2001. **276**(35): p. 32933-9.

120. Fisher, A.J., et al., *Crystal structure of baculovirus P35: role of a novel reactive site loop in apoptotic caspase inhibition.* EMBO J, 1999. **18**(8): p. 2031-9.

121. Xu, G., et al., *Covalent inhibition revealed by the crystal structure of the caspase-8/p35 complex.* Nature, 2001. **410**(6827): p. 494-7.

122. Clem, R.J. and L.K. Miller, *Control of programmed cell death by the baculovirus genes p35 and iap.* Mol Cell Biol, 1994. **14**(8): p. 5212-22.

123. Takahashi, R., et al., *A single BIR domain of XIAP sufficient for inhibiting caspases.* J Biol Chem, 1998. **273**(14): p. 7787-90.

124. Deveraux, Q.L., et al., *Cleavage of human inhibitor of apoptosis protein XIAP results in fragments with distinct specificities for caspases.* EMBO J, 1999. **18**(19): p. 5242-51.

125. Sun, C., et al., *NMR structure and mutagenesis of the inhibitor-of-apoptosis protein XIAP.* Nature, 1999. **401**(6755): p. 818-22.

126. Chai, J., et al., *Structural basis of caspase-7 inhibition by XIAP.* Cell, 2001. **104**(5): p. 769-80.

127. Riedl, S.J., et al., *Structural basis for the inhibition of caspase-3 by XIAP.* Cell, 2001. **104**(5): p. 791-800.

128. Shiozaki, E.N., et al., *Mechanism of XIAP-mediated inhibition of caspase-9.* Mol Cell, 2003. **11**(2): p. 519-27.

129. O'Riordan, M.X., et al., *Inhibitor of apoptosis proteins in eukaryotic evolution and development: a model of thematic conservation.* Dev Cell, 2008. **15**(4): p. 497-508.

Chapter 3

Vaccinia virus protein F1L is a caspase-9 inhibitor

Abstract

Apoptosis plays important roles in host defense, including eliminating virus-infected cells. The executioners of apoptosis are caspase-family proteases. We report that vaccinia virus-encoded F1L protein, previously recognized as anti-apoptotic viral Bcl-2-family protein, is a caspase-9 inhibitor. F1L binds to and specifically inhibits caspase-9, the apical protease in the mitochondrial cell death pathway, while failing to inhibit other caspases. In cells, F1L inhibits apoptosis and proteolytic processing of caspases induced by over-expression of caspase-9, but not caspase-8. An N-terminal region of F1L preceding the Bcl-2-like fold accounts for Caspase-9 inhibition and significantly contributes to the anti-apoptotic activity of F1L. Viral F1L thus provides the first example of caspase inhibition by a Bcl-2-family member, functioning both as a suppressor of pro-apoptotic Bcl-2-family proteins and as an inhibitor of caspase-9, thereby neutralizing two sequential steps in the mitochondrial cell death pathway.

Introduction

Viruses have evolved multiple strategies to prevent or delay host antiviral responses. Apoptosis is a host mechanism used to combat viral infections by eliminating virus-producing cells. By inhibiting apoptosis, viruses can ensure adequate time to

40

replicate their genomes, as well as providing a possible mechanism for achieving chronic latent infections. Suppression of apoptosis can also contribute to escape of host immune surveillance, allowing virus-infected cells to withstand attack by cytolytic T cells and thus continue viral production [1, 2].

Viruses have either evolved independently or usurped from host cells a diversity of anti-apoptotic strategies. Apoptosis is mediated by caspases, a family of intracellular cysteine proteases. Consequently, viruses often target either the caspases or their upstream cellular activators. For example, viral homologs of anti-apoptotic Bcl-2-family proteins have been identified in poxviruses, herpes viruses, adenoviruses, and other viruses. These proteins suppress a major pathway for caspase activation and cell death that involves mitochondria, often referred to as the "intrinsic" pathway (reviewed in [3]). Multiple signals converge on mitochondria, including DNA damage, hypoxia, and oxidative stress, which modulate the expression or activity of various cellular Bcl-2-family proteins that associate with these organelles. Bcl-2-family proteins either block or cause release of cytotoxic mitochondrial proteins, including cytochrome c, which binds to and induces oligomerization of Apaf-1, a central component of a caspase-9-activating complex known as the "apoptosome" [1, 2, 4]. Activation of apoptosome-associated caspase-9 initiates a proteolytic cascade, whereby activated caspase-9 cleaves and activates downstream executioner proteases, such as pro-caspases-3 and -7, resulting in apoptotic cell demise. Viruses encode homologs of cellular anti-apoptotic Bcl-2 proteins to protect infected host cells by keeping the mitochondria intact, with several viral Bcl-2 protein homologs reported to date [1, 2].

In addition to the intrinsic (mitochondrial) pathway, Tumor Necrosis Factor (TNF)-family death receptors transduce apoptotic signals into cells, constituting the so-called "extrinsic" pathway [1, 2, 5]. Upon binding TNF-family cytokine ligands, these death receptors oligomerize in membranes and recruit caspase-binding adapter proteins, forming a "death inducing signaling complex" (DISC), activating caspases-8 and -10. To interfere with this pathway, viruses encode various antagonists, including (1) vFLIPs, viral homologs of cellular FLIP (cFLIP), which bind pro-caspases-8 and -10 and inhibit their activation [1, 2, 6]; (2) CrmA, a viral serpin that binds irreversibly to and inhibits caspases-8 and -10 [7-12]; and (3) soluble decoy receptors that compete with host TNF family receptors for binding cognate ligands (reviewed in [2, 13, 14]).

Virus-encoded antagonists of caspases also include p35 of baculoviruses, a broad-spectrum irreversible inhibitor of caspases, and viral IAPs (Inhibitor of Apoptosis Proteins), found in some insect and animal viruses, which inhibit certain caspases [2, 13-15].

Vaccinia virus represents a prototypical poxvirus, a family of viruses that have large DNA genomes encoding >250 genes [2, 13, 14]. Poxviruses synthesize numerous gene products that inhibit cell death during infection and that interfere with host immune responses. For example, poxviruses produce extrinsic pathway antagonists CrmA, vFLIP, and soluble variants of the TNF-family receptors such as Myx-MT-2 and TPV-2L [1, 2, 13, 14]. Inhibitors of the intrinsic apoptotic pathway have also been identified in vaccinia virus, including the viral proteins F1L and N1L [2, 16, 17]. Although the primary sequence of N1L lacks motifs indicative of Bcl-2 homologs, the 3D-structure of N1L was shown to be very similar to Bcl-2, and the N1L protein possesses anti-apoptotic activity

resembling Bcl-2 [2, 17]. F1L shares less than 10% amino-acid sequence similarity with NIL and unlike N1L, it contains a C-terminal transmembrane domain that anchors it to mitochondrial membranes. However, F1L also has the same 3D protein fold that characterizes Bcl-2-family proteins [18] and it binds certain pro-apoptotic Bcl-2-family members (e.g. Bak and Bim), suppressing mitochondrial-dependent apoptosis [2, 19-21].

Here we provide evidence that the vaccinia virus protein F1L is a direct antagonist of caspase-9, thus revealing an additional and complementary anti-apoptotic activity for this viral protein. Interesting, unlike previously described viral anti-apoptotic proteins that either inhibit active caspases or prevent caspase activation, F1L possesses the ability to do both: it inhibits the activity of active caspase-9, and also inhibits the recruitment and activation of procaspase-9 by the apoptosome. F1L thus represents the first example of direct caspase inhibition by a member of the Bcl-2 family.

Results

F1L inhibits cytochrome c-induced activation of caspases

The viral caspase inhibitor CrmA is a well-characterized anti-apoptotic protein of vaccinia virus. Nevertheless, vaccinia strains with CrmA gene deletions are still able to protect cells against numerous cell death signals, indicating that additional anti-apoptotic mechanisms are operative. A previous search for alternative mechanisms led to the discovery of F1L, a protein specific for inhibiting the intrinsic cell death pathway [2, 16]. F1L is anchored to mitochondria via its C-terminal hydrophobic tail. F1L was shown to

inhibit apoptosis via binding to the pro-apoptotic Bcl-2-family proteins, Bak and Bim [2, 19, 20].

Unlike Bcl-XL, we noticed that recombinant F1L protein inhibits caspase activation induced in cell extracts by cytochrome C (**Figure 3-1A**), the first step downstream of mitochondria in the intrinsic pathway for apoptosis (reviewed in [2, 22, 23]).

Specifically, we found that F1LΔTM recombinant F1L protein (aa 1-206, produced without its C-terminal transmembrane domain to aid solubility) at 1 μM potently suppressed cytochrome c-induced caspase activation in cytosolic extracts, whereas another anti-apoptotic vaccinia protein, N1L, did not. As controls, we also tested the activities of other recombinant anti-apoptotic proteins in cell extracts, including baculovirus p35, cowpox virus CrmA, human cellular XIAP, and Bcl-XL. The p35 protein is a broad-spectrum caspase inhibitor, while XIAP inhibits several caspases within the cytochrome c-activated pathway, including the proximal protease caspase-9 and its downstream substrates caspases-3 and -7 (reviewed in [2, 15]). As expected, 1 μM p35 or XIAP potently inhibited cytochrome c-induced caspase activity in cell extracts (**Figure 3-1A**). CrmA inhibits caspases involved in the extrinsic pathway (e.g. caspases-8 and -10) but not the intrinsic pathway. As expected, CrmA had little effect on activation of DEVD-cleaving effector caspases in cytochrome c-stimulated extracts. Similarly, Bcl-XLΔTM had no effect (**Figure 3-1A**), consistent with prior studies demonstrating that the mechanism of anti-apoptotic Bcl-2 proteins resides upstream of cytochrome c [24]. These findings raised the possibility that F1L might have additional targets besides pro-apoptotic Bcl-2 family proteins that control mitochondrial membrane integrity.

To determine whether F1L is a broad-spectrum inhibitor of caspases, we stimulated effector caspase activation in cell extracts by addition of recombinant active caspase-8, thus mimicking the extrinsic pathway [5]. In contrast to cytochrome c stimulation, F1LΔTM failed to inhibit caspase-8-mediated induction of DEVD-cleaving effector caspase activity in cell extracts (**Figure 3-1B**). As expected, CrmA was inhibitory in these assays, consistent with its ability to directly bind to, and irreversibly inhibit, caspase-8 [8]. p35 and XIAP were also inhibitory, as anticipated, while Bcl-XL was not. Thus, our data demonstrate that F1L selectively inhibits caspase activation within the intrinsic pathway activated by cytochrome c, butnot in the extrinsic pathway activated by caspase-8. Moreover, addition of F1LΔTM to S-100 extracts after (rather than before) stimulation with cytochrome c failed to suppress DEVDase activity (**Figure 3-2C**). Thus, F1L does not directly suppress DEVD-cleaving caspases, but rather interferes with cytochrome c-induced mechanisms leading to activation of effector caspases.
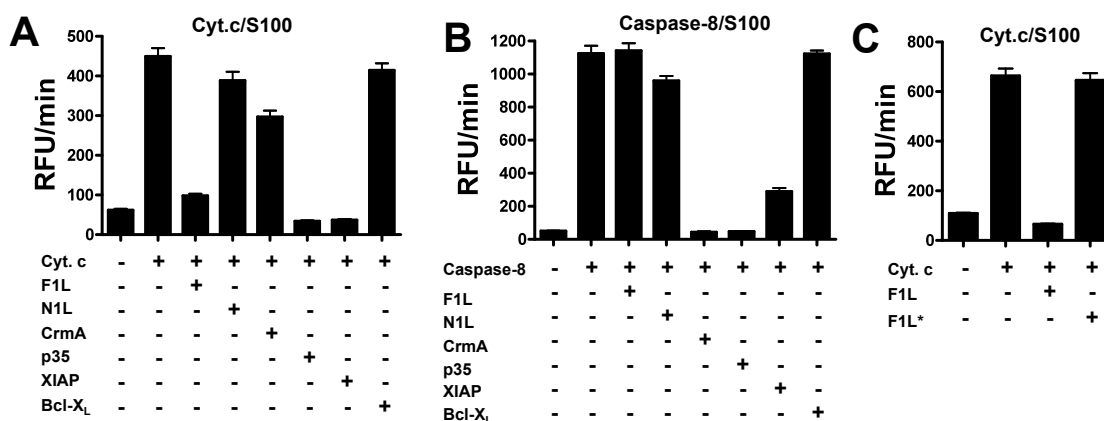
Figure 3-1. F1LΔTM inhibits cytochrome c-activated caspases in cell extracts. (A, B) F1LΔTM (without GST tag), CrmA, N1L, p35, XIAP, or Bcl-XLΔTM (1 µM) proteins were pre-incubated with HeLa cell lysate (S-100) for 10 min at 37°C, follow by addition of cytochrome c and dATP to activate apoptosome (A) or 50 nM of active caspase-8 (B) to activate pro-caspase-3/7 in HEPES buffer for 20 min at 37°C. Caspase-3/7 activity was measured by hydrolysis of Ac-DEVD-AFC. **(C)** F1LΔTM (2 µM without GST tag) was pre-incubated with HeLa cell lysate for 10 min at 37°C, follow by addition of cytochrome c (500 nM) and dATP (200 µM) to activate apoptosome for 20 min at 37°C. Alternatively, F1L (without GST tag) was added after the activation of apoptosome (indicated as *). Caspase-3 activity was measured by hydrolysis of Ac-DEVD-AFC (mean + SD; n = 3).

F1L inhibits cytochrome c-induced, Apaf-1-dependent activation of caspase-9 and apoptosome assembly in vitro

To investigate further the anti-apoptotic mechanism of F1L, we tested its activity against reconstituted apoptosomes, which form in vitro upon cytochrome c-induced oligomerization of Apaf-1, followed by recruitment and activation of pro-caspase-9 [4]. For these experiments, full-length Apaf-1 purified from insect cells was combined with recombinant pro-caspase-9, cytochrome c and dATP (a necessary cofactor for Apaf-1

oligomerization). Caspase-9 activity was measured by hydrolysis of the fluorigenic tetrapeptide Ac-LEHD-AFC. We found that preaddition of F1L at an equimolar ratio relative to Apaf-1 potently blocked cytochrome c-induced LEHDase activity (**Figure 3-2A**). As expected, XIAP had a similar effect in this assay, while N1L and Bcl-XL showed no inhibitory activity.

Next, we used gel-filtration chromatography to investigate the effect of F1L on apoptosome assembly, analyzing column fractions by immunoblotting to unambiguously identify the protein species. Recombinant Apaf-1 and pro-caspase-9 were incubated with cytochrome c and dATP, with or without F1LΔTM protein, and samples analyzed by chromatography and immunoblotting for detection of Apaf-1 and caspase-9. In the absence of F1L, most of the Apaf-1 and caspase-9 migrated as a large (> 670 kDa complex), consistent with formation of the apoptosome [25]. In contrast, when F1L was included, Apaf-1 and caspase-9 eluted from gel-filtration columns much earlier, indicating that F1L interferes with apoptosome assembly. Furthermore, in the absence of F1L, nearly all the pro-caspase-9 was processed to its ~35 kDa form while in the presence of F1L, a significant fraction of the caspase-9 remained in its ~50 kDa proform, (**Figure 3-2B**). We also noted that a significant portion of F1L protein co-eluted in fractions with caspase-9, consistant with an interaction of these proteins.In addition, we performed co-immunoprecipitation experiments to monitor association of caspase-9 with Apaf-1, in the presence versus absence of F1LΔTM protein (**Figure 3-8**). F1LΔTM reduced association of caspase-9 with Apaf-1, whereas Bcl-XLΔTM had no effect.

Although Apaf-1 normally requires cytochrome c for activation, removal of its C-terminal WD40 repeats produces a constitutively active protein (Apaf-1ΔC; residues 1-

591) that directly binds to and activates pro-caspase-9, presumably because the WD40 domains are normally engaged in an autoinhibitory interaction that is relieved by binding cytochrome c [26]. We therefore used Apaf-1ΔC to explore whether either cytochrome c or the WD40 repeats are required directly to mediate the inhibitory activities of F1L. When Apaf-1ΔC was combined with full-length procaspase-9, caspase-9 activity was induced (**Figure 3-2C**). Pre-addition of recombinant F1LΔTM protein at 5-fold molar excess relative to Apaf-1 and caspase-9 significantly inhibited Apaf-1ΔC-induced caspase-9 activity (**Figure 3-2C**). As a positive control, a fragment of XIAP (BIR1-3) that is known to inhibit apoptosome-induced caspase activation had a similar effect on caspase-9 activity. In contrast, several other proteins tested had no inhibitory activity, including N1L, Bid, Bcl-XL, and SMAC (**Figure 3-2C**). The suppression of Apaf-1ΔC-induced caspase-9 activity by F1L was dose-dependent, with half-maximal suppression occurring at approximately equimolar concentrations compared to apoptosome components (**Figure 3-2D**).

Figure 3-2. F1LΔTM inhibits apoptosome-mediated caspase-9 activation and apoptosome assembly. (A) Pro-caspase-9 was pre-incubated with F1LΔTM (lacking GST tag), N1L, XIAP, or Bcl-XLΔTM (1 μM) proteins for 10 min at 37°C, following addition of cytochrome c, dATP and recombinant full-length Apaf-1 (1 μM) for 10 min at 37°C. Caspase-9 activity was measured by hydrolysis of Ac-LEHD-AFC (mean + SD; n =3). **(B)** Pro-caspase-9 was incubated with (+) or without (-) F1L (lacking GST tag), then added to reactions containing Apaf-1 together with cytochrome c and dATP for 10 min. The samples were size-fractionated by S-200 gel-filtration chromatography and the resulting fractions were analyzed by SDS-PAGE/immunoblotting using caspase-9 Apaf-1, or F1L antibodies. The fifth panel represents a chromatography of F1LΔTM alone, which migrated as an apparent dimer. Molecular weight standards are indicated in kDa. **(C)** Recombinant F1LΔTM, N1L, XIAP, Bid, Bcl-XLΔTM or SMAC (10 μM) proteins were pre-incubated with Apaf-1ΔWD-40 recombinant protein (1 μM) for 10 min, then pro-caspase-9 (100 nM) was introduced for 10 min. Caspase-9 activity was measured by hydrolysis of Ac-LEHD-AFC (mean + SD; n =3). **(D)** Various concentrations of F1L (μM) proteins (without GST tag) were pre-incubated with active caspase-9 (200 nM) pre-activated by Apaf-1ΔWD-40 recombinant protein (1μM) for 10 min. Caspase-9 activity was measured by hydrolysis of Ac-LEHD-AFC (mean + SD; n =3).
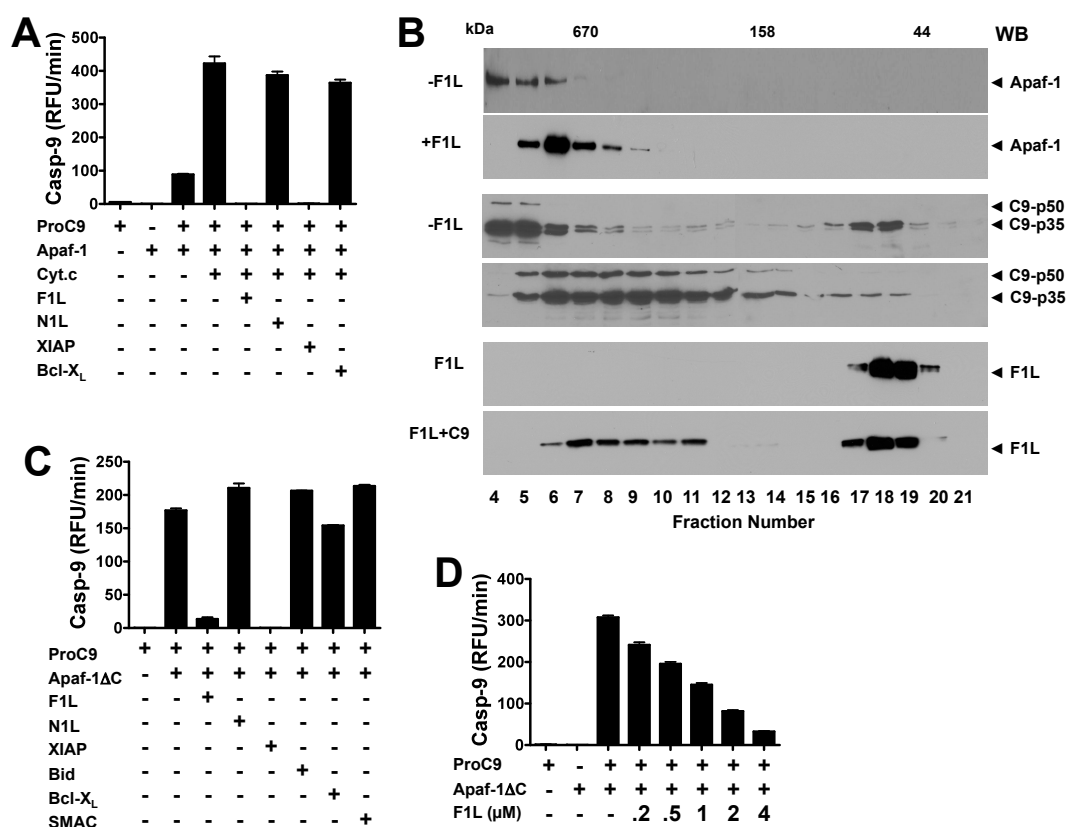
Figure 3-2. F1LΔTM inhibits apoptosome-mediated caspase-9 activation and apoptosome assembly.

F1L is a direct and selective caspase-9 inhibitor

To further explore how F1L inhibits apoptosome-mediated caspase-9 activation, we compared the ability of F1LΔTM protein to inhibit caspase-9 activated by an alternative, Apaf-1-independent mechanism involving incubation with high concentrations of the kosmotropic salt sodium citrate, as previously described [27]. F1LΔTM protein inhibited sodium citrate-activated caspase-9 in a dose-dependent manner in vitro (**Figure 3-3A**), suggesting that F1L acts as a direct inhibitor of caspase-9,

rather than an inhibitor of Apaf-1. When compared with other caspase-9 inhibitors using the same assay, we found that F1LΔTM and XIAP (BIR1-3 domains) displayed similar potencies, with IC_{50} values of 0.17 μM and 0.13 μM, respectively. Recombinant baculovirus p35 was slightly less potent, with IC_{50} of 0.34 μM. However, the viral CrmA protein displayed much weaker inhibitory activity, while the control viral protein N1L had no effect (**Figure 3-3A**).

We next examined the specificity of the caspase inhibition by F1L. As expected, **figure 3B-F** show that F1LΔTM strongly inhibited caspase-9, and slightly inhibited caspase-2, but failed to inhibit caspases-3, -7, or -8 in vitro. Thus, F1L is a selective inhibitor of caspase-9.

We also explored the ability of F1L to inhibit caspase-9 in the context of its physiological substrates, examining proteolytic processing and activity of caspases-3 and -7 in vitro, resulting in similar results (**Figure 3-9**) and indicating that F1L inhibits caspase-9-mediated cleavage and activation of its downstream physiological substrates.

The association rate (k_a) for the interaction between F1L and caspase-9 (activated by apoptosome) was determined under pseudo-first order conditions. The process of caspase-9 inhibition was represented as a simple decay with a rate, k_{obs}. The k_{obs} values obtained at different concentrations were plotted against the inhibitor concentrations. The slope of the line k' and the Km were used to calculate the overall second order rate constant. The k_a for F1LΔTM inhibition of caspase-9 was 0.91×10^3 $M^{-1}S^{-1}$ (**Figure 3-3G**).
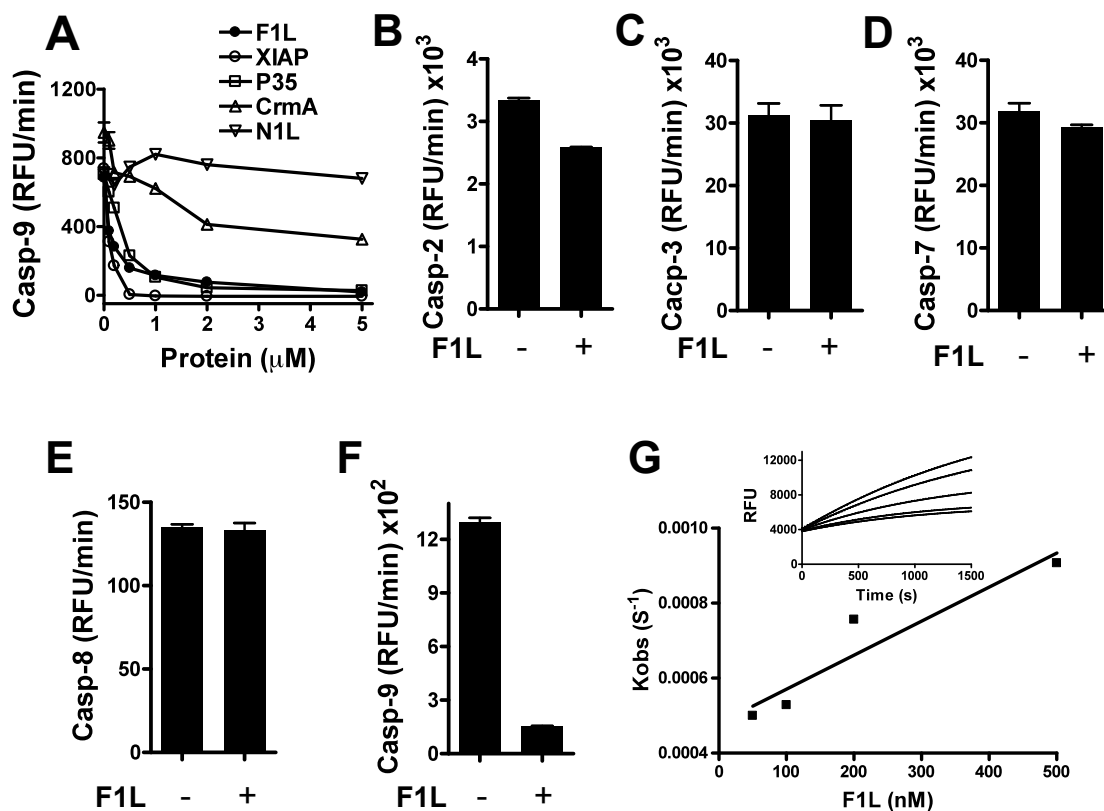
Figure 3-3. F1L selectively inhibits caspase-9 activity. (A) Various concentrations of F1LΔTM (without GST tag), XIAP BIR1-3 domain, p35, CrmA or N1L (μM) proteins were pre-incubated with active caspase-9 (200 nM) pre-activated by Na_2Citrate. Caspase-9 activity was measured by hydrolysis of Ac-LEHD-AFC (mean + SD; n = 3). **(B-F)** Active caspase-2 (B), caspase-3 (C), caspase-7 (D), caspase-8 (E), or caspase-9 (F) was incubated with (+) or without (-) F1LΔTM (2 mM without GST tag) protein for 10 min before addition of fluorigenic substrate peptides. Caspase activity was measured by hydrolysis of Ac-DEVD-AFC (caspase-2, -3, -7), Ac-IETD-AFC (caspase-8) or Ac-LEHD-AFC (caspase-9) (mean + SD; n =3). **(G)** Apoptosome-preactivated caspase-9 (100 nM) was mixed with various concentrations of F1LΔTM (without GST tag). Caspase activity was measured immediately by hydrolysis of Ac-LEHD-AFC at 37°C for 30 min. The rate of inhibition (K_{obs}) and second-order rate constant (Ka) were calculated.

F1L binds caspase-9

To determine whether F1L binds caspase-9, we first performed GST pull-down assays using GST-F1LΔTM fusion protein immobilized on glutathione Sepharose beads, which were incubated with recombinant citrate-activated caspase-9. We observed that GST-F1LΔTM but not GST control protein binds caspase-9 in vitro (**Figure 3-4A**). These results were corroborated by an independent method, whereby binding of activated caspase-9 to GST-F1LΔTM protein was assessed using an ELISA assay in which GST- or GST-F1LΔTM was adsorbed to microtiter plates, incubated with activated caspase-9, and binding was detected using anti-caspase-9 antibody (**Figure 3-4B**). This method also showed that GST-F1L but not GST binds caspase-9 in vitro in a dose-dependent manner (demonstrating sigmoidal binding characteristics) (EC_{50} = 1.6 μM). While an EC50 is provided here using citrate-activated caspase-9, we note that a formal determination of Kd for caspase-9 under physiological conditions is problematic because the native caspase-9 protein is known to require association with active Apaf-1 to assume an active conformation and thus the preformed apoptosome (Apaf1:caspase-9:cytochrome c) is required, making precise determination of protein concentrations problematic [28]. Also, the term Kd implies an entirely reversible mechanism, a subject requiring further analysis.

Finally, gel-filtration chromatography was used to interrogate F1L binding to caspase-9. The elution of both unprocessed pro-caspase-9 and citrate-activated processed caspase-9 from gel filtration columns was retarded by F1L (**Figure 3-4C, D**), consistent with high affinity binding of F1L to both the unprocessed and processed forms of caspase-9. Note that addition of 5 μM F1LΔTM protein to 1 μM caspase-9 resulted in

nearly complete loss of monomeric caspase-9, with most of the caspase-9 protein migrating as a large protein complex upon binding F1LΔTM. The elution characteristics of the F1L/caspase-9 complex suggest formation of a multimeric complex, which could be due to the ability of F1L and caspase-9 to each form homodimers, thus creating the opportunity for heterocomplexes of mixed stoichiometry.
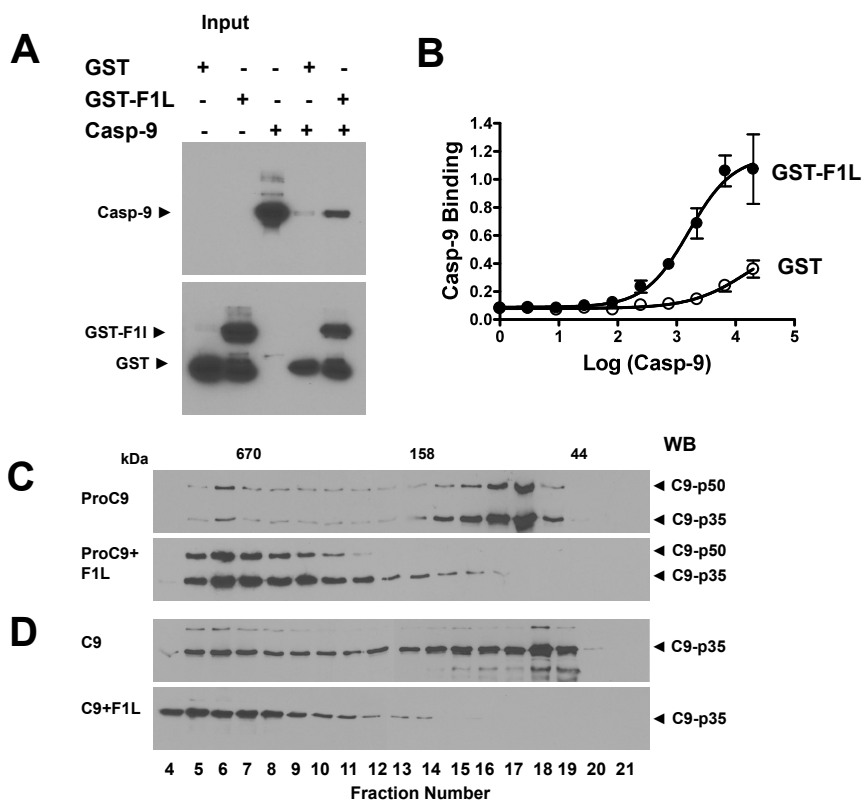
Figure 3-4. F1L binds caspase-9. (A) Recombinant GST or GST-F1LΔTM proteins (1 µg) were incubated with 1 µg active caspase-9 for 4 hrs together with 10 µl Glutathione Sepharose 4B resin. The resin was washed 3-times and associated proteins were analyzed by SDS-PAGE/immunoblotting using anti-caspase-9 or GST antibodies. **(B)** Caspase-9 binding to GST-F1L demonstrated by ELISA assays. F1LΔTM (dark symbols) or GST (white symbols) was incubated with various concentrations of caspase-9. **(C, D)** Pro-caspase-9 (C) or sodium citrate-activated caspase-9 (D) was incubated with (+) or without (-) GST-F1LΔTM, then analyzed by 2S00 gel-sieve chromatography. Eluted fractions were analyzed by SDS-PAGE/immunoblotting using caspase-9 antibody. Molecular weight standards are indicated in kDa. Note the bacterially-expressed pro-caspase-9 contained both uncleaved p50 and cleaved p35 caspase-9 (top), which was reduced to cleaved p35 caspase-9 following activiation with Na_2-Citrate. Addition of F1LΔTM shifted both unprocessed (p50) and processed (p35) caspase-9.

The caspase-9 inhibitory mechanism of F1L differs from XIAP

XIAP is a well-characterized mammalian inhibitor of caspase-9, which binds with high affinity to the proteolytically processed form of caspase-9 but not unprocessed procaspase-9 [29, 30]. We therefore compared the caspase-9 inhibitory mechanisms of F1L and XIAP.

The BIR3 domain of XIAP binds and inhibits caspase-9, mediated in part by interaction of a crevice on BIR3 with the first four amino acids of the unique N-terminus of caspase-9 produced by cleavage at Asp[315]. The binding of processed caspase-9 to this crevice on BIR3 of XIAP is competitively inhibited by the mitochondrial protein SMAC, which similarly binds XIAP via a proteolytically processed N-terminal segment of four amino-acids [31]. Thus, the tetrapeptide, AVPI, corresponding to the N-terminus of the mature SMAC protein, binds the BIR3 domain of XIAP, competitively displacing processed caspase-9. Unlike F1LΔTM, which inhibits recruitment of pro- caspase-9 to Apaf-1 (see **figure 3-2B** above), XIAP reportedly does not interfere with caspase-9 association with Apaf-1 or with apoptosome assembly [32, 33]. Using fluorescence polarization assays, we further determined that F1L does not bind SMAC peptide, in contrast to the XIAP BIR3 domain, which displayed an apparent affinity of ~ 50 nM (**Figure 3-5A**). Moreover, unlike XIAP-BIR3, SMAC peptide does not neutralize the caspase-9 inhibitory activity of F1L (**Figure 3-5B**). Thus, the mechanism by which F1L inhibits active caspase-9 presumably involves structural features distinct from those employed by XIAP.

We further explored the mechanism by which F1L inhibits caspase-9 using non-cleavable mutants. Though caspase-9 is typically cleaved during the protease activation

process, it has been shown that cleavage is not necessary for activation [34, 35]. C9-5A is a noncleavable mutant of caspase-9, in which Asp[315], Asp[330] and GluAspGlu[304-306] have been mutated to alanines, but which nevertheless can be activated with Apaf-1 or sodium citrate [36]. We compared the ability of F1LΔTM protein and XIAP to inhibit the C9-5A mutant. While XIAP-BIR3 failed to inhibit the activity of C9-5A, F1L demonstrated dose-dependent suppression, achieving approximately half-maximal inhibition at an approximately equimolar ratio, with $IC_{50} \approx 0.5$ μM (**Figure 3-5C**). Thus, unlike XIAP, cleavage of caspase-9 is not required for suppression by F1L.

To further examine the mechanism of F1L, we explored the role of the CARD domain. Capase-9 is the only CARD (caspase recruitment domain)-containing caspase in which proteolytic cleavage does not remove the N-terminal prodomain where the CARD resides [31]. We therefore compared the inhibitory activity of F1L against activated full-length caspase-9 and truncated caspase-9 lacking the CARD domain. In assays where caspase-9 activity was measured based on hydrolysis of Ac-LEHD-AFC, F1LΔTM protein showed partial loss of its caspase-9 inhibitory activity against CARD-less caspase-9 compared to full-length caspase-9. In contrast, XIAP inhibited both forms of caspase-9 with similar potency (**Figure 3-5D, E**).

Next, to further interrogate the role of the CARD, we tested F1L for inhibitory activity against a chimeric caspase containing the CARD domain of caspase-9 combined with the catalytic domain of caspase-8 [37]. F1L did not inhibit this chimeric caspase, as measured by hydrolysis of the caspase-8 substrate Ac-IETD-AFC (**Figure 3-5E**). In contrast, CrmA inhibited the chimeric caspase. We conclude therefore that the CARD makes important contributions to the inhibitory mechanism of F1L, but that the catalytic

domain of caspase-9 is also required. Also, F1L binds in vitro to both the full-length caspase-9 protein and caspase-9 lacking the CARD, but does not bind the isolated CARD domain (**Figure 3-10**).

Further studies of the mechanism of F1L-mediated inhibition of caspase-9 in vitro showed that F1L is not cleaved by caspase-9 (indicating that it is not a substrate of this protease) and that the inhibition is reversible (**Figure 3-11 and 3-12**). Thus, the mechanism of caspase inhibition by F1L differs from CrmA, which is an irreversible inhibitor.

Figure 3-5. Studies of mechanism of F1L-mediated inhibition of caspase-9. (A) The fluorescence polarization assay (FPA) method was used to monitor binding of rhodamine (Rd)-labeled SMAC peptide to F1LΔTM (no GST tag). Various concentrations of F1LΔTM, XIAP BIR1-3 domain, Bid or Bcl-XLΔTM were incubated with 20 mM Rd-conjugated SMAC peptide. Fluorescence polarization (milli-Polars) was measured after 10 min. XIAP BIR1-3 domain (0.5 µM), or F1LΔTM (no GST tag) (1 µM) proteins were pre-incubated with active caspase-9 (200 nM) with or without SMAC protein (2 µM) for 10 min. Caspase-9 activity was measured by hydrolysis of Ac-LEHD-AFC (mean + SD; n = 3). **(B)** XIAP BIR1-3 domain (0.5 µM), or F1LΔTM (1 µM) proteins were pre-incubated with active caspase-9 (200 nM) with or without SMAC protein (2 µM) for 10 min. Caspase-9 activity was measured by hydrolysis of Ac-LEHD-AFC (mean + SD; n = 3). **(C)** Various concentrations of F1LΔTM (lacking GST) or XIAP BIR1-3 domain (µM) proteins were pre-incubated with active caspase-9-5A (single chain) mutant (200 nM) for 10 min. Caspase-9 activity was measured by hydrolysis of Ac-LEHD-AFC (mean + SD; n = 3). **(D, E)** F1LΔTM (no GST tag) or XIAP(BIR1-3) proteins (2 µM) were pre-incubated with active full-length caspase-9 (activated by sodium citrate) or caspase-9 protein lacking the CARD domain for 10 min. Caspase-9 activity was measured by hydrolysis of Ac-LEHD-AFC (mean + SD; n = 3). **(F)** Various concentrations of F1LΔTM (no GST tag) or CrmA proteins (µM) were pre-incubated with caspase-9/8 protein (10 nM) for 10 min prior to addition of substrate. Caspase-8 activity was measured by hydrolysis of Ac-IETD-AFC (mean + SD; n = 3).
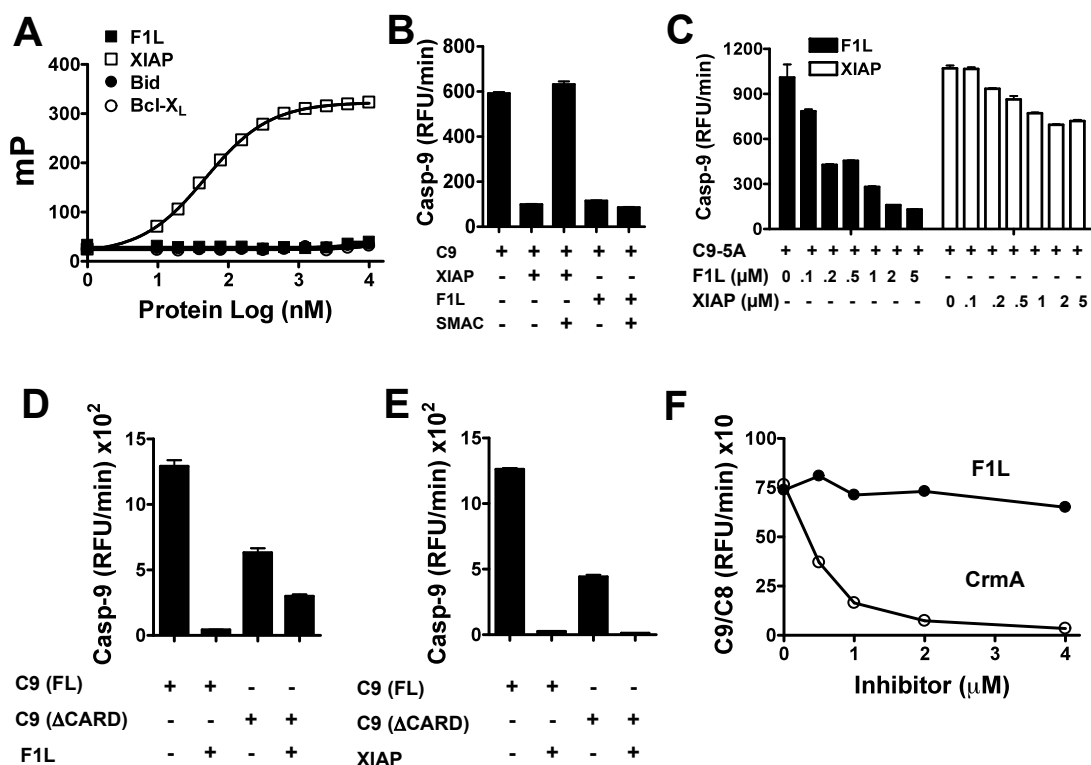
Figure 3-5. Studies of mechanism of F1L-mediated inhibition of caspase-9.

F1L inhibits caspase-9-induced cell death

Expression of F1L occurs rapidly after infection of host cells by vaccinia virus and has been shown to suppress apoptosis induced by stimuli that trigger the intrinsic pathway [38]. We tested whether F1L can suppress caspase activation and apoptosis induced directly by caspase-9 over-expression in mammalian cells, and compared this with caspase-8 over-expression. Accordingly, HEK293T cells were transfected with plasmids encoding flag-tagged caspase-9 or caspase-8 in combination with plasmids encoding F1L. After 1 day, caspase activity was either measured in cell lysates or proteolytic processing of caspases was evaluated by immunoblotting (**Figure 3-6A-C**).

Alternatively, the percentage of apoptotic cells was determined by DAPI staining (**Figure 3-6D**). When overexpressed in cells, caspase-9 undergoes auto-cleavage and is activated, thereby leading to cell death, similar to other caspases [39]. Co-transfecting plasmids encoding full-length F1L and full-length pro-caspase-9 resulted in concentration-dependent reductions in caspase activity and apoptosis (**Figure 3-6A, B, D**). Proteolytic processing of caspase-9 in cells was also inhibited by F1L (**Figure 3-13**). In contrast to F1L, co-expressing Bcl-X_L with procaspase-9 did not suppress activation of effector caspases or apoptosis (**Figure 3-6B, D**), excluding an indirect mechanism for the F1L results related to its suppression of pro-apoptotic Bcl-2 family proteins.

Interestingly, F1L lacking its C-terminal TM domain was equally effective as full-length F1L at inhibiting apoptosis induced by either caspase-9 overexpression or by treatment with staurosporine (STS) (**Figure 3-14**), an agonist of the mitochondria-dependent intrinsic pathway for cell death. In contrast to caspase-9, F1L failed to suppress apoptosis of cells transfected with caspase-8-producing plasmid (**Figure 3-6C, D**), demonstrating its specificity for caspase-9. F1L also failed to inhibit apoptosis induced by agonistic anti-Fas antibody (**Figure 3-15**), an activator of caspase-8. Thus, the anti-apoptotic activity of F1L is specific for the intrinsic rather than extrinsic pathway.
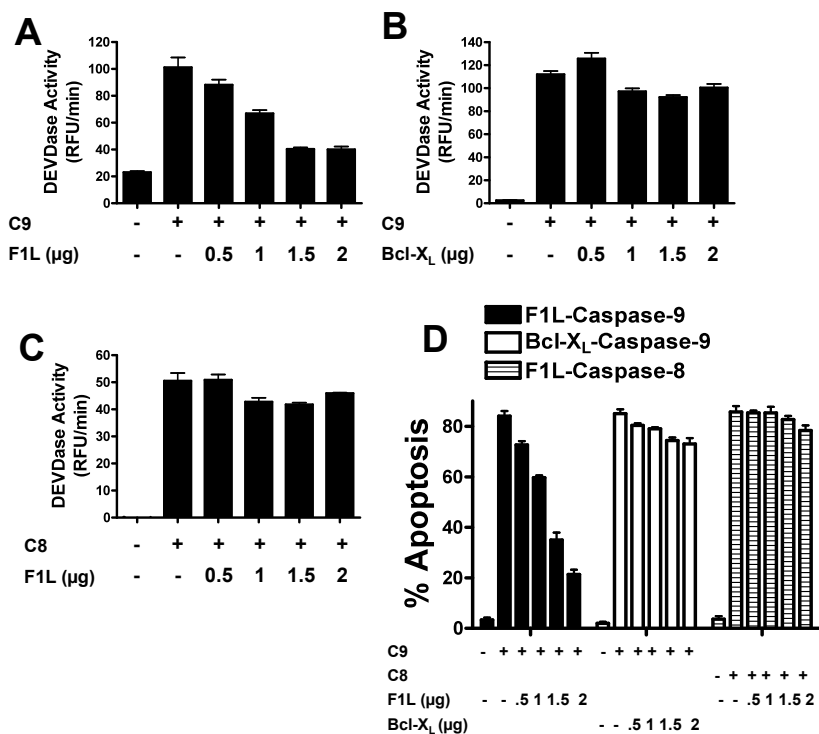
Figure 3-6. F1L suppresses caspase-9-induced apoptosis. (A-C) HEK293T cells were transfected with various amounts of plasmids (pcDNA3 alone denoted by "-") encoding full-length Flag-F1L or Bcl-XL (0-2.0 µg), with or without Flag-caspase-9 (A, B, 0.5 µg) or caspase-8 (C, 1 µg) plasmid, maintaining total DNA constant at 3 µg by addition of pcDNA3. Cell lysates were prepared 20 hrs after transfection, normalized for protein content (10 µg), and incubated with caspase-3/7 substrate Ac-DEVD-AFC. Enzyme activity was determined by generation of fluorescent AFC product, and Vmax was calculated (mean + SD; n = 3). **(D)** HEK293T cells were transfected with various amounts of plasmids encoding GFP (denoted by "-"), GFP-F1L, or Bcl-XL (0-2.0 µg), with or without Flag-caspase-9 (0.5 µg) or caspase-8 (1 µg) plasmids, maintaining total DNA constant at 3 µg by addition of pcDNA3. At 20 hrs post-transfection, both floating and adherent cells were collected, fixed, and stained with 0.1 µg/ml DAPI. The percentages of apoptotic cells were determined by counting the GFP-positive cells having nuclear fragmentation and/or chromatin condensation (mean + S.D.; n = 3).

Analysis of F1L mutants that fail to bind caspase-9 or Bak

To distinguish the role of caspase-9 binding from binding to pro-apoptotic Bcl-2 family proteins such as Bak in terms of the anti-apoptotic activity of the F1L protein, we compared the functions of alanine substitution mutants of F1L with differential loss of binding to either caspase-9 or Bak. We first determined by deletional analysis that the N-terminal region of F1L preceding the Bcl-2-like fold is required for caspase-9 inhibition (not shown). Through sitedirected mutagenesis studies, we determined that converting the cysteine at position 7 to alanine in an N-terminal α-helix of F1L ablated binding to caspase-9, while having no effect of Bak binding (**Figure 3-7A**), as determined by co-immunopreciptiation analysis (**Figure 3-7B**). Conversely, the mutant M67P, previously reported to lack Bak-binding activity [38], retained caspase-9-binding activity (**Figure 3-7B**). The C7A mutant but not the M67P mutant of F1L also lacks in vitro caspase-9 inhibitory activity, as shown by experiments comparing the wild-type and mutant F1L proteins expressed as recombinant proteins (**Figure 3-7C**). Moreover, adding recombinant Bid protein or synthetic Bak BH3 peptide to reactions did not interfere with the ability of F1LΔTM to suppress caspase-9 activity in vitro (**Figure 3-16**). Thus, F1L binds and inhibits caspase-9 independent of its interactions with pro-apoptotic Bcl-2 family proteins.

In cell transfection experiments using Apaf-1-/- MEFs, full-length F1L and full-length F1L M67P equally suppressed activation of effector caspases (not shown) and inhibited apoptosis induced by over-expression of pro-caspase-9, whereas F1L-C7A was inactive (**Figure 3-7D**). These experiments with the C7A mutant thus demonstrate that F1L's ability to bind and suppress caspase-9 correlates with its ability to suppress

caspase-9-induced apoptosis. The use of Apaf1-/- cells excludes a role in these experiments for cytochrome c, a molecule whose release from mitochondria is mediated by pro-apoptotic Bcl-2 family proteins. Moreover, F1L lacking its mitochondria-targeting C-terminal transmembrane domain was equally effective as full-length F1L at blocking apoptosis induced by over-expression of caspase-9 (**Figure 3-14**). Immunoblotting experiments showed equivalent levels of expression of the various F1L proteins (not shown). We conclude therefore that F1L is capable of inhibiting caspase-9 and suppressing caspase-9-induced apoptosis independently of its interactions with pro-apoptotic Bcl-2-family proteins.

To compare the roles of caspase-9- and Bak-binding in F1L-mediated apoptosis suppression, we expressed the C7A (caspase-9-defective) and M67P (Bak-defective) in HEK293 cells and induced apoptosis by treating cells with staurosporine (STS), an activator of the mitochondrial cell death pathway. Cells were transfected with various amounts of F1L-encoding plasmid DNA to compare potency. F1L and F1L-M67P reduced the percentage of apoptotic cells with comparable efficiency, whereas F1L-C7A showed significantly less anti-apoptotic activity (**Figure 3-7E**). Thus, ablating the caspase-9-binding site on F1L reduces the anti-apoptotic activity of F1L, at least in some cellular contexts. A double mutant of F1L (C7A plus M67P) was completely inactive in terms of apoptosis suppression (**Figure 3-14**).

Figure 3-7. Analysis of F1L mutants. (A) Depiction of F1L and Bcl-XL proteins. The locations of some of the α-helices of F1L and Bcl-XL are shown and the C-terminal transmembrane (TM) domains. The regions required for caspase-9 and Bak/Bim/Bid binding are shown, illustrating the alanine substsitutions that ablate protein interactions at C7A (caspase-9) and M67P (Bak). Numbers indicate amino-acid residues that define the borders of the indicated structural elements. **(B)** Immunoprecipitation of caspase-9 or Bak with GFP-tagged wild-type and mutant F1L. HEK293T cells were co-transfected with GFP-F1L and Flag-caspase-9 plasmids, as indicated. After 24 hrs, cell lysates were prepared and analyzed by co-immunoprecitation assay, using anti-GFP antibody (IP). Immune-complexes (IP) (top) or cell lysates (bottom) were analyzed by SDS-PAGE/immunoblotting (WB) using antibodies specific for GFP, caspase-9 or Bak. Pro-caspase-9 (~50 kDa) versus processed caspase-9 large subunit (LS) (~35 kDa) are indicated. Asterisks mark the light chain of anti-GFP used in co-immunoprecipitation. Selected molecular weight markers are indicated in kDa. **(C)** Recombinant GST-tagged F1LΔTM, or GST-F1LΔTM(M67P) (1 µM) were pre-incubated with Na_2Citrate-activated caspase-9 (200 nM). Caspase-9 activity was measured by hydrolysis of Ac-LEHD-AFC (mean + SD; n = 3). **(D)** MEF Apaf-1-/- cells were transfected with various amounts of plasmids (pcDNA3 alone denoted by "-") encoding GFP-F1L, F1L(C7A) or F1L(M67P) (0-2.0 g), with or without Flag-pro-caspase-9 (0.5 µg) plasmid, maintaining total DNA constant at 3 µg by addition of pcDNA3. At 20 hrs post-transfection, both floating and adherent cells were collected, fixed, and stained with 0.1 µg/ml DAPI. The percentages of apoptotic cells were determined by counting the GFP-positive cells having nuclear fragmentation and/or chromatin condensation (mean ± S.D.; n = 3). **(E)** HEK293T cells were transfected with various amounts of plasmid DNA encoding GFP (denoted by "-"), GFP-F1L, GFP-F1L(C7A), or GFP-F1L(M67P), maintaining total DNA constant at 3 $µg$ by addition of GFP plasmid. After 20 hrs, cells were treated with 0.1 $µM$ staurosporine (STS) for 16 hrs. Both floating and adherent cells were collected, fixed, and stained with 0.1 $µg$/ml DAPI. The percentages of apoptotic cells (condensed chromatin and/or fragmented nucleus) among GFP-positive cells was determined by UV-microscopy. Data represent the % of non-apoptotic GFP-positive cells (mean ± SD; n = 3).
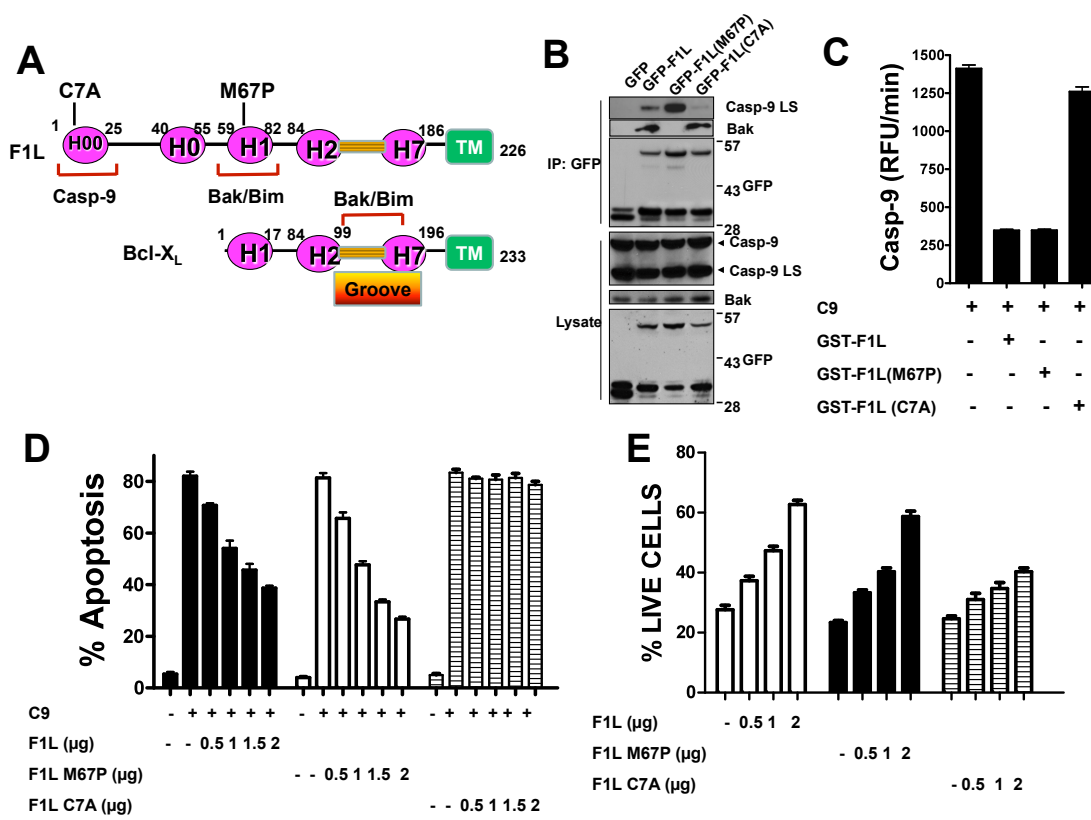
Figure 3-7. Analysis of F1L mutants.
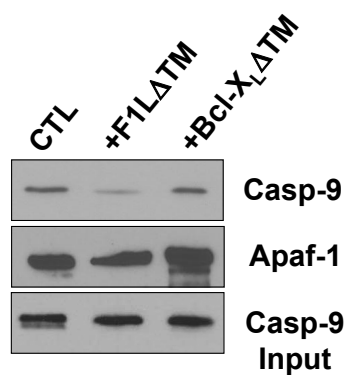
Figure 3-8. F1L reduces association of caspase-9 with Apaf-1. Pro-caspase-9 was incubated with (+) or without (-) F1LΔTM (5 µM, untagged), or His6-Bcl-XLΔTM (5 µM), then added to reactions containing Apaf-1 together with cytochrome c and dATP for 10 min. The samples were incubated with 10 µl protein G beads containing rabbit Apaf-1 antibody at 4°C for 6 hrs. The beads were washed three times and the samples were analyzed by SDS-PAGE/immunoblotting using anti-caspase-9 (top) or Apaf-1 (bottom) antibodies. Caspase-9 input control is shown at bottom.
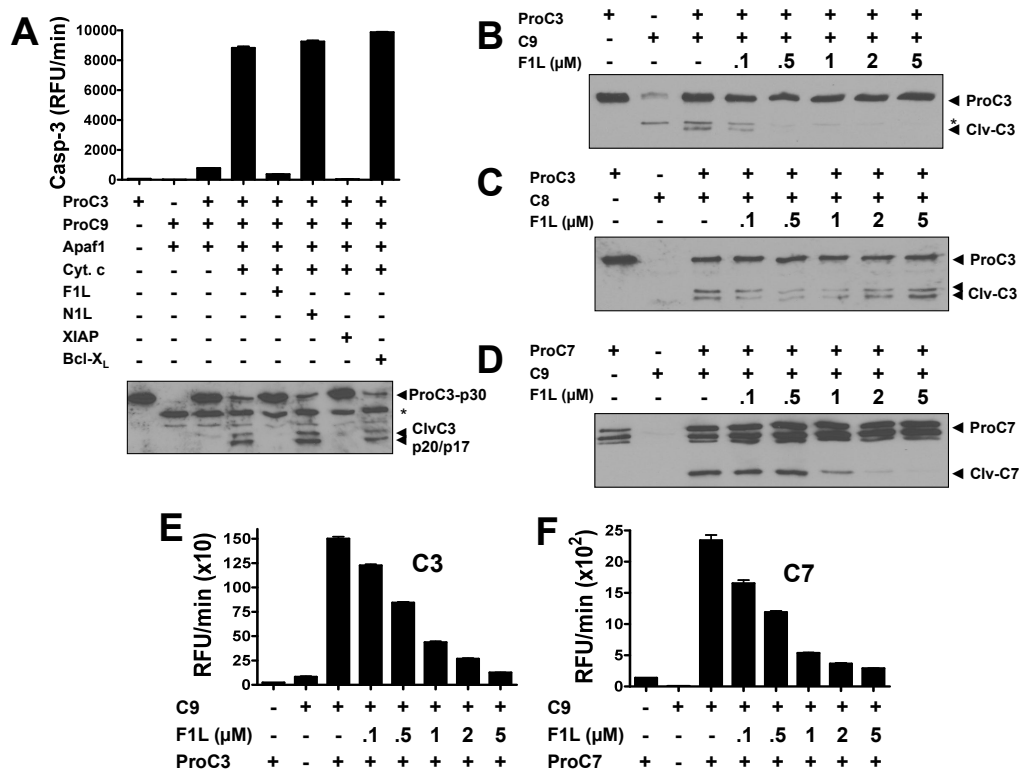
Figure 3-9. F1L inhibits caspase 9-induced activation of effector proteases, caspases-3 and -7. (A) Pro-caspase3 was added to reactions as indicated for figure 3-3A. Caspase-3 activity was measured by hydrolysis of Ac-DEVD-AFC (mean + SD; n =3). Processing of caspase-3 was monitored by SDS-PAGE/immunoblotting using anti-caspase-3 antibody. Asterisk indicates non-specific band. **(B, C, D)** Various concentrations of F1LDTM protein (untagged) were pre-incubated with active caspase-9 (B,D) or caspase-8 (C) (200 nM) for 10 min, follow by addition of pro-caspase-3 (2 nM, B, C) or pro-caspase-7 (10 nM, D). After 1 hr, the samples were analyzed by SDS-PAGE/immunoblotting using anti-caspase-3 or -caspase-7 antibodies. Asterisk indicates non-specific band. **(E, F)** Various concentrations of F1L proteins (untagged) were pre-incubated with active caspase-9 (200 nM) for 10 min, followed by addition of pro-caspase-3 (2 nM) or pro-caspase-7 (10 nM). Caspase activity was measured by hydrolysis of Ac-DEVD-AFC (mean + SD; n = 3).
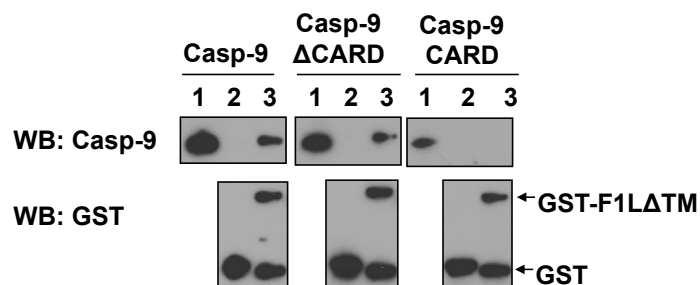
Figure 3-10. F1L does not bind CARD domain of caspase-9. Purified caspase-9-His6, caspase-9ΔCARD-His6 or His6-caspase-9 CARD (10 µg) was incubated with 10 mg of GST (lane 2) or GST-F1LDTM (lane 3). After 10 min at room temperature, Glutathione Sepharose beads were added and incubated at room temperature for 10 min. Beads were then washed three times with PBS plus 0.2% triton X-100 and 20 mM imidazole, and subjected to immunoblot analysis. Purified caspase-9 or its truncated mutants were included in gels (lane1) as "input" controls. The caspase-9-His6 and caspase-9ΔCARD-His6 proteins were detected by anti-caspase-9 antibody. His-caspase-9 CARD was detected by anti-His antibody. GST-tagged proteins were detected by anti-GST antibody.
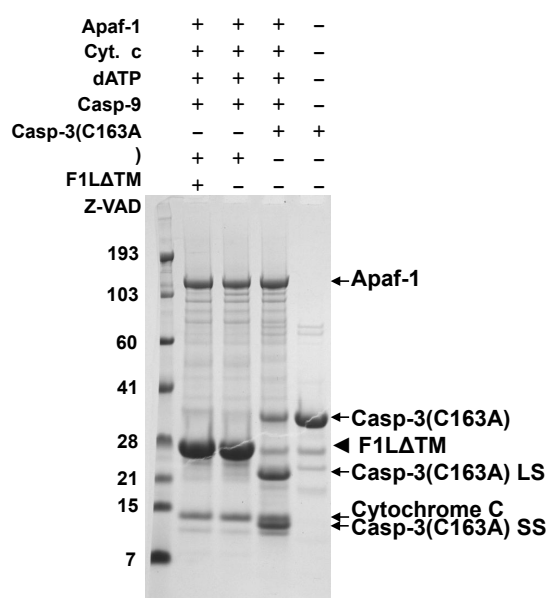
Figure 3-11. F1L is not cleaved by caspase-9. F1LΔTM (40 µM, untagged) or caspase-3(C163A) (40 µM) was mixed with Apaf-1 (4 µM), cytochrome c (10 µM), caspase-9 (4 µM) and dATP (200 µM), with or without Z-VAD (10 µM) as indicated, in caspase assay buffer, and incubated at 37 ºC for 20 hrs. Samples were analyzed by SDS-PAGE and stained with Coumassie blue. Molecular weight standards are indicated in kDa.
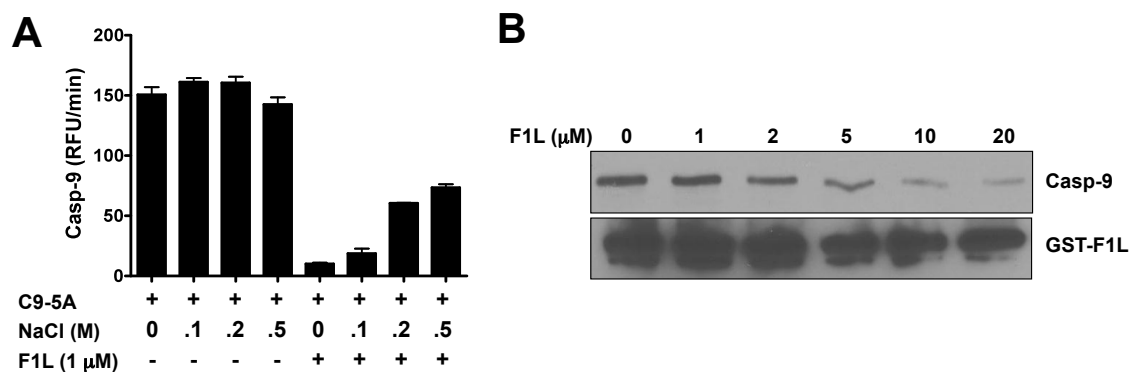
Figure 3-12. F1L-mediated inhibition of caspase-9 is reversible. (A) Na2-citrated-activated caspase-9 (5A non-cleavable mutant) at 100 nM was incubated without (-) or with (+) F1LΔTM protein (untagged) at 1µM at 37 °C for 10 minutes. Then, various concentrations of NaCl were introduced and incubated for 20 min at 37 °C. Caspase-9 activity was measured by hydrolysis of Ac-LEHD-AFC (mean + SD; n = 3). Note that high salt partially restores caspase activity, indicating reversibility. The caspase-9 mutant protein employed here retains activity better than the wild-type protein when withdrawn from Na2-citrate. **(B)** Recombinant GST-F1L proteins (7 µg) were incubated with 7 µg active caspase-9 for 4 hrs together with 10 µl Glutathione Sepharose 4B resin. The resin was washed 3-times and split into aliquots. Various concentrations of untagged F1LΔTM protein were added to the resin to compete with the binding of caspase-9 to GST-F1LΔTM for overnight at 4°C. The resin were washed three times and analyzed by SDSPAGE/immunoblotting using anti-caspase-9 or GST antibodies. Note that untagged F1L competes with GST-F1L for binding to caspase-9, indicating reversible binding.
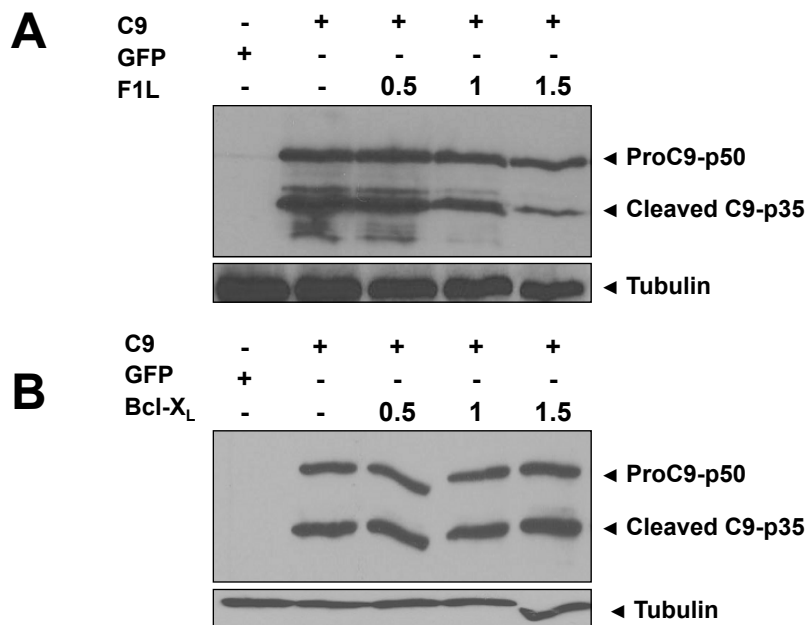
Figure 3-13. F1L inhibits proteolytic processing of pro-caspase-9 in vivo. HEK293T cells were transfected with various amounts of plasmids encoding GFP, GFP-F1L (A), or GFP-Bcl-XL (B) (0-1.5 µg), with or without Flag-caspase-9 (0.5 µg) plasmid, maintaining total DNA constant at 3 µg by addition of pcDNA3. Cell lysates were prepared 20 hrs after transfection, and were analyzed by SDS-PAGE/immunoblotting using anti-caspase-9 or tubulin antibodies. Note that over-expression of pro-caspase-9 results in its autoprocessing from ~50 kDa proform to ~35 kDa processed form. F1L partially inhibits processing, while Bcl-XL does not.
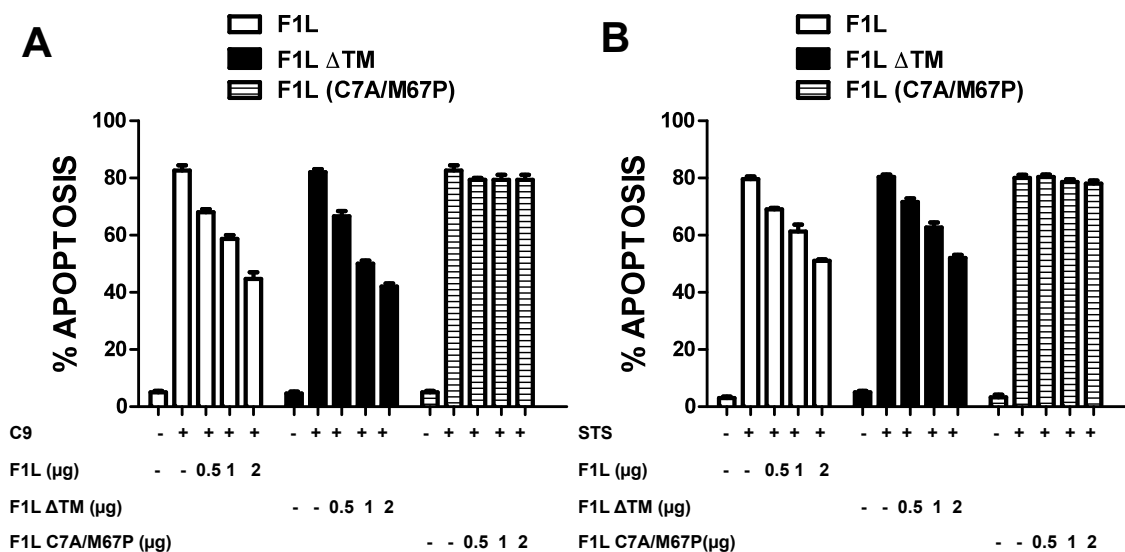
Figure 3-14. Comparison of anti-apoptotic activity of F1L mutants. (A, B) HEK293T cells were transfected with various amounts of plasmids encoding GFP (denoted by "-"), GFP-F1L, GFP-F1L ΔTM, or GFP-F1L double mutant (GFP-F1L C7A/ M67P, 0-2.0 µg), with or without Flag-caspase-9 (0.5 µg) plasmids, maintaining total DNA constant at 3 µg by addition of GFP plasmids. At 20 hrs post-transfection, cells without caspase-9 transfection were treated with 0.2 µM staurosporine for 10 hrs. Both floating and adherent cells were collected, fixed, and stained with 0.1 µg/ml DAPI. The percentages of apoptotic cells were determined by counting the GFP-positive cells having nuclear fragmentation and/or chromatin condensation (mean + S.D.; n = 3).
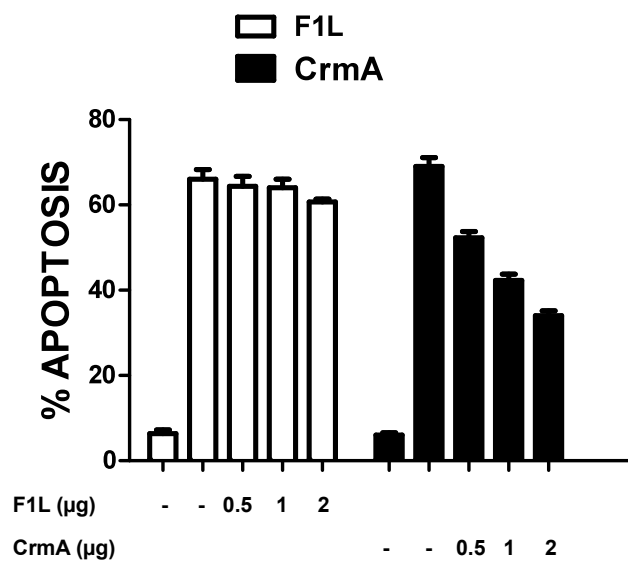
Figure 3-15. F1L fails to rescue cell death induced by an extrisinc pathway agonists. HT1080 cells (which are "Type 1" cells in which Bcl-2 fails to block the extrinsic pathway) were transfected with various amounts of plasmids encoding Flag-F1L, or pcDNA3-myc-CrmA, together with 0.5 µg of plasmids encoding GFP indicative of transfection efficiency. After 12 hrs transfection, the cells were treated with anti Fas antibody CH11 (20 ng/ml) for 12 hrs. Both floating and adherent cells were collected, fixed, and stained with 0.1 µg/ml DAPI. The percentages of apoptotic cells were determined by counting the GFP-positive cells having nuclear fragmentation and/or chromatin condensation (mean + S.D.; n = 3).
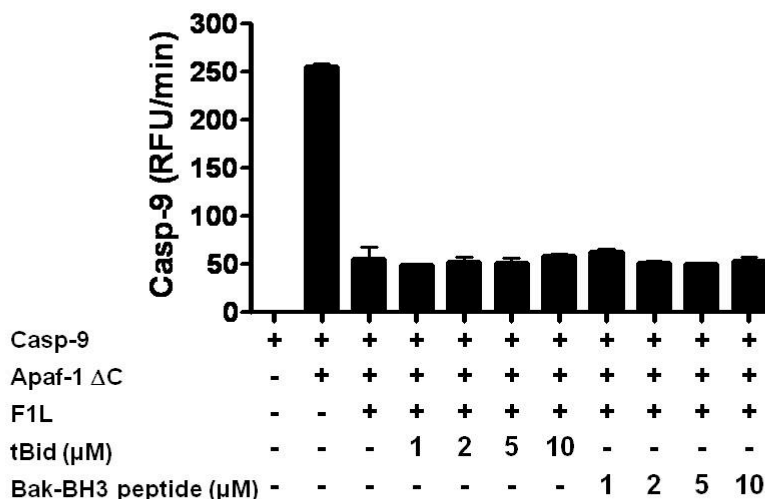
Figure 3-16. tBid protein or Bak peptide does not interfere with F1L-mediated inhibition of caspase-9. Various amounts of recombinant tBid protein or Bak BH3 peptide were pre-incubated with F1L for 10 min, then active caspase-9 was introduced for 10 min at 37 °C. Caspase-9 activity was measured by hydrolysis of Ac-LEHD-AFC (mean + SD; n = 3). Note that neither tBid protein nor Bak peptide interfered with F1L-mediated inhibition of caspase-9.

Discussion

The anti-apoptotic protein F1L specifically inhibits the intrinsic cell death pathway. It has previously been shown that F1L binds and regulates several pro-apoptotic Bcl-2-family proteins, including Bak and Bim [16, 19, 20, 38].

Here, we provide evidence that F1L has another activity as a selective inhibitor of capase-9, the apical protease in the intrinsic (mitochondrial) pathway. The inhibitory activity of F1L is comparable to other known caspase inhibitors, including viral p35 and CrmA, and cellular XIAP. In vitro, F1L also slightly inhibited caspase-2, the caspase most closely related to caspase-9, but not the extrinsic pathway apical protease caspase-8,

nor the downstream effector proteases, caspases-3 and -7. By suppressing caspase-9 activity, F1L inhibits proteolytic processing and activation of its physiological substrates pro-caspases-3 and -7 in vitro and also blocks caspase-9-induced apoptosis of cells. Thus, F1L interrupts the intrinsic pathway at two points – upstream of cytochrome c release through its actions on pro-apoptotic Bcl-2 family proteins as previously reported and downstream of cytochrome c release through its inhibition of caspase-9. Moreover, at least in some cellular contexts, such as STS-induced apoptosis of HEK293T cells, the caspase-9-binding function of F1L appears to be more important than the Bak-binding function.

Unlike other caspase inhibitors, F1L inhibited recruitment of pro-caspase-9 to Apaf-1, and appeared to bind the caspase-9 CARD, in addition to its ability to inhibit caspase-9 activity directly. Most proteins that inhibit caspases either inhibit activation or inhibit the active protease, but not both. For example, viral p35 and CrmA inhibit active caspases by serving as pseudosubstrates, becoming covalently bound to the active site cysteine [15, 40]. XIAP only binds the proteolytically processed forms of caspases, not the inactive zymogens [29, 30]. In contrast, viral FLIPs prevent binding of pro-caspases-8 and -10 to their activating protein FADD. Similarly, the cellular CARD-only proteins, Iceberg and COP, bind pro-caspase-1 via interactions with the N-terminal CARD-containing prodomains of the zymogen forms of these proteases, blocking activation but failing to suppress once the proteases have become activated [6, 41-43]. Our studies suggest that both the N-terminal CARD of caspase-9 and the catalytic domain make contributions to the inhibitory mechanisms of F1L, raising the possibility that F1L interacts cooperatively with both regions in caspase-9 or that the CARD is required for

establishing conformational states of caspase-9 that are optimally inhibited by F1L. We observed however that F1L does not bind to the isolated CARD domain, arguing in favor of the protein conformation model but a 2-site interaction model, where the catalytic domain drives cooperative interactions with the CARD cannot be excluded. Importantly, among the caspases, only caspase-9 retains its N-terminal prodomain where the CARD resides following activation and proteolytic processing [31], thus making the CARD relevant to both zymogen and processed (active) protease. Determination of the 3D-structure of F1L in complex with full-length caspase-9 would therefore be insightful.

Unlike CrmA and p35, which are irreversible inhibitors, our studies suggest that F1L-mediated inhibition of caspase-9 is reversible, which is analogous to the mechanism used by XIAP. However, XIAP binding and inhibition require proteolytic processing of caspase-9, while F1L does not. Also, SMAC peptides block XIAP-mediated inhibition of casaspe-9, but have no effect on F1L. Thus, XIAP and F1Lsuppress caspase-9 by different mechanisms.

F1L is mostly anchored in the mitochondrial membrane via a C-terminal transmembrane domain, with the extra-membrane portion oriented towards the cytosol, similar to cellular members of the Bcl-2 family. How membrane-anchoring impacts the role of F1L as a caspase-9 inhibitor was not explored in detail here, though we did demonstrate that F1LΔTM is equally effective as full-length F1L in inhibiting apoptosis induced by over-expression of caspase-9 or by treatment with staurosporine. It is interesting to note however that some reports have demonstrated pro-caspase-9 association with mitochondria in certain tissues and cell lines [44-46]. Other studies have suggested that some caspases, including caspase-9, tend to localize to mitochondria after

activation [47, 48]. Thus, by placing F1L at the surface of mitochondria, it may be suitably located to interact with caspase-9 in the context of cytochrome c-mediated activation of the protease.

The notion that Bcl-2 family proteins can interact with two or more classes of cellular target proteins is not without precedent, thus making it entirely plausible that F1L inhibits pro-apoptotic Bcl-2-family proteins such as Bim and Bak, while also inhibiting caspase- 9. For example, while cellular Bcl-2 has a central function related to its binding to BH3 domains of pro-apoptotic Bcl-2 family proteins, it also interacts with a variety of cellular proteins including inositol triphosphate receptors (IP3Rs), Bax Inhibitor-1 (BI-1), Bifunctional Apoptosis Regulator (BAR), and Bap31 in membranes of the endoplasmic reticulum (reviewed in [49]) and the autophagy protein Beclin [50], as well as also directly binding and suppressing cytosolic NLR-family proteins such as NALP1 (NLRP1) [51]. It will be interesting therefore to explore whether F1L has additional unrecognized cellular targets, analogous to cellular Bcl-2. Regardless, our data provide the first demonstration of direct caspase inhibition by a Bcl-2-family protein, a theme that may eventually be found for other viral or cellular members of this protein family. Moreover, we mapped the caspase-9-binding domain in F1L to an N-terminal α-helix preceding the Bcl-2-like fold, thus suggesting that this viral Bcl-2 homolog acquired an additional functional domain relative to its cellular counterparts. Computer-assisted searches of genomic databases failed to reveal a clear cellular analog of either the full-length F1L protein or its N-terminal caspase-9-binding domain.

Most strains of vaccinia and variola virus (59 of 60) possess genes encoding both F1L and CrmA. As such, vaccinia virus is armed with anti-apoptotic tools for suppressing

the apical caspases in both the intrinsic and extrinsic pathways for apoptosis. Genetic analysis of vaccinia virus has demonstrated that ablation of F1L leads to apoptosis of infected host cells, indicating that F1L is crucial for blocking vaccinia virus-induced cell death [20, 38]. Moreover, it seems likely that F1L is a dual inhibitor that neutralizes both pro-apoptotic Bcl-2 family proteins, blocking the intrinsic pathway upstream of cytochrome c release [19, 38], as well as inhibiting caspase-9, thus also arresting the pathway downstream of cytochrome c release. In contrast, the related vaccinia virus gene product, N1L, neutralizes pro-apoptotic Bcl-2-family proteins but does not inhibit caspase-9. Therefore, these poxviruses are armed with both complementary and partially redundant weapons for suppressing host cell apoptosis, presumably affording them with the ability to maintain survival of their infected hosts for purposes of viral production.

Experimental procedures

Materials

Cytochrome c (from bovine heart), dATP, and anti-alpha-tubulin antibody were purchased from Sigma. Rabbit anti-caspase-3 and anti-SMAC antibodies have been described [52, 53]. Anti-caspase-7 antibody (clone #9494) was purchased from Cell Signaling Technology (Danvers, MA). Anti-Apaf-1 antibody (clone 94408) was purchased from R&D Systems, Inc. (Minneapolis, MN). Anti-caspase-9 antibody (clone 96-2-22) was purchased from Upstate Biotechnology (Charlottesville, VA). F1L antibody was a gift from Michael Way (Cancer Research UK London Research Institute).

The caspase peptidyl substrates were purchased from BIOMOL. GST mouse monoclonal antibody was produced in our laboratory.

Plasmids

The gene encoding F1L from Vaccinia Virus strain Western Reserve was subcloned into pEGFP-C1 or pFlag-CMV2 for mammalian cell expression (full-length, residues 1-226) or into pGEX 4T1 vector for bacterial expression ("F1LΔTM": C-terminal truncated, residues 1-206, lacking the C-terminal transmembrane domain). F1L mutants C7A,M67P and double mutant C7A/M67P were made by using a one-step, PCR-based mutagenesis kit (Stratagene; Quik-Change). Plasmids encoding mouse Bid, human Bcl-XL, viral N1L, human caspase-3, caspase-7, caspase-8, caspase-9, caspase-9ΔCARD (residues 138-416), caspase-C9-5A, human XIAP BIR1-3, human full-length Apaf-1 and Apaf-1ΔC (residues 1-591) have been described [17, 36, 37, 53-55]. Genes or cDNAs encoding SMAC (AA 56-239, pET-15b), p35, and CrmA were subcloned into pET-21b plasmid for expression in bacteria as His6-fusion proteins.

Protein Expression and Purification

Bid, Bcl-XL, Apaf-1ΔC (1-591), SMAC, p35, CrmA, and caspases-2, -3, -7, -8 and -9 proteins were produced in bacteria as His6-tagged proteins and purified using Ni-chelate agarose beads following previously described methods [34]. GST-F1LΔTM GST-F1LΔTM C7A and GST-F1LΔTM M67P fusion proteins wereexpressed in bacteria and affinity purified using gluthathione-Sepharose, followed by proteolytic removal of GST by thrombin digestion, essentially as described [56]. Full-length Apaf-1 protein was

expressed in Sf9 insect cells at 27°C for 60 hrs and purified by FPLC chromatography as described [54].

Fluorescence Polarization Assays (FPAs)

Binding of SMAC peptide to F1LΔTM or XIAP proteins was measured by fluorescence polarization assays (FPAs), according to published procedures [57]. Briefly, various concentrations of F1LΔTM or XIAP proteins were incubated in the dark in 384 well black plates (Greiner bio-one) with 10 20 nM of rhodamine-conjugated SMAC peptide (AVPIAQK-Rhodamine) dissolved in water. Fluorescence polarization was measured using an Analyst TM AD Assay Detection System (LJL Biosystem, Sunnyvale, CA) in phosphate-buffered saline (PBS) at pH 7.4. EC_{50} determinations were performed using GraphPad Prism software (GraphPad, Inc., San Diego, CA).

Caspase Activity Assays

Caspases were pre-incubated with F1LΔTM or other inhibitors for 10 min at 37°C in 20 mM HEPES buffer (pH 7.2) and the reaction was performed in 100 μL standard caspase assay buffer (50 mM HEPES, pH 7.4, 10% sucrose, 1 mM EDTA, 0.1% CHAPS, 100 mM NaCl, and 5 mM DTT) for 30 min at 37°C. Caspase activity was measured by monitoring cleavage of the fluorogenic tetrapeptide substrates Ac-DEVD-AFC (caspase-2, -3 and -7), Ac-IETD-AFC (caspase-8) or Ac-LEHD-AFC (caspase-9) (BIOMOL, Plymouth, PA) at 100 μM.. Generation of fluorogenic AFC (7-amino-4-trifluoromethyl coumarin) product was measured with a Molecular Devices fMAX fluorometer plate reader operating in kinetic mode for 30 min at 37°C using excitation and emission wavelengths of 405 nm and 510 nm, respectively. Caspase-8 and -9 activity was also

measured by monitoring the cleavage of their natural substrates, pro-caspase-3 and -7. The reactions were performed in caspase assay buffer at 37°C for 60 min. The resulting samples were boiled and analyzed by SDS-PAGE/immunoblotting using anti-caspase-3 or -7 antibodies.

Enzyme Kinetics

Enzyme inhibition rates (k_a) were determined. First, under pseudo-first order conditions, a constant amount of caspase-9 (activated by the apoptosome) was mixed with different concentrations of inhibitors and excess substrate. The amount of product formation (P) proceeds at an initial velocity (V) and is inhibited over time (t) at a rate of (k_{obs}): $P=V/k_{obs}*(1-e^{-kobs*t})+C$. Then, an apparent second order rate constant (k') was determined by measuring the slope of various k_{obs} values. The value of the second order rate constant k_a was then calculated as $k_a=k'*(1+[S]/Km)$, where the Km for caspase-9 in the assays was 0.6 mM [36].

Caspase Cleavage Assays

Recombinant F1LΔTM (40 μM) or caspase-3(C163A) (40 μM) was mixed with Apaf-1 (4 μM), cytochrome c (10 μM), pro-caspase-9 (4 μM) and dATP (200 μM), with or without Z-VAD-fmk (10 μM) in standard caspase assay buffer, and incubated at 37ºC for 20 hrs. Samples were analyzed by SDS-PAGE and stained with Coumassie blue.

Apoptosome Assembly

S-100 cell lysates from HeLa cells were obtained as previously reported [4] and activated by adding bovine cytochrome c (1 μM) and dATP (200 μM) for 20 min at 37°C in reconstitution buffer (20 mM HEPES, pH 7.2, 2 mM $MgCl_2$, 10 mM KCl). For in vitro

reconstituted apoptosomes, recombinant pro-caspase-9 (200 nM) was incubated with 200 μM dATP, and with either recombinant Apaf-1ΔC in the absence of cytochrome c or with full-length Apaf-1 (1 μM) together with cytochrome c for 10 min at 37°C. Caspase-9 activity was measured by hydrolysis of the peptide substrate, acetyl-Leucinyl-Glutamyl-Histidinyl-Aspartyl-amino-fluoro-coumarin (Ac-LEHD-AFC) as described above.

Cell Culture, Transfection, and Apoptosis Assays

HEK293T, HeLa or MEF Apaf-1-/-cells were maintained in Dulbecco's modified Eagle's medium (Irvine Scientific; Irvine, CA) supplemented with 10% fetal bovine serum (FBS), 1 mM L-glutamine, and antibiotics. For transient transfection apoptosis assays, cells (5 x 10^5) in six-well plates were co-transfected using Lipofectamine 2000 (Invitrogen; Carlsbad, CA) with 0.5 μg each of pEGFP-C1 (Clontech; Mountain View, CA) or pcDNA3-Flag-caspase-9 or -8, together with various amounts of GFP-F1L or Flag-F1L plasmids or F1L mutant M67P. For caspase assays, cell lysates were prepared 20 hrs after transfection, normalized for protein content, and then 10 μg aliquots of cell lysates were incubated with 100 μM Ac-DEVD-AFC; enzyme activity was determined by the loss of AFC-fluorescence.

Apoptosis was assessed by DAPI-staining of cells. Briefly, 20 hrs after transfection, both floating and adherent cells were collected, fixed with PBS containing 3.7% formaldehyde, and stained with 0.1 mg/ml 4, 6-diamidino-2-phenylindole (DAPI) in PBS. The percentages of apoptotic cells were determined by UV microscopy, counting GFP-positive cells having nuclear fragmentation and/or chromatin condensation. All assays were performed in triplicate.

In Vitro Protein Binding or competition Assays

For binding assays, recombinant GST, GST-F1LΔTM proteins (1 μg) were incubated with 1 μg of active caspase-9 at 4°C for 4 hrs in PBS together with 10 μl glutathione-Sepharose 4B resin.   For competition assays, GST-F1LΔTM was pre-incubated with caspase-9 at 4°C for 4 hrs, the resin was spit into equal parts, various concentrations of untagged recombinant F1L proteins was introduced to compete the binding at 4°C for overnight. The resulting resin was washed 3 times using PBS buffer, and the associated proteins were boiled and analyzed by SDS-PAGE/immunoblotting using anti-caspase-9 or anti-GST antibodies.

Gel Filtration Assay

A Superdex 200 HR 10/30 column (Amersham-Pharmacia) was equilibrated with buffer (20 mM HEPES, pH 7.4, 100 mM NaCl). Then, 100 μl of samples in 20 mM HEPES buffer were loaded onto the column, and 0.5 ml fractions were collected. Samples (100 μl) consisted of 1 μM caspase-9, alone, or premixed with 5 μM F1LΔTM or with apoptosome components: 5 μM Apaf-1, 5 μM cytochrome c and 500 μM dATP at 37°C for 10 min prior to loading. Aliquots (30 μL) were analyzed by SDS-PAGE, followed by immunoblotting using antibodies recognizing caspase-9,Apaf-1 or F1L.

Acknowledgment

Chapter 3, in full, is a reprint of the publication in "Vaccinia virus protein F1L is a caspase-9 inhibitor" Journal of Biological Chemistry, 2010. 285(8):5569-80, by Dayong Zhai*, Eric Yu*, Chaofang Jin, Kate Welsh, Chung-wei Shiau, Lili Chen, Guy S. Salvesen, Robert Liddington, and John C. Reed. The dissertation author was one of two co-primary investigators and authors of this paper (*co-first author credit given). Both the dissertation author and Dayong Zhai conceived the project, designed and performed experiments, analyzed data, and wrote the initial draft of the manuscript.

References

1. Cuconati, A. and E. White, *Viral homologs of BCL-2: role of apoptosis in the regulation of virus infection.* Genes Dev, 2002. **16**(19): p. 2465-78.

2. Boya, P., et al., *Viral proteins targeting mitochondria: controlling cell death.* Biochim Biophys Acta, 2004. **1659**(2-3): p. 178-89.

3. Danial, N.N. and S.J. Korsmeyer, *Cell death: critical control points.* Cell, 2004. **116**(2): p. 205-19.

4. Li, P., et al., *Cytochrome c and dATP-dependent formation of Apaf-1/caspase-9 complex initiates an apoptotic protease cascade.* Cell, 1997. **91**(4): p. 479-89.

5. Peter, M.E. and P.H. Krammer, *The CD95(APO-1/Fas) DISC and beyond.* Cell Death Differ, 2003. **10**(1): p. 26-35.

6. Thome, M., et al., *Viral FLICE-inhibitory proteins (FLIPs) prevent apoptosis induced by death receptors.* Nature, 1997. **386**(6624): p. 517-21.

7. Ray, C.A., et al., *Viral inhibition of inflammation: cowpox virus encodes an inhibitor of the interleukin-1 beta converting enzyme.* Cell, 1992. **69**(4): p. 597-604.

8.   Zhou, Q., et al., *Target protease specificity of the viral serpin CrmA. Analysis of five caspases.* J Biol Chem, 1997. **272**(12): p. 7797-800.

9.   Tewari, M. and V.M. Dixit, *Fas- and tumor necrosis factor-induced apoptosis is inhibited by the poxvirus crmA gene product.* J Biol Chem, 1995. **270**(7): p. 3255-60.

10.   Talley, A.K., et al., *Tumor necrosis factor alpha-induced apoptosis in human neuronal cells: protection by the antioxidant N-acetylcysteine and the genes bcl-2 and crmA.* Mol Cell Biol, 1995. **15**(5): p. 2359-66.

11.   Enari, M., H. Hug, and S. Nagata, *Involvement of an ICE-like protease in Fas-mediated apoptosis.* Nature, 1995. **375**(6526): p. 78-81.

12.   Los, M., et al., *Requirement of an ICE/CED-3 protease for Fas/APO-1-mediated apoptosis.* Nature, 1995. **375**(6526): p. 81-3.

13.   Everett, H. and G. McFadden, *Poxviruses and apoptosis: a time to die.* Curr Opin Microbiol, 2002. **5**(4): p. 395-402.

14.   Taylor, J.M. and M. Barry, *Near death experiences: poxvirus regulation of apoptotic death.* Virology, 2006. **344**(1): p. 139-50.

15.   Stennicke, H.R., C.A. Ryan, and G.S. Salvesen, *Reprieval from execution: the molecular basis of caspase inhibition.* Trends Biochem Sci, 2002. **27**(2): p. 94-101.

16.   Wasilenko, S.T., et al., *Vaccinia virus encodes a previously uncharacterized mitochondrial-associated inhibitor of apoptosis.* Proc Natl Acad Sci U S A, 2003. **100**(24): p. 14345-50.

17.   Aoyagi, M., et al., *Vaccinia virus N1L protein resembles a B cell lymphoma-2 (Bcl-2) family protein.* Protein Sci, 2007. **16**(1): p. 118-24.

18.   Kvansakul, M., et al., *Vaccinia virus anti-apoptotic F1L is a novel Bcl-2-like domain-swapped dimer that binds a highly selective subset of BH3-containing death ligands.* Cell Death Differ, 2008. **15**(10): p. 1564-71.

19.   Wasilenko, S.T., et al., *The vaccinia virus F1L protein interacts with the proapoptotic protein Bak and inhibits Bak activation.* J Virol, 2005. **79**(22): p. 14031-43.

20.   Taylor, J.M., et al., *The vaccinia virus protein F1L interacts with Bim and inhibits activation of the pro-apoptotic protein Bax.* J Biol Chem, 2006. **281**(51): p. 39728-39.

21.   Fischer, S.F., et al., *Modified vaccinia virus Ankara protein F1L is a novel BH3-domain-binding protein and acts together with the early viral protein E3L to block virus-associated apoptosis.* Cell Death Differ, 2006. **13**(1): p. 109-18.

22.   Riedl, S.J. and G.S. Salvesen, *The apoptosome: signalling platform of cell death.* Nat Rev Mol Cell Biol, 2007. **8**(5): p. 405-13.

23.   Bao, Q. and Y. Shi, *Apoptosome: a platform for the activation of initiator caspases.* Cell Death Differ, 2007. **14**(1): p. 56-65.

24.   Haraguchi, M., et al., *Apoptotic protease activating factor 1 (Apaf-1)-independent cell death suppression by Bcl-2.* J Exp Med, 2000. **191**(10): p. 1709-20.

25.   Cain, K., et al., *Apaf-1 oligomerizes into biologically active approximately 700-kDa and inactive approximately 1.4-MDa apoptosome complexes.* J Biol Chem, 2000. **275**(9): p. 6067-70.

26.   Riedl, S.J., et al., *Structure of the apoptotic protease-activating factor 1 bound to ADP.* Nature, 2005. **434**(7035): p. 926-33.

27.   Boatright, K.M., et al., *A unified model for apical caspase activation.* Mol Cell, 2003. **11**(2): p. 529-41.

28.   Chen, L., et al., *Differential targeting of prosurvival Bcl-2 proteins by their BH3-only ligands allows complementary apoptotic function.* Mol Cell, 2005. **17**(3): p. 393-403.

29.   Srinivasula, S.M., et al., *A conserved XIAP-interaction motif in caspase-9 and Smac/DIABLO regulates caspase activity and apoptosis.* Nature, 2001. **410**(6824): p. 112-6.

30.   Shiozaki, E.N., et al., *Mechanism of XIAP-mediated inhibition of caspase-9.* Mol Cell, 2003. **11**(2): p. 519-27.

31.   Shi, Y., *Caspase activation, inhibition, and reactivation: a mechanistic view.* Protein Sci, 2004. **13**(8): p. 1979-87.

32.   Hill, M.M., et al., *Analysis of the composition, assembly kinetics and activity of native Apaf-1 apoptosomes.* EMBO J, 2004. **23**(10): p. 2134-45.

33.   Bratton, S.B., et al., *Recruitment, activation and retention of caspases-9 and -3 by Apaf-1 apoptosome and associated XIAP complexes.* EMBO J, 2001. **20**(5): p. 998-1009.

34.   Stennicke, H.R., et al., *Caspase-9 can be activated without proteolytic processing.* J Biol Chem, 1999. **274**(13): p. 8359-62.

35.   Rodriguez, J. and Y. Lazebnik, *Caspase-9 and APAF-1 form an active holoenzyme.* Genes Dev, 1999. **13**(24): p. 3179-84.

36.   Renatus, M., et al., *Dimer formation drives the activation of the cell death protease caspase 9.* Proc Natl Acad Sci U S A, 2001. **98**(25): p. 14250-5.

37.   Pop, C., et al., *The apoptosome activates caspase-9 by dimerization.* Mol Cell, 2006. **22**(2): p. 269-75.

38.   Postigo, A., et al., *Interaction of F1L with the BH3 domain of Bak is responsible for inhibiting vaccinia-induced apoptosis.* Cell Death Differ, 2006. **13**(10): p. 1651-62.

39.   Boatright, K.M. and G.S. Salvesen, *Mechanisms of caspase activation.* Curr Opin Cell Biol, 2003. **15**(6): p. 725-31.

40.   Xu, G., et al., *Covalent inhibition revealed by the crystal structure of the caspase-8/p35 complex.* Nature, 2001. **410**(6827): p. 494-7.

41.   Postigo, A. and P.E. Ferrer, *Viral inhibitors reveal overlapping themes in regulation of cell death and innate immunity.* Microbes Infect, 2009. **11**(13): p. 1071-8.

42.   Lee, S.H., C. Stehlik, and J.C. Reed, *Cop, a caspase recruitment domain-containing protein and inhibitor of caspase-1 activation processing.* J Biol Chem, 2001. **276**(37): p. 34495-500.

43.   Humke, E.W., et al., *ICEBERG: a novel inhibitor of interleukin-1beta generation.* Cell, 2000. **103**(1): p. 99-111.

44.   Susin, S.A., et al., *Mitochondrial release of caspase-2 and -9 during the apoptotic process.* J Exp Med, 1999. **189**(2): p. 381-94.

45.   Krajewski, S., et al., *Release of caspase-9 from mitochondria during neuronal apoptosis and cerebral ischemia.* Proc Natl Acad Sci U S A, 1999. **96**(10): p. 5752-7.

46.   Costantini, P., et al., *Pre-processed caspase-9 contained in mitochondria participates in apoptosis.* Cell Death Differ, 2002. **9**(1): p. 82-8.

47.   Chandra, D. and D.G. Tang, *Mitochondrially localized active caspase-9 and caspase-3 result mostly from translocation from the cytosol and partly from caspase-mediated activation in the organelle. Lack of evidence for Apaf-1-mediated procaspase-9 activation in the mitochondria.* J Biol Chem, 2003. **278**(19): p. 17408-20.

48. Chandra, D., et al., *Association of active caspase 8 with the mitochondrial membrane during apoptosis: potential roles in cleaving BAP31 and caspase 3 and mediating mitochondrion-endoplasmic reticulum cross talk in etoposide-induced cell death.* Mol Cell Biol, 2004. **24**(15): p. 6592-607.

49. Kim, I., W. Xu, and J.C. Reed, *Cell death and endoplasmic reticulum stress: disease relevance and therapeutic opportunities.* Nat Rev Drug Discov, 2008. **7**(12): p. 1013-30.

50. Levine, B. and G. Kroemer, *Autophagy in the pathogenesis of disease.* Cell, 2008. **132**(1): p. 27-42.

51. Bruey, J.M., et al., *Bcl-2 and Bcl-XL regulate proinflammatory caspase-1 activation by interaction with NALP1.* Cell, 2007. **129**(1): p. 45-56.

52. Krajewska, M., et al., *Immunohistochemical analysis of in vivo patterns of expression of CPP32 (Caspase-3), a cell death protease.* Cancer Res, 1997. **57**(8): p. 1605-13.

53. Zhai, D., et al., *Humanin binds and nullifies Bid activity by blocking its activation of Bax and Bak.* J Biol Chem, 2005. **280**(16): p. 15815-24.

54. Kim, H.E., et al., *Formation of apoptosome is initiated by cytochrome c-induced dATP hydrolysis and subsequent nucleotide exchange on Apaf-1.* Proc Natl Acad Sci U S A, 2005. **102**(49): p. 17545-50.

55. Deveraux, Q.L., K. Welsh, and J.C. Reed, *Purification and use of recombinant inhibitor of apoptosis proteins as caspase inhibitors.* Methods Enzymol, 2000. **322**: p. 154-61.

56. Zhai, D., et al., *Comparison of chemical inhibitors of antiapoptotic Bcl-2-family proteins.* Cell Death Differ, 2006. **13**(8): p. 1419-21.

57. Zhai, D., et al., *Characterization of the anti-apoptotic mechanism of Bcl-B.* Biochem J, 2003. **376**(Pt 1): p. 229-36.

Chapter 4

Identification of a novel motif of vaccinia virus Bcl-2-like F1L that is sufficient for caspase-9 inhibition

Abstract

In multi-cellular organisms, programmed cell death (apoptosis) is one of the key mechanisms for the host to defend against viral infection. Apoptosis is mediated by activation of different caspase-family protease cascades. Therefore, viruses have evolved a variety of strategies to inhibit caspase activation in order to productively replicate in the host cell. In the mitochondrial cell death pathway, release of cytochrome c from the mitochondria into the cytosol leads to formation of the apoptosome, resulting in activation of caspase-9 and effector caspases, and subsequently apoptosis. We previously showed that the vaccinia virus-encoded Bcl-2-like protein, F1L, which suppresses cytochrome c release by binding Bcl-2 family proteins, is also a caspase-9 inhibitor. Here we further characterize the inhibition of caspase-9 mediated by F1L, and identify a novel motif within the F1L N-terminus that is required and sufficient for the interaction and inhibition of caspase-9. Based on the results of coimmunoprecipitations and caspase activity assays, we show by structural model that the F1L peptide binds to the substrate binding site of casapse-9 in reverse orientation, which is reminiscent of the mechanism of mammalian XIAP-mediated caspase-3/-7 inhibition. In addition, coimmunoprecipitation assays reveal that the Bcl-2-like domain of F1L is able to bind to both pro- and active

caspase-9, implying this domain also possesses a caspase-9 binding site supplementary to the N-terminal motif of F1L.

Introduction

Through the process of host-pathogen co-evolution, the host has developed a variety of defense mechanisms to cope with viral infection. Since viruses are intracellular parasites, programmed cell death (apoptosis) of infected cells is one of the key defense mechanisms to inhibit viral replication in multi-cellular organisms [1-4]. Apoptosis is mediated by activation of the caspase-family protease cascades. In general, signaling pathways leading to apoptosis are known as either the mitochondria-dependent/intrinsic pathway, or the death receptor-dependent/extrinsic pathway [1, 5]. In the mitochondrial pathway, pro-apoptotic signals converge to mitochondria, resulting in permeabilization of its outer membrane, which leads to the release of cytochrome c into the cytosol. Bound with cytochrome c in the cytosol, apoptotic protease activating factor 1 (Apaf-1) oligomerizes together with pro-caspase-9 to form a multi-protein complex, named apoptosome. After forming apoptosome with Apaf-1, pro-caspase-9 is processed and activated. Active caspase-9 then converts downstream pro-caspase-3 and -7 into their active forms, and subsequently leads to apoptosis [6-10].

The release of cytochrome c is regulated by the Bcl-2 family proteins. The BH3-only members of the Bcl-2 protein family, such as Bid and Bim, induce oligomerization of the pro-apoptotic Bcl-2 family proteins on the outer mitochondrial membrane, such as Bak and Bax, leading to cytochrome c release, while other Bcl-2 family proteins, such as

Bcl-2 and Bcl-XL, repress this event [5, 11, 12]. In addition to the cellular Bcl-2 family proteins, there is a collection of functional Bcl-2 homologues encoded by DNA viruses, including adenovirus E1B-19k, African swine fever virus A179L, cytomegalovirus vMIA, Epstein-Barr virus (EBV) BHRF1, fowlpox virus FPV039, Kaposi sarcoma-associated herpesvirus (KSHV) KSBcl-2, myxoma virus M11L, Orf virus ORFV125, vaccinia virus (VACV) F1L and N1L, [3, 4]. Despite the lack of sequence similarity, most of these viral Bcl-2 (vBcl-2) proteins have been shown to adopt a Bcl-2-like structure.

The vaccinia virus-encoded vBcl-2, F1L, has been shown to inhibit apoptosis during infection by interacting with pro-apoptotic proteins, such as Bak and Bim [13-16]. Previously, we showed that F1L also binds to and selectively inhibits caspase-9, the apical caspase in the mitochondrial cell death pathway. Here we identify a highly conserved 15 amino acid-long motif at the N-terminus of F1L preceding the Bcl-2-like domain that is necessary and sufficient for the interaction and inhibition of caspase-9. We further show by caspase-9 activity assays that the peptide derived from this motif is able to suppress a constitutively active mutant of caspase-9 that is independent from the presence of apoptosome, suggesting that the peptide directly blocks to the catalytic site of caspase-9. In addition, coimmunoprecipitation assays reveal that the Bcl-2-like domain of F1L might also act as a supplementary caspase-9 binding site to the N-terminal motif. In summary, our evidence implies a novel mechanism of caspase-9 inhibition mediated by F1L that is distinct from other known caspase inhibitor proteins.

Results

N-terminal region of F1L is necessary for caspase-9 inhibition and interaction

The alignment of all the F1L protein sequences in the Orthopoxvirus family shows that F1L is highly conserved among different strains. The C-terminal Bcl-2-like domain (amino acids 55-226 of F1L in VACV-WR) shares >95% sequence identity, while the N-terminus of F1L is highly variable (**Figure 4-6** & data not shown). Although there is a short conserved motif at the N-terminus of F1L, this sequence is followed by a highly variable "loop" region that varies in length among different strains (**Figure 4-6** & data not shown). Moreover, secondary structure estimation and the result of limited proteolysis (data not shown) implicate that the N-terminal region of F1L is independent from the C-terminal Bcl-2-like domain. Thus, we sought to investigate whether the N-terminus of F1L is important for caspase-9 inhibition.

Caspase-9 activity assays were conducted with recombinant F1LΔTM proteins with different N-terminal truncations. The results of these assays show that even deletion of only the first 23 amino acids substantially reduced the ability of F1L to inhibit caspase-9 (**Figure 4-1A**). Consistently, F1LΔTM without its N-terminus failed to bind caspase-9 in the GST pull down assays (**Figure 4-1B**, lane 4-6). Addition of the N-terminal peptide corresponding to the first 47 amino acids of F1L, F1L(1-47), disrupted the interaction between GST-F1LΔTM and caspase-9 (**Figure 4-1B**, compare lane 3 & 7). Further, GST-F1L(1-47) was able to interact with caspase-9 (**Figure 4-1B**, lane 2). This interaction was much weaker than that of GST-F1LΔTM (**Figure 4-1B**, compare lane 2 & 3), probably due to interference from the GST tag. These results demonstrate

that the N-terminus (the first 23 amino acids) of F1L is required for the interaction and inhibition of caspase-9 *in vitro*.

To confirm the importance of F1L N-terminus on caspase-9 interaction, coimmunoprecipitations of wild type and catalytically inactive mutant (C287A) of caspase-9 were performed with GFP-tagged F1L with different N-terminal truncations (**Figure 4-1C**). Consistent to the results of GST pull down assays, F1L without N-terminus could not bind wild type caspase-9 in these coimmunoprecipitation assays (**Figure 4-1C**, left panel, lane 3-6). In contrast to recombinant caspase-9 from bacterial cultures, which exclusively appeared as cleaved caspase-9, both unprocessed pro-caspase-9 (Casp-9 FL) and processed caspase-9 (detected by the presence of its large subunit (Casp-9 LS)) were present in mammalian cell lysates (**Figure 4-1C**, left panel). Significantly, GFP-F1L binds only to cleaved caspase-9, but not the unprocessed pro-enzyme (**Figure 4-1C**, left panel), indicating the exclusive binding of F1L to activated caspase-9. Contrary to wild type caspase-9, catalytically inactive caspase-9(C287A) mutant can also bind to N-terminally truncated F1Ls (**Figure 4-1C**, right panel). Caspase-9(C287A) is an inactive mutant of which the cysteine at the catalytic center has been mutated to alanine. This mutant cannot carry out auto-processing and appears as unprocessed pro-enzyme (**Figure 4-1C**, right panel). Therefore, it is possible that the interaction between caspase-9(C287A) and the C-terminal region of F1L depends on the cleavage of the caspase. Moreover, we found that more caspase-9(C287A) bound to GFP-F1LΔN59 and GFP-F1LΔN75, when compared to other GFP-F1L proteins (**Figure 4-1C**, right panel, lane 5 & 6). Since the interaction of Bak to these mutants of F1L were much weaker, these results implicate that the binding of caspase-9(C287A) and Bak to F1L

might be mutually exclusive (**Figure 4-1C**, right panel). In conclusion, these results indicate that the N-terminal region of F1L is essential for interaction and inhibition of caspase-9.
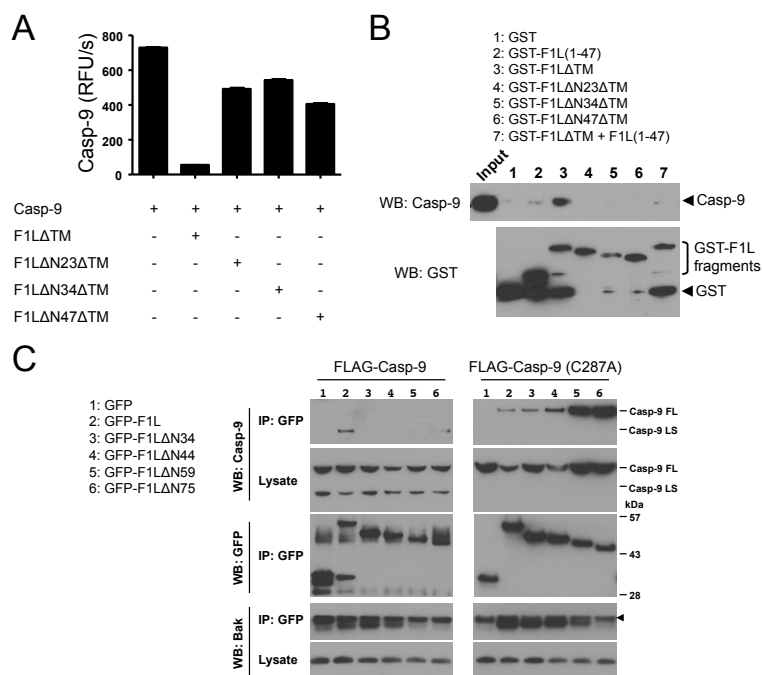
Figure 4-1. N-terminal region of F1L is crucial for caspase-9 interaction and inhibition. (A) F1LΔTM or its fragments with N-terminal truncation (2 µM) were pre-incubated with active caspase-9 (200 nM) pre-activated by sodium citrate. Caspase 9 activity was measured by hydrolysis of Ac-LEHD-AFC (mean ± S.D.; n = 3). **(B)** Recombinant GST, GST-F1LΔTM or its truncated fragments (1 µg) was incubated in PBS with 1 µg caspase-9 for 15 min at room temperature. For lane 7, 0.1 µg of purified F1L(1-47) peptide was mixed with caspase-9 before addition of GST-F1LΔTM. 10 µl of glutathione sepharose resin was then added to the mixture. The resin was washed 3-times and bound proteins were analyzed by SDS-PAGE/immunoblotting using caspase-9 or GST antibodies as indicated. "Input" corresponds to 10% of total caspase-9 used the assays. **(C)** HEK29T cells were transfected with plasmids containing GFP, GFP-F1L or its truncated mutants, together with FLAG-Caspase-9 or FLAG-Caspase-9 (C287A), as indicated. After 17 hrs, cells were harvested and lysed using lysis buffer. Cell lysates were coimmunoprecipitated with anti-GFP. Immuno-complexes (IP) and cell lysates were analyzed by SDS-PAGE/immunobloting with GFP, FLAG or Bak antibodies as indicated. "Casp-9 FL" and "Casp-9 LS" represent full-length caspase-9 and large subunit of processed caspase-9, respectively. Arrowhead indicates a non-specific band.

F1L binds to caspase-9 with two distinct sites

Our evidence show that the N-terminus of F1L is required for the interaction with wild type caspase-9, while caspase-9(C287A) could bind to F1L C-terminal region (**Figure 4-1B & C**), implicating two possible binding sites of caspase-9 on F1L. To further investigate the mechanism of the interaction between F1L and caspase-9, coimmunoprecipitations of various caspase-9 mutants (C287A, 5A, F404D, Dimer) with F1L having different truncations (F1LΔN34, F1L(1-36)) were performed (**Figure 4-2A**). As shown in **Figure 4-2A**, wild type caspase-9 exists as either unprocessed (Casp-9 FL) or processed enzymes (Casp-9 LS) upon overexpression in mammalian cells. The inactive mutant, caspase-9(C287A), appears as uncleaved pro-enzyme. Caspase-9(5A), is a non-cleavable mutant of caspase-9, in which all the possible caspase cleavage sites between the large and small subunits of caspase-9 (Asp^{315}, Asp^{330} and Glu-Asp-Glu$^{304-306}$) have been mutated to alanines. Nonetheless, it could form dimers and have similar catalytic activity when compared to wild type caspase-9 [17]. Caspase-9(F404D) is another inactive mutant of which the phenylalanine at the center of the homodimerization interface has been mutated to a negatively charged residue, aspartic acid, thus this mutant exists exclusively as monomers and cannot be activated [18]. Caspase-9(Dimer) is an engineered form of caspase-9, of which five residues in its homodimerization interface (Gly-Cys-Phe-Asn-Phe$^{402-406}$) have been replaced by those in caspase-3's (Cys-Ile-Val-Ser-Met$^{264-268}$). It has been shown that this mutant caspase-9 is dimeric in solution, and therefore constitutively active [19].

The results of coimmunoprecipitation assays show that all five forms of caspase-9 tested were able to bind GFP-F1L (**Figure 4-2A**, lane 2). F1L without N-terminus, GFP-

F1LΔN34, could interact with all the mutants of caspase-9, but not wild type caspase-9 (**Figure 4-2A**, lane 3). Notably, only caspase-9 mutants that can be active (wild type, 5A, Dimer) were able to bind GFP-F1L(1-36) (**Figure 4-2A**, lane 4). Altogether, these results confirm the notion that there are two distinct caspase-9 binding sites in the N-terminus and C-terminal region of F1L, respectively. Although our data demonstrate that the N-terminus of F1L is required for interaction and inhibition of caspase-9, it is possible that the C-terminal Bcl-2-like domain of F1L plays a supplementary role to further stabilize this interaction. Moreover, as the C-terminal region of F1L is able to bind the monomeric mutant of caspase-9 (F404D), this domain may bind to monomeric pro-caspase-9, and prevent the zymogen from dimerization and consequent activation. It is interesting to note that F1L N-terminus only bind to caspase-9 that can be active, implying that the N-terminus of F1L might exclusively bind to activated caspase-9.

To study the interaction between F1L and caspase-9 *in vitro*, we performed GST pull down assays using various caspase-9 mutants (C287A, 5A, F404D, Dimer) with F1L having different truncations (F1LΔTM and F1LΔN23ΔTM) purified from *E.coli* cultures (**Figure 4-2B**). Similar to the results of coimmunoprecipitation assays, all five forms of caspase-9 tested were able to bind GST-F1LΔTM, but not GST. All the mutants that exist as unprocessed protein (C287A, 5A, F404D) also bind weakly to the N-terminally truncated F1L (GST-F1LΔN23ΔTM). Contrary to the results of coimmunoprecipitations, the constitutively dimeric mutant, caspase-9(Dimer), failed to bind GST-F1LΔN23ΔTM (**Figure 4-2B**). Nonetheless, these results confirm that the C-terminal region of F1L can directly interact with unprocessed form of caspase-9.
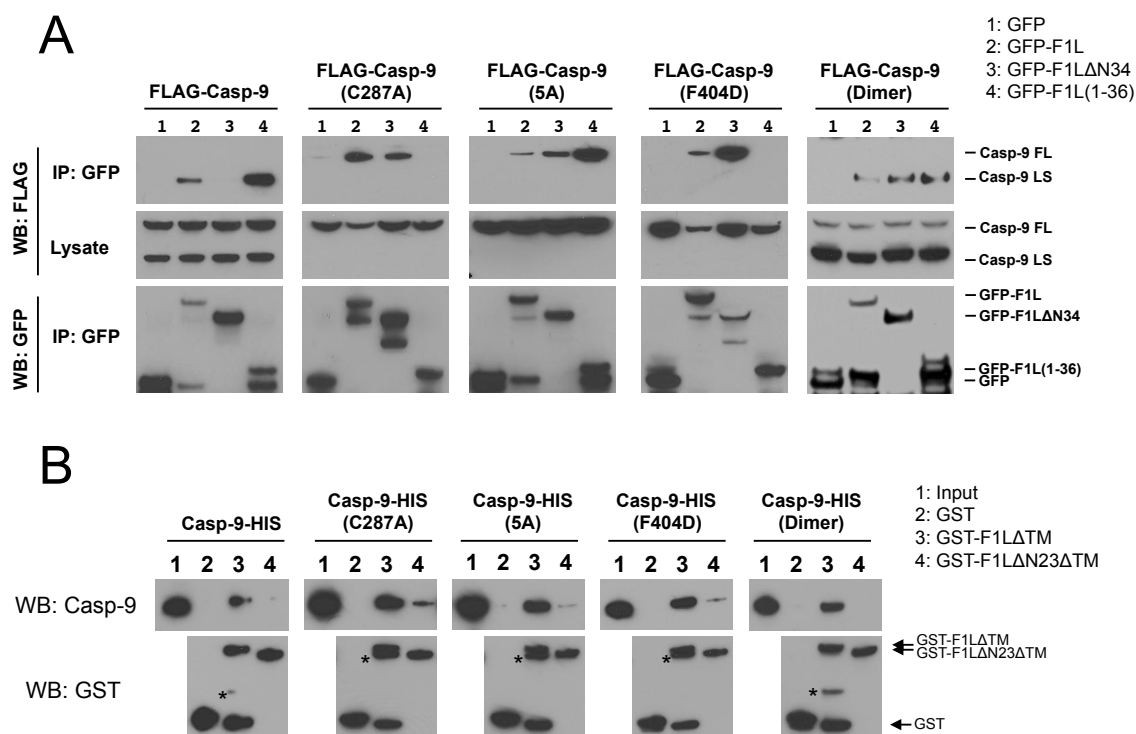
Figure 4-2. F1L interacts with caspase-9 via two distinct binding sites. (A) HEK29T cells were transfected with plasmids containing GFP, GFP-F1L, GFP-F1LΔN34 or GFP-F1L(1-36) together with various FLAG-Caspase-9 mutants, as indicated. After 17 hrs, cells were harvested and lysed using lysis buffer. Cell lysates were coimmunoprecipitated with anti-GFP. Immuno-complexes (IP) and cell lysates were analyzed by SDS-PAGE/immunobloting with GFP or FLAG antibodies. "Casp-9 FL" and "Casp-9 LS" represent full-length caspase-9 and large subunit of processed caspase-9, respectively. **(B)** Recombinant GST, GST-F1LΔTM or GST-F1LΔN23ΔTM (1 μg) was incubated in PBS with 1 μg of different caspase-9-HIS mutants, as indicated, for 15 min at room temperature. 10 μl of Glutathione Sepharose 4B resin was then added to the mixture. The resin was washed 3-times and bound proteins were analyzed by SDS-PAGE/immunoblotting using caspase-9 or GST antibodies as indicated. "Input" corresponds to 10% of total caspase-9 used the assays. Asterisk indicates residual signal from caspase-9 antibody on the same blot.

A peptide derived from F1L N-terminus is sufficient to inhibit caspase-9

Our data of coimmunoprecipitations demonstrate that the 36-amino acid-long region at the F1L N-terminus is sufficient to interact with caspase-9 (**Figure 4-2A**). Therefore, we synthesized a collection of 25-amino acid-long peptides covering the entire N-terminal flexible region (first 47 amino acids) of F1L to identify minimal sequence that is sufficient to suppress caspase-9 activity (**Figure 4-7**). In caspase activity assays, both F1L(1-47) and F1L(1-25) peptides possess similar inhibitory activity to caspase-9 in a dose-dependent manner, while all other peptides we tested, including the F1L(7-31) peptide, failed to inhibit caspase-9 (**Figure 4-7B**). These results indicate that the first 6 amino acids at the N-terminus of F1L are critical for the inhibition of caspase-9. Since the first 15 amino acids of F1L are highly conserved among all the F1L orthologues (**Figure 4-3A**, **4-6** & data not shown), we examined whether this motif is able to bind and inhibit caspase-9. The results of coimmunoprecipitation and caspase-9 activity assays show that the F1L(1-15) peptide is sufficient to bind and inhibit caspase-9 (**Figure 4-3B & 4-4A**).

Characterization of the interaction of F1L N-terminus with caspase-9

Although the 15-amino acid-long motif of the F1L that we used in this study is extremely conserved among all the F1L orthologues available, there are variations in certain positions (Ser^3, Cys^7 and Tyr^{13}). This conserved motif is followed by a "loop" region that is greatly variable in sequence and length. In addition, there are four extra amino acids (Met-Tyr-Asn-Ser) at the N-terminus and a S3P variation in the F1L orthologues of all the variola virus strains (**Figure 4-3A**, **4-6** & data not shown). To investigate whether F1Ls from other strains in the Orthopoxvirus family, especially the

variola virus strains that cause smallpox, are able to bind caspase-9, we selected two representative sequences of F1L from other strains (VACV-MVA and VARV-YUG72) as references to mutate the N-terminal region of F1L from the VAVC-WR strain (**Figure 4-3A**). Performing coimmunoprecipation assays, we show that caspase-9 is able to interact with all these F1L variants. Moreover, F1L without the "loop" region (F1LΔ16-37) can bind to caspase-9 (**Figure 4-3B**). These data suggest that F1L from different strains in the Orthopoxvirus family are capable to bind, and probably inhibit caspase-9, even though there are variations in the N-terminal region.

To further characterize the role of the 15 residues of F1L on caspase-9 interaction, point mutations were introduced in selected positions based on the sequence alignment of F1L. Conducting coimmunoprecipation assays with these F1L mutants, we found that L2A, S3P, M4A, F5S and C7A mutations dramatically reduced the binding of F1L to caspase-9, confirming the importance of these residues on the interaction (**Figure 4-8**). Intriguingly, the C7Y mutation that presents in the F1L sequences of all monkeypox and certain cowpox strains, and D12A mutation, enhanced the interaction, while V14A and D15A mutations had no significant effect (**Figure 4-8**). To rule out the possibility that the mutation at the N-terminus might disrupt proper folding of the F1L protein and thus affect its interaction with caspase-9, we tested the F1L(1-15) peptide with selected mutations (C7A, C7Y and C7Y/D12A) (**Figure 4-9A**). Consistent to the results of coimmunoprecipitations with full-length F1L mutants, C7A mutation diminished the interaction of F1L(1-15) with caspase-9, while C7Y and C7Y/D12A mutations enhanced the interaction (**Figure 4-9A**). Although C7Y or D12A mutation alone was able to enhance the binding of F1L to caspase-9, the C7Y/D12A double mutations acted in

synergy to further enhance the interaction of F1L(1-15) with caspase-9, when compared to C7Y mutation (**Figure 4-9A**). Therefore, we sought to examine if this C7Y/D12A double mutant peptide possesses stronger inhibition to caspase-9. A variety of F1L(1-36) peptides (Wild Type, C7A and C7Y/D12A) were tested with caspase-9 activity assays (**Figure 4-9B**). As expected, the C7A mutation significantly decreased the ability of the F1L(1-36) peptide to suppress caspase-9 when compared to the wild type peptide. Contrary to the results of coimmunoprecipitation assays, the F1L(1-36)-C7Y/D12A peptide possesses similar inhibitory potency on caspase-9 when compared to the wild type peptide (**Figure 4-9B**). Nonetheless, these results confirm that the conserved motif at the N-terminus of F1L is crucial for caspase-9 inhibition.

Our data show that the N-terminal region of F1L is sufficient for the interaction and inhibition of caspase-9. Notably, we show by coimmunoprecipitation assays that F1L(1-36) can not bind to caspase-9(C287A), of which its catalytic cysteine has been mutated to alanine. In contrast, F1L(1-36) is able to interact with other active variants of caspase-9 (Wild Type, 5A, Dimer) (**Figure 4-2A**). These results suggest that the binding site of the conserved N-terminal motif of F1L is proximal to the active site of caspase-9. Interestingly, the C-terminal Bcl-2-like domain of F1L (F1LΔN) alone can interact with all the unprocessed forms of caspase-9 (C287A, 5A, F404D), and possibly also the dimeric form of the caspase (Dimer) (**Figure 4-2**). However, a single point mutation within the N-terminal motif of F1L disrupted the interaction and inhibition of caspase-9. Therefore, we hypothesized that the N-terminal motif of F1L binds and blocks the active site of caspase-9, while there is a second supplementary binding site of caspase-9 in the C-terminal domain of F1L that stabilizes this interaction. To verify this hypothesis, we

examined the ability of various F1L fragments (F1LΔTM, F1LΔN34ΔTM, F1L(1-15)) to suppress different caspase-9 mutants (Wild Type, 5A, Dimer) (**Figure 4-4**). As expected, both F1LΔTM protein and F1L(1-15) peptide inhibited all the caspase-9 mutants we tested in a dose-dependent manner, giving comparable $K_{i,app.}$ values in low micromolar range (**Figure 4-4D**). Importantly, F1L(1-15) was able to suppress the activity of caspase-9(Dimer), which is constitutively active regardless the presence of apoptosome (**Figure 4-4C & D**). Thus, it is evident that the peptide targets and blocks the active site of caspase-9 directly. Surprisingly, the C-terminal domain of F1L (F1LΔN34ΔTM) could also inhibit caspase-9 in a dose-dependent manner, although the potency is 10-15 times lower than that of F1LΔTM and F1L(1-15) (**Figure 4-4**). Nonetheless, this inhibition is not due to nonspecific protein aggregation because another Bcl-2-like protein from vaccinia virus, N1L, had no inhibitory effect across the range of concentrations we examined (**Figure 4-4**). Given that the C-terminal domain of F1L can interact with caspase-9(Dimer) mutant (**Figure 4-2A**), the C-terminal domain may also bind to activated caspase-9 and stabilize the binding of the N-terminal motif of F1L to the active site of caspase-9. Taken together, these results imply that the N-terminal motif of F1L is the major site for caspase-9 interaction and inhibition, while the C-terminal domain of F1L is the supplementary site that might stabilize the F1L/caspase-9 complex.

Since the C-terminal Bcl-2-like domain of F1L can bind to the monomeric mutant of caspase-9 (F404D), and also the dimeric mutant (Dimer) (**Figure 4-2**), the mechanism of the interaction between this domain and caspase-9 remains elusive. It is possible that the F1L C-terminal domain interacts with monomeric caspase-9 and prevents the caspase to dimerize, or forms aggregates with caspase-9. Since the C-terminal domain of F1L can

also interact with caspase-9(Dimer) mutant (**Figure 4-2A**), the C-terminal domain may also bind to activated caspase-9 and stabilize the binding of the N-terminal motif of F1L to the active site of caspase-9.
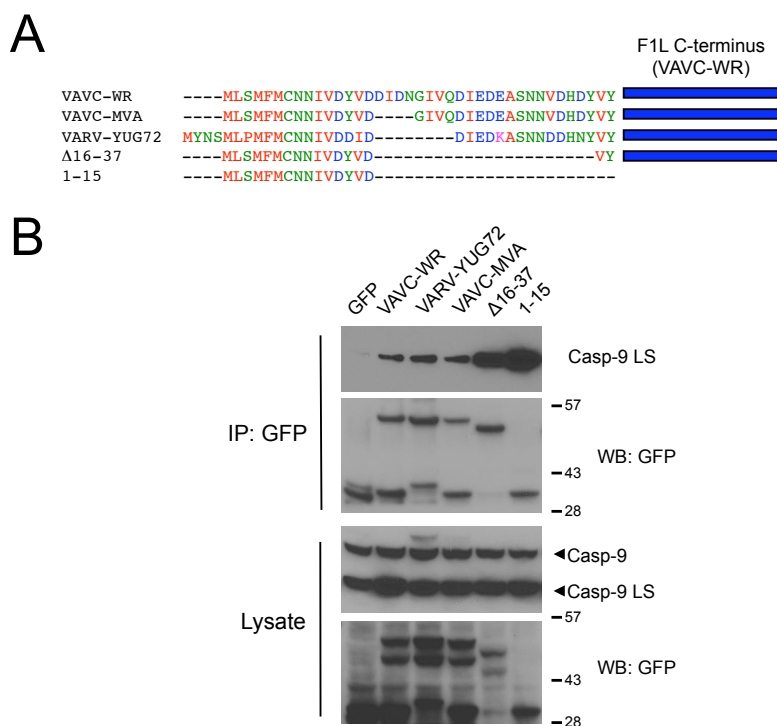
Figure 4-3. N-terminal peptide of F1L is sufficient to bind caspase-9. (A) A schematic picture showing the F1L sequences used in the coimmunoprecipation assays presented in (B). Corresponding mutations were introduced in the F1L sequence of the VAVC-WR strain. The blue bars represent the C-terminus of VAVC-WR F1L (a.a. 40-226) sequence. **(B)** HEK29T cells were transfected with plasmids containing GFP or different GFP-F1L mutants, together with FLAG-Caspase-9, as indicated. After 17 hrs, cells were harvested and lysed using lysis buffer. Cell lysates were coimmunoprecipitated with anti-GFP. Immuno-complexes (IP) and cell lysates were analyzed by SDS-PAGE/immunoblotting with GFP or FLAG antibodies. "Casp-9" and "Casp-9 LS" represent full-length caspase-9 and large subunit of processed caspase-9, respectively.
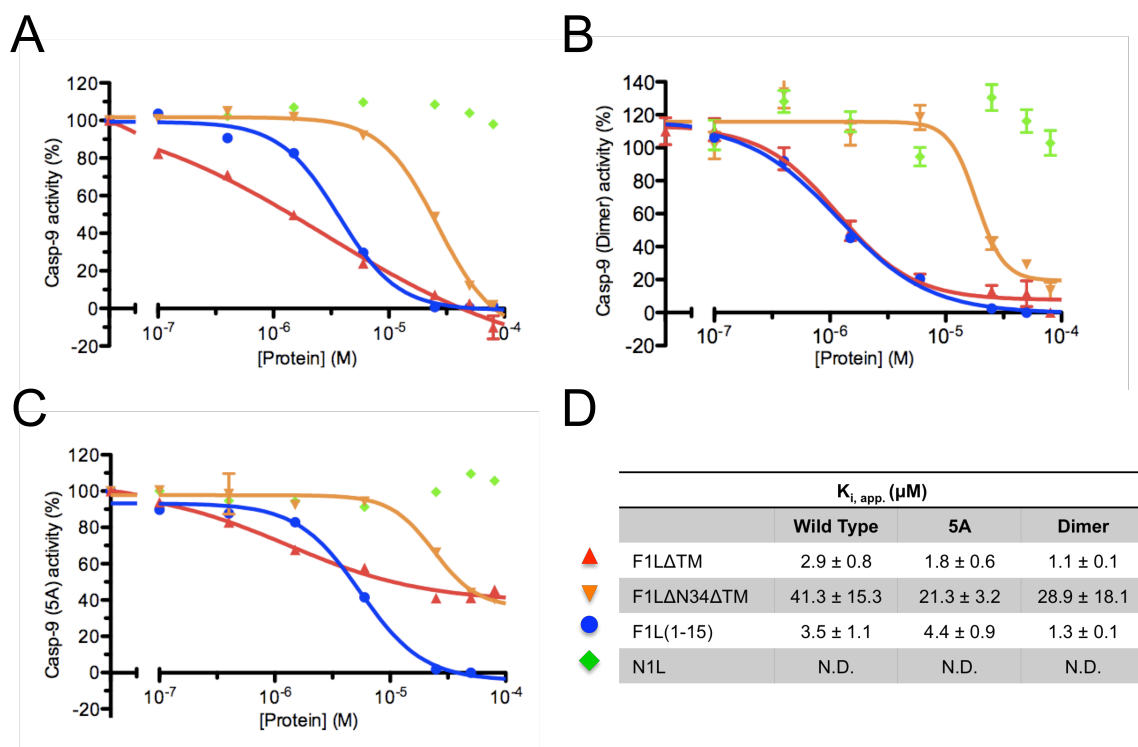
Figure 4-4. N-terminal peptide of F1L is sufficient to directly inhibit caspase-9. (A-C) A series of concentrations of different F1L proteins (F1LΔTM, F1LΔN34ΔTM, F1L(1-15)) or N1L were mixed with pro-caspase-9 (A), pro-caspase-9 (5A) (B) or active caspase-9 (Dimer) (C). Pro-caspase-9 and pro-caspase-9 (5A) were activated by addition of cytochrome c, dATP and recombinant full-length Apaf-1 (1 µM), and incubated at 37°C for 10 min. Caspase 9 activity was measured by hydrolysis of Ac-LEHD-AFC. The values measured were normalized by assigning the activities of pro-caspase-9 or pro-caspase-9 (5A) as 0%, while that of activated caspases by apoptosome as 100% (A & B). Since caspase-9 (Dimer) is constitutively active, the activity of caspase-9 (Dimer) alone was assigned as 100%, while caspase-9 (Dimer) with 50 µM F1LΔTM as 0% (C). The calculated percentage values are presented as mean ± S.D (n = 3). **(D)** Summary of apparent inhibition constants ($K_{i, app.}$) of different proteins tested on inhibition of various caspase-9 mutants in (A-C) by curving fitting with dose-respond equation. $K_{i, app.}$ values are mean ± S.D. derived from three independent experiments.

Molecular model of caspase-9 in complex with F1L peptide

To gain insights of the mechanism of caspase-9 inhibition mediated by the F1L N-terminal motif, we generated a docking model with online protein docking servers (see Experimental Procedures). Since the results of coimmunoprecipitation and caspase-9 activity assays show that the first 12 amino acids at the N-terminus of F1L are crucial for caspase-9 inhibition, we used F1L(1-12) peptide and wild type caspase-9 structure (PDB 1JXQ) for docking studies. As exemplified in **Figure 4-5**, the top hits of the docking models fit the F1L peptide to the active site of caspse-9 in reverse orientation compared to substrate binding. Consistent to our mutagenesis studies (**Figure 4-8**), the docking model shows that the interaction between caspase-9 and the F1L peptide is mainly mediated by hydrophobic interactions (**Figure 4-5**). Interestingly, reversal of relative orientation of the F1L peptide bound to caspase-9 resembles the mechanism of caspase-3/-7 inhibition by XIAP, a renowned mammalian inhibitor of caspases [20, 21].
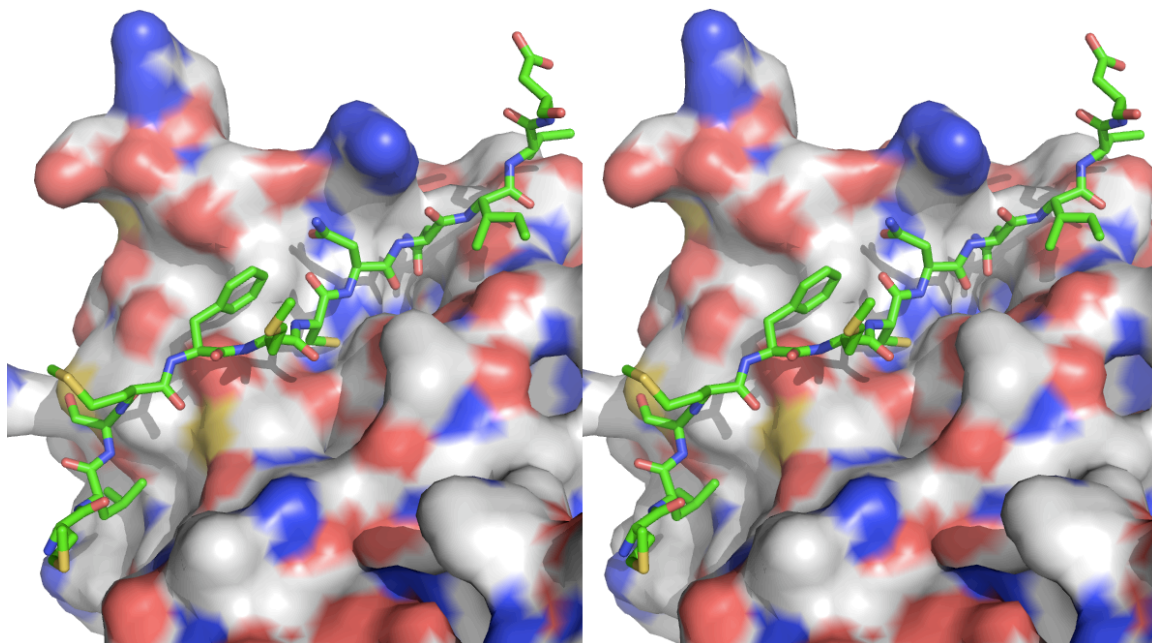
Figure 4-5. Molecular model of caspase-9 bound to F1L peptide. A docking model calculated by protein docking servers. The F1L peptide is docked into the substrate-binding site of caspase-9 in a relatively reverse orientation when compared to substrate binding. The caspase-9 is in surface representation, while the F1L peptide is in green sticks.

```
VAVC-WR        ----MLSMFMCNNIVDYVD--------------------DIDNGIVQDIEDEASNNVDH 35
VAVC-MVA       ----MLSMFMCNNIVDYVD------------------------GIVQDIEDEASNNVDH 31
VAVR-YUG72     MYNSMLPMFMCNNIVDDID----------------------------DIEDKASNNDDH 31
CPXV-BR        MDNSMLSMFMYNNIVDYVDDDVDDGIDNGIVPDIDNGIVPDIDNGIVPDIEDEASDNDDH 60
MPXV-USA       ----MLSMFMYNNIIDYVH--------------------------VHDIDDEASDNDDR 29
                   **.*** ***:* :.                        **:*:**:* *:


VAVC-WR        DYVYPLPENMVYRFDKSTNILDYLSTERDHVMMAVRYYMSKQRLDDLYRQLPTKTRSYID 95
VAVC-MVA       DYVYPLPENMVYRFDKSTNILDYLSTERDHVMMAVRYYMSKQRLDDLYRQLPTKTRSYID 91
VAVR-YUG72     NYVYPLPENMVYRFNKSTNILDYLSTERDHVMMAVQYYMSKQRLDDLYRQLPTKTRSYID 91
CPXV-BR        NYVYPLPENMVYRFDKSTNILDYLSTERDHVMMAVQYYMSKQRLDDLYRQLPTKTRSYID 120
MPXV-USA       DYVYPLPENMVYRFDKSTNILDYLSTERDHVMMAVQYYMSKQRLDDLYRQLPTKTRSYVD 89
                :************:********************:********************:*


VAVC-WR        IINIYCDKVSNDYNRDMNIMYDMASTKSFTVYDINNEVNTILMDNKGLGVRLATISFITE 155
VAVC-MVA       IINIYCDKVSNDYNRDMNIMYDMASTKSFTVYDINNEVNTILMDNKGLGVRLATISFITE 151
VAVR-YUG72     IINMYCDKVNNDYNRDMNIMYDMASTESFTVYDINNEVNTILMDNKGLGVRLATISFITE 151
CPXV-BR        IINMYCDKVNNDYNRDMNIMYDMASTESFTVYDINNEVNTILIDNKGLGVRLATISFITE 180
MPXV-USA       IINTYCDKVNNDYNSDMNIMCDMASTESFTVYDINNEVNTILMNNKGLGVRLATISFITE 149
               *** *****.**** ***** *****:***************::***************


VAVC-WR        LGRRCMNPVETIKMFTLLSHTICDDYFVDYITDISPP-DNTIPNTSTREYLKLIGITAIM 214
VAVC-MVA       LGRRCMNPVKTIKMFTLLSHTICDDCFVDYITDISPP-DNTIPNTSTREYLKLIGITAIM 210
VAVR-YUG72     LGKRCMNPVETIKMFTLLSHTICDDCFIDYITDISPP-DNTIPNISTREYLKLIGITAIM 210
CPXV-BR        LGRRCMNPVETIKMFTLLSHTICDDCFVDYITDISPP-DNTIPNTSTREYLKLIGITAIM 239
MPXV-USA       LGRRCMNPVETIKMFTLLSHTICDDYFVDYITYISAPRDNAIH--STREYLKIMGIAVIM 207
               **:******:************** *:**** **.* **:*   *******::**:.**


VAVC-WR        FATYKTLKYMIG 226
VAVC-MVA       FATYKTLKYMIG 222
VAVR-YUG72     FATYKTLKYMIG 222
CPXV-BR        FATYKTLKYMIG 251
MPXV-USA       FATYKTLKYMIG 219
               ************
```

Figure 4-6. Sequence alignment of F1L. Alignment of F1L sequences from vaccinia virus strains Western Reserve (VAVC-WR) and modified vaccinia Ankara (VAVC-MVA), variola virus strain Yugoslavia 1972 V72-164 (VARV-YUG72), cowpox virus strain Brighton Red (CPXV-BR), and monkeypox virus strain USA_2003_039 (MPXV-USA). Note that F1L from VAVC-WR was used for all the experiments in this study.

Figure 4-7. Identification of a N-terminal peptide of F1L that is sufficient to inhibit caspase-9. (A) A schematic picture showing the peptides used in caspase-9 activity assays presented in (B). **(B)** A series of concentrations of different F1L N-terminal peptides were mixed with pro-caspase-9 (200 nM) in HEPES buffer, followed by addition of cytochrome c, dATP and recombinant full-length Apaf-1 (1 μM), and incubated at 37°C for 10 min. Caspase 9 activity was measured by hydrolysis of Ac-LEHD-AFC (mean ± S.D.; n = 3). F1L(1-47) peptide was purified from bacterial cultures, while other peptides were chemically synthesized. All the methionines on F1L(1-25) sequence are replaced by norleucines on F1L(1-25)_Nle.
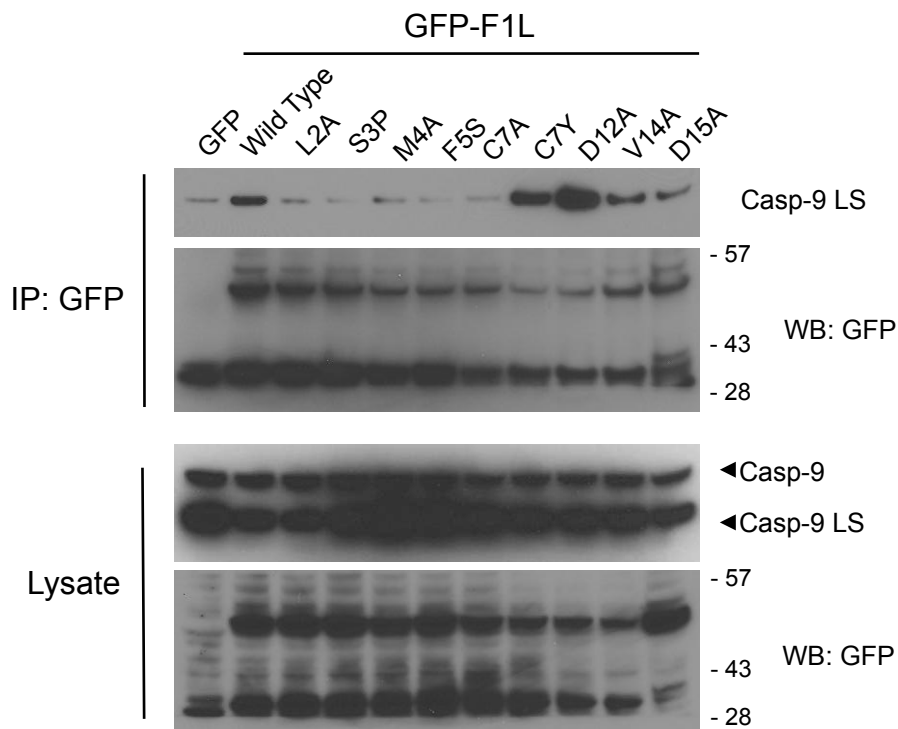
Figure 4-8. Identification of point mutations on F1L that affect its interaction with caspase-9. HEK29T cells were transfected with plasmids containing GFP or different GFP-F1L mutants, together with FLAG-Caspase-9, as indicated. After 17 hrs, cells were harvested and lysed using lysis buffer. Cell lysates were coimmunoprecipitated with anti-GFP. Immuno-complexes (IP) and cell lysates were analyzed by SDS-PAGE/immunobloting with GFP or FLAG antibodies. "Casp-9" and "Casp-9 LS" represent full-length caspase-9 and large subunit of processed caspase-9, respectively.
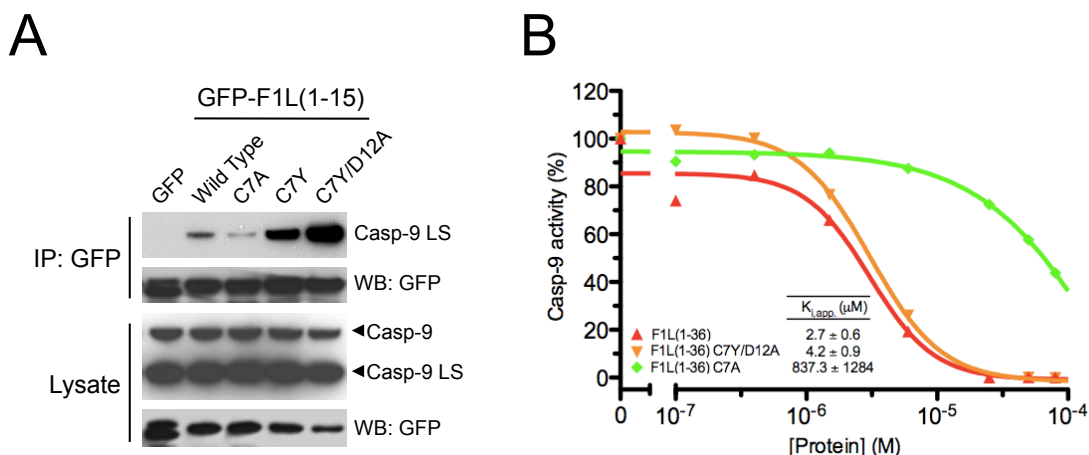
Figure 4-9. C7A mutation on F1L N-terminal peptide disrupts the interaction and inhibition of caspase-9. (A) HEK29T cells were transfected with plasmids containing GFP or different GFP-F1L(1-15) mutants, together with FLAG-Caspase-9, as indicated. After 17 hrs, cells were harvested and lysed using lysis buffer. Cell lysates were coimmunoprecipitated with anti-GFP. Immuno-complexes (IP) and cell lysates were analyzed by SDS-PAGE/immunoblotting with GFP or FLAG antibodies. "Casp-9" and "Casp-9 LS" represent full-length caspase-9 and large subunit of processed caspase-9, respectively. **(B)** A series of concentrations of different F1L(1-36) peptides (Wild Type, C7A or C7Y/D12A) were mixed with pro-caspase-9 in HEPES buffer, followed by addition of cytochrome c, dATP and recombinant full-length Apaf-1 (1 µM), and incubated at 37°C for 10 min. Caspase-9 activity was measured by hydrolysis of Ac-LEHD-AFC (mean ± S.D.; n = 3).

```
XIAP 138   —DYLLRTGQVVDISD   151
F1L    1   MLSMFMCNNIVDYVD    15
```

Figure 4-10. Sequence alignment of caspase-3/-7-binding motif of human XIAP and caspase-9-binding motif of F1L (Vaccinia virus strain Western Reserved).

Discussion

Viruses are intracellular parasites that require host cell's resources to replicate. Although the molecular pathways remain unclear, there are multiple mechanisms that induce apoptosis in infected cells as an immune response against viral infection. Therefore, viruses have evolved a variety of strategies to subvert host cell apoptosis in order to replicate effectively in the host [1-4, 22]. The vaccinia virus-encoded protein, F1L, is functionally related to cellular Bcl-2 proteins, which inhibits apoptosis during infection by interacting with pro-apoptotic proteins, such as Bak and Bim [13-16]. Previously, we showed that F1L binds to and selectively inhibits caspase-9, the apical caspase in the mitochondrial cell death pathway. Although we demonstrated that the N-terminal region of F1L preceding the Bcl-2-like domain might be responsible for caspase-9 inhibition, the underlying mechanism of this inhibition is still elusive.

F1L does not retain significant sequence homology to any other Bcl-2 family proteins except to its immediate orthologues in related poxviruses. The C-terminal region (amino acid 55-226) of F1L resembles a Bcl-2-like fold with an unusual N-terminal extension (amino acid 1-54) that is not required for interaction with Bak [16, 23]. Here we show that this unusual N-terminal extension of F1L is necessary for the interaction and inhibition of caspase-9 (**Figure 4-1**). Based on the remarkably high sequence identity of the N-terminal motif among the orthologues of F1L, we further illustrate that the N-terminal 15-amino acid-long motif is sufficient for caspase-9 interaction and inhibition (**Figure 4-3B & 4-4**). Presumably, F1L possess two functional domains: (i) A Bcl-2-like domain that interacts with pro-apoptotic Bcl-2 family proteins to prevent cytochrome c

release. (ii) A novel N-terminal motif preceding the Bcl-2-like domain that acts downstream of cytochrome c release through its inhibition to caspase-9.

Although the N-terminal motif of F1L is required for the interaction with processed wild type caspase-9, our data suggest that the Bcl-2-like domain alone can bind to those mutants that are not processed (C287A, 5A, F404D), and possibly to the dimeric mutant (Dimer) (**Figure 4-1C & 4-2**). Therefore, F1L might have a second caspase-9 binding site in the Bcl-2-like domain. We have previously demonstrated by gel filtration chromatography that F1L forms large complex (>200 kDa) with both unprocessed pro-caspase-9 and activated caspase-9. Here we show that the Bcl-2-like domain of F1L can interact with the monomeric mutant, F404D, and also the dimeric mutant, Dimer (**Figure 4-2**). Although the underlying mechanism is still not clear, these results implicate that F1L prevents activation of pro-caspase-9, and also inhibits active caspase-9 by forming a large complex with the protease. Indeed, the Bcl-2-like domain of F1L (F1LΔN34ΔTM) alone was able to suppress caspase-9 at high concentrations (> 20 μM) (**Figure 4-4**). This inhibition is not due to non-specific protein aggregation because another vaccinia virus-encoded, Bcl-2-like protein, N1L had no effect on caspase-9 activity across the range of concentrations tested (**Figure 4-4**). Although the significance of the interaction of caspse-9 mediated by the Bcl-2-like domain of F1L is not known, it is possible that this caspase-9 binding site might be supplementary to the N-terminal motif of F1L, and further stabilize the interaction between the two proteins. In addition, this bulky Bcl-2-like domain might also interfere with the recruitment of pro-caspase-9 to Apaf-1 as we previously showed. Interestingly, F1L with its putative BH4 domain deleted (F1LΔN75) could still bind caspase-9(C287A), but not Bak, suggesting different binding mechanisms

between these two interactions (**Figure 4-1C**). Additionally, we found that the binding of caspase-9(C287A) and Bak to F1L is mutually exclusive since more caspase-9(C287A) bound to those F1L mutants that can not bind Bak (F1LΔN59 and F1LΔN75), when compared to wild type F1L (**Figure 4-1C**).

Our data show that the peptide derived from the N-terminal motif of F1L was able to inhibit constitutively active caspase-9(Dimer) with potency similar to that of wild type caspase-9 and caspase-9(5A) that are activated by apoptosome, indicating this inhibition is independent of the presence of the apoptosome (**Figure 4-4**). Further, the N-terminal motif binds only to processed caspase-9, but not to the mutants that cannot be active (**Figure 4-2A**). It is evident that the N-terminal motif of F1L binds to a proximal site to the active site of caspase-9. However, contrary to other suicide substrate inhibitors, including CrmA and p35 [24-27], F1L is not cleaved by caspase-9. Consistent to our data, the docking model of caspase-9 with the F1L N-terminal peptide suggests that this interaction may resemble the inhibition of caspase-3/-7 by the mammalian caspase inhibitor, XIAP (**Figure 4-5**) [20, 21]. In the case of XIAP-mediated caspase-3/-7 inhibition, the 18-residue linker between the BIR1 and BIR2 domains of XIAP docks into the substrate binding site of caspase-3/-7 in reserve orientation, and thus sterically blocks the activities of the protease [20, 21]. Intriguingly, our docking model shows that the F1L N-terminal motif may binds to the substrate-binding site of caspase-9 through hydrophobic interactions in a similar manner (**Figure 4-5**). The highly conserved N-terminal motif does not share homology to any known protein nor caspase-9 substrate, implicating a unique binding mechanism. Interestingly, this conserved motif shares some homology with the caspase-3/-7 binding region of XIAP (**Figure 4-10**). Mutagenesis

studies of the F1L N-terminal motif revealed that L2A, S3P, M4A, F5S and C7A mutations dramatically reduced the binding of F1L to caspase-9, confirming the importance of these residues on the interaction (**Figure 4-8**). It is interesting to note that all the variola virus orthologues possess a proline, instead of serine, at the third position of the F1L sequence used in this study, while having extra four amino acids at their N-termini (Met-Tyr-Asn-Ser). Although S3P mutation disrupts the interaction of F1L with caspase-9, the presence of the extra N-terminal sequence, Met-Try-Asn-Ser, can somehow rescue this interaction (**Figure 4-3**). Moreover, we found that the C7Y and D12A mutations do not affect the interaction and inhibition of caspase-9 mediated by F1L, when compared to wild type F1L (**Figure 4-8 & 4-9**). Notably, the F1L sequences of all monkeypox and certain cowpox strains have the same cysteine to tyrosine variation at the seventh position (C7Y). Therefore, it is probable that all the orthologues of F1L are able to bind and inhibit caspase-9.

The N-terminal extension region of F1L is highly variable in sequence and length. However, the N-terminal motif of F1L that is responsible for caspase-9 inhibition is extremely conserved among all the F1L orthologues in related poxviruses. This implies the importance of caspase-9 inhibition. In addition, we have shown that C7A mutation, which specifically abolishes the interaction of F1L with caspase-9, reduced the ability of F1L to protect cells from apoptosis induced by staurosporine, thus it would be insightful to study the role of this inhibition during infection. In conclusion, F1L inhibits apoptosis by suppressing pro-apoptotic Bcl-2 family proteins and caspase-9, which involve in two sequential steps in the mitochondrial cell death pathway. Intriguingly, caspase-9 has also been implicated in apoptosome-independent lysosomal cell death pathway induced by

tumor necrosis factor (TNF), indicating a complex network of the cell death pathways [28, 29]. Although the significance of this apoptosome-independent cell death pathway during infection is not known, inhibition of caspase-9 mediated by F1L might play a role in this pathway.

Experimental procedures

Materials

HEK 293T cells were obtained from the ATCC. Cytochrome c (from bovine heart), dATP and Anti-FLAG M2-Peroxidase *(*HRP*)* antibody were purchased from Sigma-Aldrich Co. (St. Louis, MO). Rabbit monoclonal anti-caspase-9 (clone E23) was purchased from Abcam Inc. (Cambridge, MA). Mouse anti-GST was purchased from BD Pharmingen (San Diego, CA). Dynabeads Protein G, anti-Bak, mouse monoclonal (clone 3E6) and rabbit polyclonal anti-GFP were obtained from Invitrogen (San Diego, CA). The caspase peptidyl substrate, Ac-LEDH-AFC was purchased from BIOMOL. Glutathione Sepharose 4B resin was obtained from GE Healthcare Biosciences.

Plasmids

The gene encoding F1L (full-length, residues 1-226), F1LΔN34, F1L(1-36) and F1L(1-15) from vaccinia virus strain Western Reserve were subcloned into pEGFP-C1 (BD Biosciences Clontech) for mammalian cell expression. F1LΔN44-pGFP, F1LΔN59-pGFP and F1LΔN75-pGFP were generous gifts from Dr. Michael Way (Cancer Research UK London Research Institute). F1LΔTM (without the C-terminal transmembrane motif,

residues 1-206), F1LΔN23ΔTM, F1LΔN34ΔTM, F1LΔN47ΔTM, F1L(1-36) and F1L(1-47) were subcloned into pGEX-4T-1 (GE Healthcare Biosciences) for bacterial expression. F1L mutants L2A, S3P, M4A, F5A, C7A, C7Y, D12A, V14A and D15A, and F1L(1-15) or F1L(1-36) mutants C7A, C7Y and double mutant C7A/D12A were made by using the QuikChange site-directed mutagenesis kit (Stratagene). Plasmids encoding viral N1L, caspase-9, caspase-9(C287A), caspase-9(5A), caspase-9(F404D), caspase-9(Dimer) and human full-length Apaf-1 have been described [17-19, 30, 31]. Caspase-9(Dimer)-pET21b, received from Dr. Yigong Shi (Tsinghua University, Beijing, China), was used to generate caspase-9(Dimer)-pFLAG-CMV2.

Protein expression and purification

Caspase-9 and its mutant proteins were produced in bacteria as His_6-tagged proteins and purified using Ni-NTA resin (Qiagen) following the methods described by the manufacturer's instructions. GST-tagged F1LΔTM, F1LΔN23ΔTM, F1LΔN34ΔTM, F1LΔN47ΔTM, F1L(1-47) and F1L(1-36) were expressed in bacteria and affinity purified using Glutathione Sepharose (GE Healthcare Biosciences). For purification of F1LΔTM, F1LΔN34ΔTM, F1L(1-47) and F1L(1-36), GST tag was removed by on-column proteolytic cleavage by thrombin (Sigma Aldrich). F1LΔTM and F1LΔN34ΔTM were purified by gel filtration chromatography, while F1L(1-47) and F1L(1-36) were further purified by Amicon Ultra centrifugal filter units with 30 kDa-cut-off (Millipore). Full length His-tagged Apaf-1 protein was expressed in Sf9 insect cells at 27°C for 60 hrs and purified as described [30].

In vitro protein binding assays

Recombinant GST, GST-F1LΔTM or its truncated proteins (1 µg) were incubated with 1 µg of active caspase-9 at 25 °C for 15 min in PBS. 10 µl of Glutathione Sepharose resin (GE Healthcare Biosciences) was then added to the mixture. The GST protein-bound resin was washed 3 times using PBS buffer plus 20 mM imidazole and 0.1% Triton X-100, and all the associated proteins were boiled and analyzed by SDS-PAGE/immunoblotting using anti-caspase-9 or anti-GST antibodies.

Coimmunoprecipitation assays

12×10^6 HEK29T cells were transfected using Lipofectamine 2000 (Invitrogen) with plasmids containing GFP or different GFP-F1L mutants, together with FLAG-caspase-9 or its mutants, as indicated. After 17 hrs, cells were harvested and lysed using lysis buffer (20 mM HEPES pH 7.5, 150 mM NaCl, 5 mM MgCl2, 2 mM EDTA, 0.2% NP-40, 2 mM DTT and protease inhibitors (Roche)). Cell lysates were coimmunoprecipitated with Dynabeads Protein G (Invitrogen) using mouse monoclonal anti-GFP 3E6 (Invitrogen). Dynabeads were then washed 3 times with lysis buffer. Immuno-complexes (IP) and cell lysates were analyzed by SDS-PAGE/immunobloting with GFP or FLAG antibodies.

Caspase activity assays

Different F1LΔTM proteins, F1L N-terminal peptides or N1L were mixed with pro-caspase-9 (200 nM) in 20 mM HEPES buffer (pH 7.0), followed by addition of cytochrome c (1 µM), dATP (40 µM) and recombinant full-length Apaf-1 (1 µM), and incubated at 37°C for 10 min. Reaction was performed in 100 µL standard caspase assay

buffer (20 mM HEPES, pH 7.5, 2 mM MgCl$_2$, 10 mM KCl and 5 mM DTT) for 30 min at 37°C. Caspase 9 activity was measured by hydrolysis of the fluorogenic tetrapeptide substrate, Ac-LEHD-AFC (BIOMOL) at 100 μM.

Peptide synthesis and purification

F1L peptides were synthesized and purified essentially as described previously [32]. Peptides were synthesized using Rink Amide ChemMatrix resin (Matrix Innovation) employing Fmoc synthesis and DIC/HOBt coupling with an Advanced ChemTech Apex 396 multiple peptide synthesizer. The peptides were acetylated on their N-termini and were amidated on their C-terminal. Peptides were cleaved from the resin using standard cleavage and deprotection conditions and purified by HPLC on a preparative C4 column (Higgins Proteo 300 5μm, 250 x 20mm) eluting at 8 mL/min with a 50-80% linear gradient for 40 min. Purified peptides were all single peaks (>99% purity) by analytical HPLC and their mass was confirmed by MALDI mass-spectroscopy.

Protein docking

Crystal structure of dimeric mutant of caspase-9 without CARD, caspase-9(Dimer)ΔCARD, was used as a model for docking of F1L(1-12) peptide. GRAMM-X and ZDOCK protein-protein docking servers were used for calculations [33, 34]. Both of these servers generated similar results. One of the top hits from these calculations was selected and refined with Refmac.

Acknowledgement

We thank Christina Pop and Mika Aoyagi for providing reagents, Prof. Yigong Shi for the dimeric caspase-9 mutant construct.

Chapter 4, in part, is a manuscript prepared for publication titled "Identification of a novel motif of vaccinia virus Bcl-2-like F1L that is sufficient for caspase-9 inhibition", by Eric Chi-Wang Yu, Dayong Zhai, Naran Gombosuren, Yinong Zong, Ge Wei, Arnold Satterthwait, John C. Reed Robert C. Liddington. The dissertation author was the primary investigators and authors of this paper. The dissertation author conceived the project, designed and performed experiments, analyzed data, and wrote the initial draft of the manuscript.

References

1.   Benedict, C.A., P.S. Norris, and C.F. Ware, *To kill or be killed: viral evasion of apoptosis.* Nat Immunol, 2002. **3**(11): p. 1013-8.

2.   Cuconati, A. and E. White, *Viral homologs of BCL-2: role of apoptosis in the regulation of virus infection.* Genes Dev, 2002. **16**(19): p. 2465-78.

3.   Galluzzi, L., et al., *Viral control of mitochondrial apoptosis.* PLoS Pathog, 2008. **4**(5): p. e1000018.

4.   Postigo, A. and P.E. Ferrer, *Viral inhibitors reveal overlapping themes in regulation of cell death and innate immunity.* Microbes Infect, 2009. **11**(13): p. 1071-8.

5.   Creagh, E.M., H. Conroy, and S.J. Martin, *Caspase-activation pathways in apoptosis and immunity.* Immunol Rev, 2003. **193**: p. 10-21.

6.   Liu, X., et al., *Induction of apoptotic program in cell-free extracts: requirement for dATP and cytochrome c.* Cell, 1996. **86**(1): p. 147-57.

7. Zou, H., et al., *Apaf-1, a human protein homologous to C. elegans CED-4, participates in cytochrome c-dependent activation of caspase-3.* Cell, 1997. **90**(3): p. 405-13.

8. Li, P., et al., *Cytochrome c and dATP-dependent formation of Apaf-1/caspase-9 complex initiates an apoptotic protease cascade.* Cell, 1997. **91**(4): p. 479-89.

9. Du, C., et al., *Smac, a mitochondrial protein that promotes cytochrome c-dependent caspase activation by eliminating IAP inhibition.* Cell, 2000. **102**(1): p. 33-42.

10. Verhagen, A.M., et al., *Identification of DIABLO, a mammalian protein that promotes apoptosis by binding to and antagonizing IAP proteins.* Cell, 2000. **102**(1): p. 43-53.

11. Youle, R.J. and A. Strasser, *The BCL-2 protein family: opposing activities that mediate cell death.* Nat Rev Mol Cell Biol, 2008. **9**(1): p. 47-59.

12. Kroemer, G., L. Galluzzi, and C. Brenner, *Mitochondrial membrane permeabilization in cell death.* Physiol Rev, 2007. **87**(1): p. 99-163.

13. Wasilenko, S.T., et al., *The vaccinia virus F1L protein interacts with the proapoptotic protein Bak and inhibits Bak activation.* J Virol, 2005. **79**(22): p. 14031-43.

14. Taylor, J.M., et al., *The vaccinia virus protein F1L interacts with Bim and inhibits activation of the pro-apoptotic protein Bax.* J Biol Chem, 2006. **281**(51): p. 39728-39.

15. Campbell, S., et al., *Vaccinia virus F1L interacts with Bak using highly divergent BCL-2 homology domains and replaces the function of Mcl-1.* J Biol Chem, 2009.

16. Postigo, A., et al., *Interaction of F1L with the BH3 domain of Bak is responsible for inhibiting vaccinia-induced apoptosis.* Cell Death Differ, 2006. **13**(10): p. 1651-62.

17. Renatus, M., et al., *Dimer formation drives the activation of the cell death protease caspase 9.* Proc Natl Acad Sci U S A, 2001. **98**(25): p. 14250-5.

18. Shiozaki, E.N., et al., *Mechanism of XIAP-mediated inhibition of caspase-9.* Mol Cell, 2003. **11**(2): p. 519-27.

19. Chao, Y., et al., *Engineering a dimeric caspase-9: a re-evaluation of the induced proximity model for caspase activation.* PLoS Biol, 2005. **3**(6): p. e183.

20. Riedl, S.J., et al., *Structural basis for the inhibition of caspase-3 by XIAP.* Cell, 2001. **104**(5): p. 791-800.

21. Chai, J., et al., *Structural basis of caspase-7 inhibition by XIAP.* Cell, 2001. **104**(5): p. 769-80.

22. Best, S.M., *Viral subversion of apoptotic enzymes: escape from death row.* Annu Rev Microbiol, 2008. **62**: p. 171-92.

23. Kvansakul, M., et al., *Vaccinia virus anti-apoptotic F1L is a novel Bcl-2-like domain-swapped dimer that binds a highly selective subset of BH3-containing death ligands.* Cell Death Differ, 2008. **15**(10): p. 1564-71.

24. Komiyama, T., et al., *Inhibition of interleukin-1 beta converting enzyme by the cowpox virus serpin CrmA. An example of cross-class inhibition.* J Biol Chem, 1994. **269**(30): p. 19331-7.

25. dela Cruz, W.P., P.D. Friesen, and A.J. Fisher, *Crystal structure of baculovirus P35 reveals a novel conformational change in the reactive site loop after caspase cleavage.* J Biol Chem, 2001. **276**(35): p. 32933-9.

26. Fisher, A.J., et al., *Crystal structure of baculovirus P35: role of a novel reactive site loop in apoptotic caspase inhibition.* EMBO J, 1999. **18**(8): p. 2031-9.

27. Xu, G., et al., *Covalent inhibition revealed by the crystal structure of the caspase-8/p35 complex.* Nature, 2001. **410**(6827): p. 494-7.

28. Gyrd-Hansen, M., et al., *Apoptosome-independent activation of the lysosomal cell death pathway by caspase-9.* Mol Cell Biol, 2006. **26**(21): p. 7880-91.

29. McDonnell, M.A., et al., *Caspase-9 is activated in a cytochrome c-independent manner early during TNFalpha-induced apoptosis in murine cells.* Cell Death Differ, 2003. **10**(9): p. 1005-15.

30. Kim, H.E., et al., *Formation of apoptosome is initiated by cytochrome c-induced dATP hydrolysis and subsequent nucleotide exchange on Apaf-1.* Proc Natl Acad Sci U S A, 2005. **102**(49): p. 17545-50.

31. Pop, C., et al., *The apoptosome activates caspase-9 by dimerization.* Mol Cell, 2006. **22**(2): p. 269-75.

32. Faustin, B., et al., *Mechanism of Bcl-2 and Bcl-X(L) inhibition of NLRP1 inflammasome: loop domain-dependent suppression of ATP binding and oligomerization.* Proc Natl Acad Sci U S A, 2009. **106**(10): p. 3935-40.

33. Tovchigrechko, A. and I.A. Vakser, *GRAMM-X public web server for protein-protein docking.* Nucleic Acids Res, 2006. **34**(Web Server issue): p. W310-4.

34. Wiehe, K., et al., *The performance of ZDOCK and ZRANK in rounds 6-11 of CAPRI.* Proteins, 2007. **69**(4): p. 719-25.

Chapter 5

Vaccinia Virus F1L protein inhibits NLRP1 inflammasome activation and promotes virus virulence

Abstract

Host innate immune responses to double-stranded DNA (dsDNA) viruses involve members of the NOD-like Receptor (NOD) family, which collaborate with adaptor ASC to form "inflammasomes" that activate caspase-1, resulting in cleavage of pro-forms of cytokines Inerleukin-1b (IL-1b) and Interleukin-18 (IL-18). It seems likely therefore that viruses would target components of these inflammasomes in an attempt to overcome host defense mechanisms. Here we report that F1L, a Vaccinia virus (VACV) Bcl-2 homolog, is a NLRP1 inflammasome inhibitor, thus defining the first example of a viral protein that interferes with this class of innate immunity proteins. Mutant virus lacking the F1L gene (VACVΔF1L) was attenuated in its virulence in vivo, resulting in increase proteolytic processing of caspase-1 without affecting virus replication or apoptosis. Moreover, infection of macrophages in culture with VACVΔF1L caused increased caspase-1 activation and IL-1b secretion, compared to wild-type virus. Using an in vitro reconstituted system employing purified recombinant proteins, we showed that F1L functions similar to its cellular counterparts Bcl-2 and Bcl-XL to inhibit NLRP1. Furthermore, we identified a short peptidyl motif from F1L that is sufficient to inhibit the NLRP1 inflammasome in vitro, and which is required for F1L protein to bind and inhibit

NLRP1. These findings reveal a novel viral mechanism for evading the host innate immune response.

Introduction/Results/Discussion

The NOD-Like Receptors (NLRs) constitute a large family of intracellular innate immunity proteins involved in host defense [1]. Upon activation, several NLRs form large protein complexes called "inflammasomes" that bind and activate caspase-1 family proteases, resulting in proteolytic activation of pro-inflammatory cytokines (which include proIL-1β, proIL-18, and pro-IL-33) and sometime causing cell death by a variant of apoptosis known as pyroptosis [2, 3]. Members of the NLR family possess a conserved architecture that includes leucine-rich repeats (LRRs) that are thought to act as receptors for various pathogen-derived molecules. Recently, it was reported that NLRs are involved in detecting foreign double-stranded DNA (dsDNA) in cells, a function linked to host defense against DNA viruses [4-7].

The pox family viruses constitute a viridae known for their large complex dsDNA genomes. Vaccinia virus (VACV) is a prototypical member of the poxvirus family, which replicates in the cytoplasm of host cells and encodes numerous proteins that manipulate the host response to infection [8]. The viral protein F1L is a recognized homolog of mammalian anti-apoptotic protein Bcl-2 [9, 10]. Cellular Bcl-2 not only suppresses apoptosis, but it also was recently demonstrated to bind NLR family protein NLRP1 (NALP1) and to inhibit its ability to form inflammasome that stimulate caspase-1

activation and IL-1β production [11]. We therefore hypothesized that the viral Bcl-2 homolog, F1L, would similarly inhibit inflammasome activation during VACV infection.

To test this hypothesis, first, the role of F1L in virus virulence was explored. Intranasal (i.n.) administration of the VACV strain Western Reserve (WR) results in acute, productive infection of the lung. Deletion of the *F1L* gene (ΔF1L) from VACV-WR resulted in an attenuated phenotype, characterized by improved survival rates of infected mice and less severe body weight reductions without significantly impacting vivo replication (**Figure 5-1A-C & 5-5A, B**). Although Vaccina Virus-infected cells in culture were previously shown to be more sensitive to apoptosis when F1L is deleted from the viral genome [9, 12], we did not detect an increase in the percentage of apoptotic cells in the lungs of VAVCΔF1L -infected mice compared to animals infected with VAVC-WR (**Figure 5-6**). In this regard, the genome of Vaccina Virus encodes another Bcl-2 homolog, N1L, which may provide redundancy [13, 14], in addition, to other suppressors of apoptotic pathways [15].

Others have reported that intranasal administration of VACV-WR results in reduced body temperature due to the VACV gene *B15R*, which encodes the VACV IL-1b receptor − a neutralizer of IL-1b, endogenous pyrogen [16]. Interestingly, in our experiments, we observed reduced body temperatures in VACV-WR-infected mice while VACVΔF1L-infected mice showed only a slight reduction in body temperature (**Figure 5-1D & 5-5C**). This observation thus implies that mice infected with VACVΔF1L may produce more IL-1β, in excess of the neutralizing viral proteins. We therefore examined the status of caspase-1 processing in bronchial alveolar lavage (BAL) fluids recovered from the infected animals. The processed p10 subunit of caspase-1 was detected at

higher levels in BAL fluids from VACVΔF1L-infected mice compared to VACV-WR-infected mice at early stages of infection (**Figure 5-1E**).

To examine the inflammatory response to viral infection, we examined lung histology to determine the number of inflammatory foci at various times post-infection. Interestingly, an increase in inflammatory foci was present earlier in VACVΔF1L-infected mice. At day four post-infection, when little inflammatory infiltrate was found in mice infected with wild-type virus, mice infected with mutant virus already had impressive leukocyte infiltrate in lung. In contrast, VACV-WR-infected mice did not develop such lung leukocytosis until 6-8 days post-infection (**Figure 5-1F, 5-7**, and data not shown). Thus, the host inflammatory response to vaccine virus is accelerated in the absence of F1L.

Because the majority of cells in BAL fluids of the in vivo murine Vaccina Virus model are known to be activated macrophages [17], we used human macrophages generated by TPA-induced differentiation of the THP-1 monocytic cell line as an in vitro model for studying the effects of F1L deletion on caspase-1 and its physiological substrate pro-IL-1β in culture. As a control, THP-1 macrophages were also stimulated with the peptidoglycan component, muramyl-dipeptide (MDP) plus ATP, which is known to active certain caspase-1-activating NLR family proteins [11, 18, 19]. The efficiency of THP-1 cell infection was not different for VACV-WR and VACVΔF1L viruses, as monitored by expression of the E3L viral antigen (**Figure 5-8**). Analysis of THP-1 macrophages infected with wild-type versus ΔF1L viruses revealed the presence of F1L protein in the former but not the latter, whereas both expressed viral N1L at comparable levels (**Figure 5-2A**). Infection of THP-1 macrophages with VACVΔF1L resulted in

greater proteolytic processing of caspase-1 compared to infection with wild-type virus, as measured in both the intracellular compartment (where levels of the p35 processed subunit of pro-caspase-1 were clearly higher in ΔF1L virus compared to wild-type virus-infected cells [*p20 and p10 were difficult to discern in cell extracts*]) and the secreted compartment (where levels of both the p20 and p10 processed forms of mature caspase-1 were clearly higher in ΔF1L virus- compared to wild-type virus-infected cells) (**Figure 5-2B**), thus agreeing with the aforementioned in vivo findings. Furthermore, the mature, proteolytic processed form of IL-1b was detected in VACVΔF1L-infected but not VACV-WR-infected cells (**Figure 5-2C**).

In addition to processing of pro-caspase-1 and pro-IL-1β, we also measured caspase-1 activity and IL-1β secretion using THP-1 macrophages. Because the gene encoding proIL-1β is NF-κB-inducible, we employed THP-1-Blue cells containing a stably integrated NF-kB-driven secreted embryonic alkaline phosphatase (SEAP) reporter gene to simultaneously compare NF-κB activity in cells infected with wild-type, ΔF1L, or ΔN1L viruses. Measurement of VACV infection revealed no differences in viral infection due to deletion of either the *F1L* or *N1L* genes (**Figure 5-8**). When THP-1-Blue macrophages were infected with wild-type, ΔF1L, or ΔN1L viruses at 1 PFU/cell, approximately 2-fold higher levels of caspase-1 activity and IL-1b secretion were observed in VACVΔF1L-infected cultures compared to either VACV-WR- or VACVΔN1L (**Figure 5-2D, E**). In contrast, levels of NF-κB activity (**Figure 5-2F**) or IL-8 (data not shown) were not different among these various virus-infected cells. Note that the levels of caspase-1 activity and IL-1β secretion observed in ΔF1L virus-infected

cells were similar to MDP stimulation, thus providing a comparison with a known NLR activator.

Resting macrophage/monocytic cells are only minimally responsive to NLR ligands because they must first be induced to express some inflammasome components and pro-IL-1β. We therefore repeated these studies where THP-1 macrophages were primed with lipopolysaccaride (LPS) prior to VACV infection. Rational for this experimental approach is provided by reports of secondary bacterial pneumonia in the setting of viral lung infection [20-22]. THP-1 cells primed with LPS and infected with VACVΔF1L secreted strikingly higher amounts of IL-1b compared to cells infected with VACV-WR (**Figure 5-2G & 5-9**). Similar results were obtained using primary cultured peripheral blood mononuclear cells (PBMCs) primed with LPS (**Figure 5-10**). Thus, in the absence of F1L, vaccinia virus-infected cells secrete more IL-1β.

These results led us to speculate that F1L may act in a similar manner to cellular Bcl-2 and Bcl-XL to inhibit caspase-1 activation by inflammasomes. To test this possibility, we explored the ability of F1L to bind NLRP1, a NLR member inhibited by Bcl-2 and Bcl-XL [19]. As determined by co-immunoprecipitation assays, F1L, but not N1L, associated with NLRP1 (**Figure 5-3A**). In contrast, the NF-κB-activating NLR family member NOD2 (NLRC2) did not bind F1L. The interaction of F1L with NLRP1 was further confirmed by in vitro protein binding assays, using the GST pull-down method employing GST-tagged recombinant proteins. F1L bound to full-length GST-NLRP1 but not a deletion mutant lacking the LRRs (**Figure 5-3B**), binding characteristics similar to Bcl-2 and Bcl-XL [11, 23]. F1L binding was specific, as determined by comparisons with GST-control proteins.

Cellular and viral Bcl-2 family proteins are comprised of a minimum of 7 alpha-helices with connecting loops organized into a Colecin-like fold [24]. We previously demonstrated that an unstructured loop between the first and second alpha-helices of Bcl-2 is necessary and sufficient for binding to NLRP1 [19, 23]. The 3D structure of F1L together with computational modeling suggests an analogous loop at residues 30 to 42 [10]. To explore the regions within F1L required for NLRP1 binding, we first tested the binding of a N-terminal truncation mutant of F1L lacking its first 44 amino-acids, (D1-44), which encompasses the aforementioned loop. As a control, we also tested a mutant F1L protein lacking residues 57-78, which overlaps a segment constituting a BH3 like-domain (residues 64-84) that has been shown to be required for interactions with pro-apoptotic protein Bak [9]. As determined by co-immunoprecipitation assays, F1LΔ1-44 lost the ability to bind NLRP1 whereas F1LΔ57-78 did not (**Figure 5-3C & 5-11**). To determine the relevance of residues 1-44 of F1L in a cellular context, we compared the activity of full-length F1L with F1L mutants by cell transfection experiments where inflammasome components are expressed (NLRP1, ASC, pro-caspase-1, and mouse proIL-1β) and mIL-1β secretion is measured after NLRP1 stimulation with MDP, as described previously for Bcl-2 and Bcl-XL [11]. In this cellular assay, F1L and F1LΔ57-78 inhibited MDP-induced mIL-1b secretion, while F1LΔ1-44 did not (**Figure 5-3D**). As controls, Bcl-XL (binds NLRP1) and Bcl-B (does not bind NLRP1) were also compared, with the former but not the latter suppressing IL-1β production.

Next we examined the NLRP1-suppressing activity of F1L using an in vitro reconstituted system. In this regard, previously we reconstituted the NLRP1 inflammasome in vitro using recombinant proteins, showing that the combination of

MDP and ATP induces NLRP1 oligomerization and caspase-1 activation in a Bcl-2/Bcl-XL-suppressible manner [19, 23]. Various recombinant GST-F1L proteins and control proteins were added at 2-fold molar excess relative to NLRP1, followed by MDP and ATP addition, then caspase-1 activity was measured using fluorigenic peptide substrate, acetyl-Trp-Glu-His-Asp-aminomethylcourmarin (Ac-WEHD-AMC). Both F1L and Bcl-2 inhibited NLRP1-driven caspase-1 activity, whereas N1L and GST control proteins did not (**Figure 5-4A**). N-terminal truncation mutants of F1L lacking the region that contains the candidate loop (residues 30 to 42) also did not suppress NLRP1 activity in vitro. In contrast, a F1L mutant lacking the first 23 amino-acids and thus still containing the aforementioned loop, retained NLRP1 inhibitory activity. Inhibition of NLRP1 activity in vitro correlated with binding to NLRP1 among F1L mutants (**Figure 5-4B**). Experiments using a GST-F1L (1-47) fusion protein showed that the first 47 amino-acids of F1L are sufficient for suppressing NLRP1 activity in vitro (**Figure 5-12**).

To study the F1L loop in isolation, we chemically synthesized peptides corresponding to this region and other segments of F1L and examined their effects on the reconstituted NLRP1 inflammasome. Addition of the F1L loop peptide (residues 22-47) inhibited NLRP1-mediated caspase-1 activation to nearly baseline levels (**Figure 5-4C**). In contrast, F1L (22-47) peptide did not directly inhibit active recombinant caspase-1, showing NLRP1 dependence (**Figure 5-13**). In addition to using fluorigenic peptide substrate to monitor caspase-1 activity, we also monitored NLRP1-induced proteolytic processing of caspase-1, showing that synthetic F1L 22-47 peptide and recombinant GST-F1L(1-47) protein both inhibited NLRP1-driven proteolytic processing of caspase-1 (**Figure 5-14**). However, analogous to cellular Bcl-2 and Bcl-XL, GST-F1L(1-47)

protein and F1L 22-47 peptide did not inhibit caspase-1 processing induced by NLRP1ΔLRR (**Figure 5-15**), lacking the LRRs shown to be required for Bcl-2/Bcl-XL binding [11, 23]. Furthermore, the F1L 22-47 peptide binds to NLRP1, as determined by fluorescence polarization assay using a fluorescein isothiocyanate (FITC)-conjugated F1L 22-47 peptide (**Figure 5-16**). Taken together, these results demonstrate that F1L mediates inhibition of NLRP1-driven caspase-1 activation through residues in the aforementioned loop of F1L, analogous to the mechanism of Bcl-2 and Bcl-XL in suppressing NLRP1 [23].

Next, we mapped the residues within the 22-47 loop required for suppression of NLRR1 by testing the activity of shorter peptides. A hexapeptide comprised of residues 32-37 was determined to be sufficient to inhibit NLRP1 in vitro (**Figure 5-4D**).

Previously we described a 2-step mechanism for NLRP1 activation, in which MDP binding to NLRP1 induces a conformational change, rending NLRP1 competent to bind ATP, which then stimulates NLRP1 oligomerization [19]. Upon oligomerization of NLRP1, caspase-1 monomers associate with NLRP1, resulting in protease activation, presumably via an induced dimerization mechanism [25]. The binding of ATP to MDP-primed NLRP1 is readily measured using FITC-conjugated ATP, allowing us to measure ATP binding to recombinant NLPR1 in presence or absence of F1L peptides. Consistent with the ability of the 32-37 peptide to suppress NLRP1-driven caspase-1 activity, this peptide also inhibited ATP binding to NLRP1, whereas F1L peptide 41-60 did not (**Figure 5-4E**). Similarly, recombinant GST-F1L(1-47) protein also inhibited MDP-induced binding of ATP to NLRP1, while GST-N1L protein did not.

Next, we compared the concentration dependence of NLRP1 inhibition by F1L loop peptides. F1L peptides 22-37 and 32-37 both showed similar concentration-dependent NLRP1 inhibition, reducing caspase-1 activity to background levels with IC50 values of 15.0 ± 4.0 nM and 18.8 ± 6.7 nM, respectively (**Figure 5-4F**). In contrast, F1L peptide 22-32 had no effect, indicating that residues 32-37 of the F1L loop region are both necessary and sufficient to inhibit NLRP1.

We undertook a structure-activity analysis of the hexameric F1L 32-37 peptide, synthesizing a series of alanine substitutions and testing their effects on NLRP1-mediated caspase-1 activation in vitro (**Figure 5-4G**). Alanine substitutions of residues 32, 33, 35, and 37 abolished NLRP1 inhibitory activity, whereas residues 34 and 36 tolerated these substitutions. To analyze the findings with peptides in the context of the F1L protein, we produced GST-F1L mutants lacking the 32-37 hexapeptide segment as well as a V33A mutant and compared their activity with wild-type F1L and various other mutants using the in vitro reconstituted NLRP1 inflammasome. GST-F1LΔ32-37, GST-F1L(V33A), GST-F1LΔ17-37 and GST control protein all failed to inhibit NLRP1-mediated caspase-1 activation, whereas wild-type GST-F1L, GST-F1L(C7A), and GST-F1LΔ16-19 were effective inhibitors (**Figure 5-4H**). These results correlated with binding to NLRP1 (**Figure 5-17**). In conclusion, F1L residues 32-37 are necessary and sufficient to inhibit NLRP1. Interestingly, this hexapeptide sequence lacks obvious homology with a decameric sequence recently identified in Bcl-2 that inhibits NLRP1 [23], suggesting that different peptide ligands can display NLRP1 inhibitory activity.

In this report, we identify a novel function for the viral F1L protein, providing the first example of a viral inhibitor of NLR family proteins. F1L thus possesses at least two

functions – suppression of apoptosis (which is advantageous for maintaining host cell survival for viral replication or latency) and inhibition of NLR family proteins for reducing host inflammatory responses. While we focused on NLRP1 as a proto-typical target, it is possible that F1L inhibits additional NLR family members.

Caspase-1 plays several important roles in innate immune responses to viruses through its role in proteolytic processing of pro-IL-1β, pro-IL-18, and pro-IL-33. Among these cytokines, IL-18 may be particularly important in the context of viral infection because of its ability to induce interferon expression [26]. The genomes of vaccinia and many other poxviruses encode several inhibitors of the caspase-1/IL-1β axis, including (a) CrmA (SP1-2;B13R), which directly inhibits caspase-1; (b) viral soluble receptor for IL-1b (vIL-1bR), which is a IL-1R decoy that neutralizes IL-1; and (c) viral pyrin domain only protein M13L (vPOP) that competes with ASC [8, 14, 16, 27-30]. With the addition of F1L, poxviruses would appear to be capable of inhibiting at four levels (NLRs; ASC; caspase-1; IL-1β) to interfere with the bioproduction and activity of this important cytokine (**Figure 5-18**). While the relative importance of each of these points of regulation may vary depending on the host-pathogen context and timing post-infection, the observation that cells infected with F1L-deleted virus secrete more IL-1b argues that F1L is among the defenses that these viruses have evolved for interfering with host innate immune responses.

Figure 5-1. F1L deficient Vaccinia Virus exhibits reduced virulence in mice. Mice were infected (n = 14 per group) intranasally with 10^5 PFU of wild-type *vaccinia virus* Western Reserve (WR) (black circles) or F1L deleted virus (ΔF1L) (red circles), measuring **(A)** Survival (where mice that lost ≥ 30% of initial body weight were sacrificed), **(B)** body weight, and **(D)** rectal temperature daily (mean ± SEM). **(C)** At various days post-infection, four mice infected with control (black) or F1L deficient (red) virus were sacrificed and viral titers were measured in lungs. **(E)** BAL fluids were collected from mice infected with control (WR; black bars) or F1L deficient (gray bars) viruses, 10X concentrated, and analyzed by SDS-polyacrylamide gel electrophoresis (PAGE)/immunoblotting for caspase-1 cleavage using anti-p10 antibody. Results were imaged using a fluorescence imaging system employing near infrared dye-conjugated secondary antibodies, quantifying results by integrated fluorescence intensity measurements of bands (mean ± SEM; n = 4). **(F)** Lung tissue from sacrificed mice was analyzed by hematoxylin and eosin staining, quantifying number of inflammatory foci per unit area (mean ± SEM; n = 4). Representative low (*left*) and high (*right*) power magnification images are shown, where boxes show regions selected for high-power magnification imaging. (Scale bars = 100 µm). P-values for all panels were determined by pair-wise comparisons using t-tests. (With compliment to M. Gerlic)
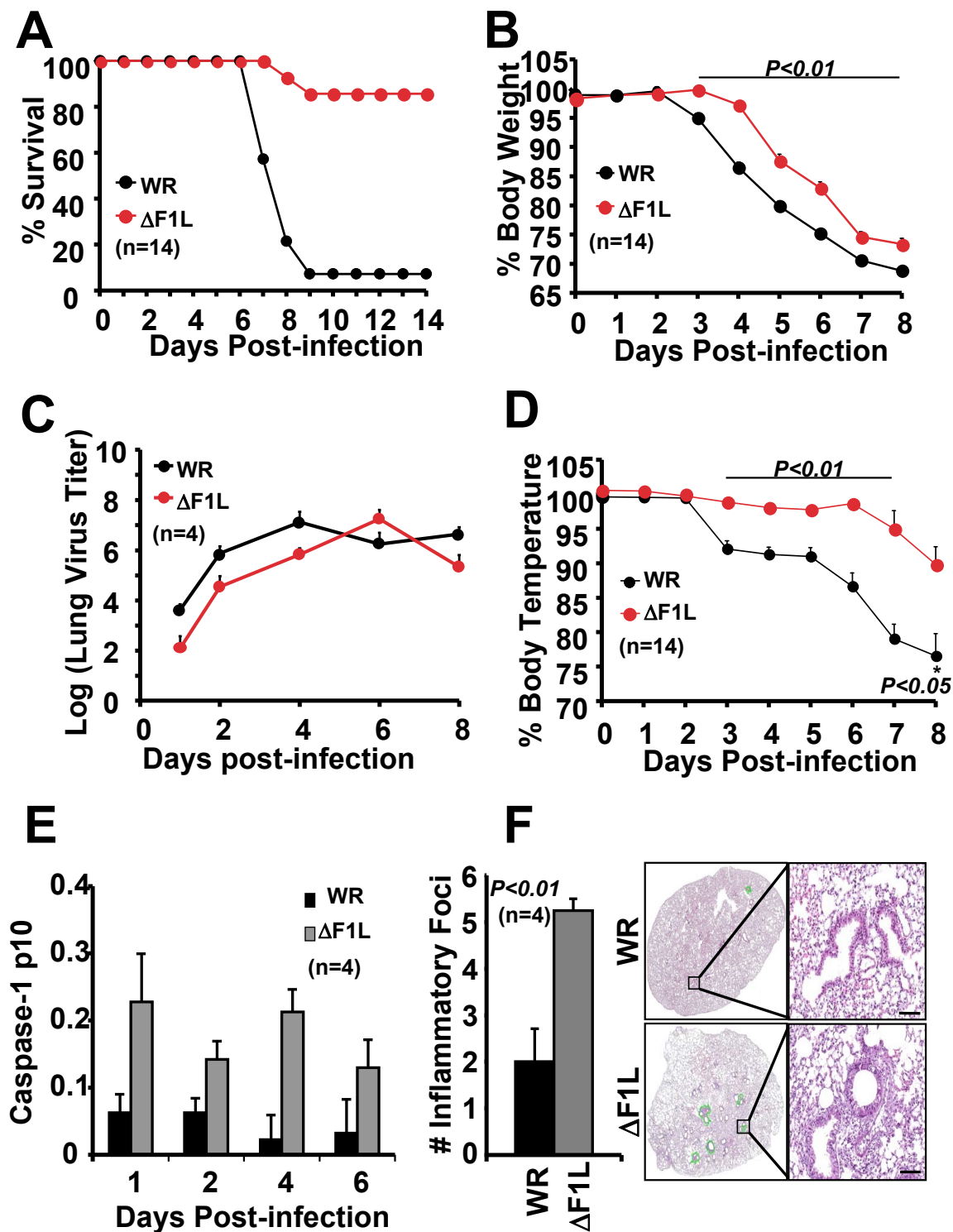
Figure 5-1. F1L deficient Vaccinia Virus exhibits reduced virulence in mice.

Figure 5-2. Increased caspase-1 cleavage, caspase-1 activity, and IL-1β production in macrophage cultures infected with F1L deficient virus. TPA-differentiated THP-1 cells (5×10^7) were infected overnight (MOI=1) with wild-type vaccinia virus Western Reserve (WR) or F1L deleted virus (ΔF1L). **(A)** Cell lysates were normalized for total protein content and analyzed by immunoblotting. F1L and N1L protein were detected using specific antibodies. **(B)** Cleaved fragments of caspase-1 were detected in either cell extracts (top) or culture supernatants (bottom) by immunoblotting using a mixture of anti-p10 and p-20 antibodies. Culture supernatants were filtered using an Amicon Ultra (100 kDa cut-off). Proteins were precipitated by Trichloroacetic acid (TCA) and washed twice with acetone. Dried pellets were resuspended, normalized for total protein content, and analyzed by SDS/PAGE/immunoblotting using a fluorescence-based imaging system. As positive control for caspase-1 cleavage, macrophages were primed 12h with LPS (50 ng/ml), incubated for 4h with MDP (2 µg/ml), followed by ATP (2.5 mM) for 20 min. **(C)** Mature IL-1β (p17) cytokine was detected in culture superntants as above, using specific antibody. **(D-F)** TPA-differentiated THP-1-Blue (InvivoGen) cells (10^6) were infected (MOI=1) with VACV-WR, VACVΔF1L or VACVΔN1L viruses. Supernatants were collected 18 hrs later for analysis. **(D)** Caspase-1 activity in culture supernatants was measured for 60 minutes by hydrolysis of Ac-WEHD-Rhodamine substrate (20 µM). **(E)** IL-1β secretion was measured using ELISA. **(F)** NF-κB activation was evaluated by measuring Alkaline Phospatase activity in culture supernatants for 180 minutes by hydrolysis of QUANTI-Blue substrate (InvivoGen). As positive control for D-F, macrophages were stimulated for 18h with MDP (5 µg/ml). **(G)** TPA-differentiated THP-1-Blue were primed 12h with LPS (50 ng/ml), followed by VACV infection. IL-1β secretion was measured using ELISA. All results are mean $\pm$ SD; n = 3. (With compliment to M. Gerlic)
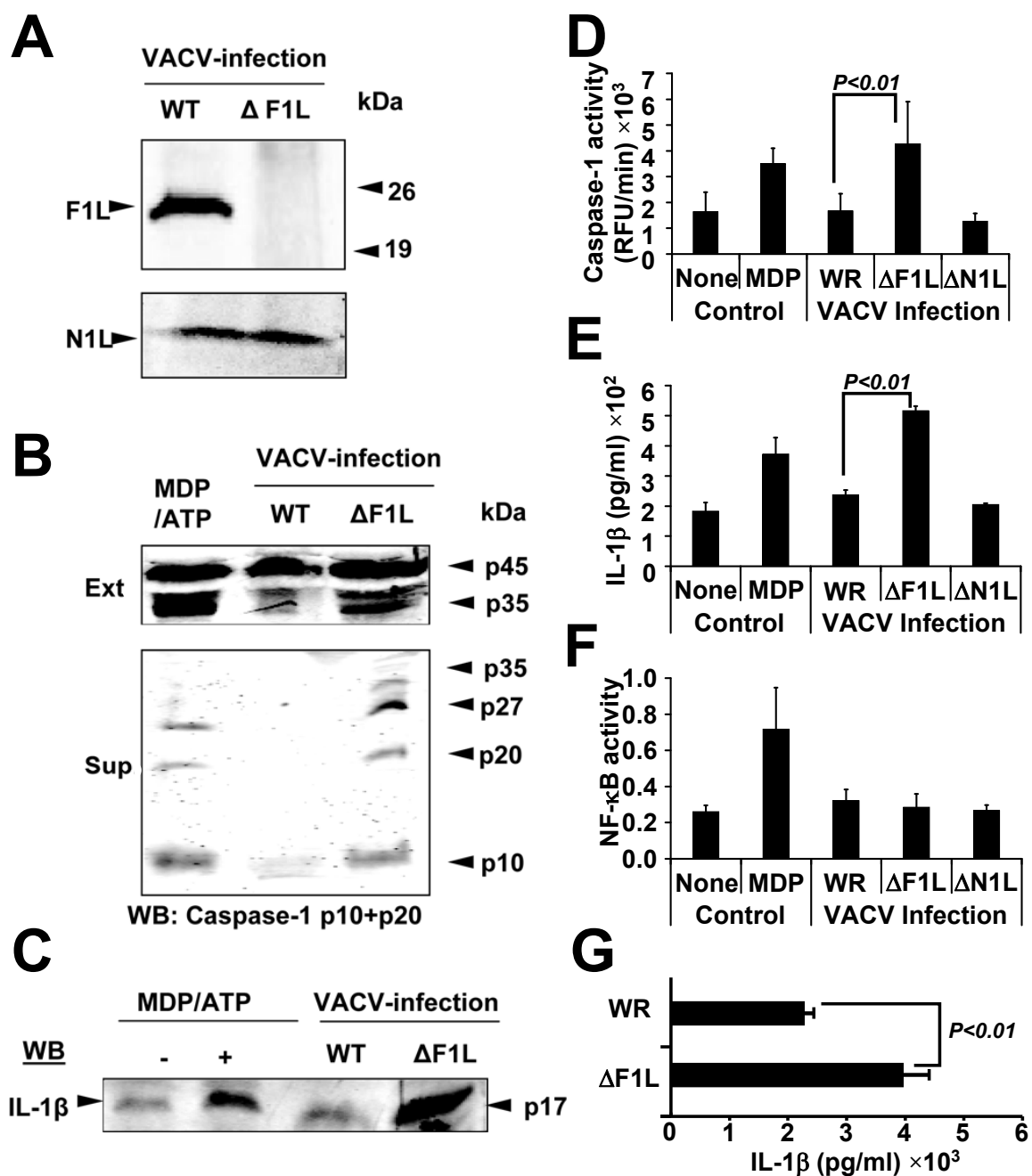
Figure 5-2. Increased caspase-1 cleavage, caspase-1 activity, and IL-1β production in macrophage cultures infected with F1L deficient virus.

Figure 5-3. F1L binds NLRP1 and inhibits cellular NLRP1 inflammasome activity.
(A) HEK293T cells were transiently co-transfected with plasmids encoding myc-tagged NOD2 or NLRP1 and either GFP-tagged N1L or GFP-tagged F1L. For co-immunoprecipitations (co-IPs), ~10^6 cells were lysed in isotonic NP-40 lysis buffer. Clarified lysates were subjected to IP using Dynabeads proteinG pre-conjugated to anti-GFP. Immune-complexes were separated by SDS/PAGE and analyzed by immunoblotting using anti-Myc and anti-GFP antibodies using a fluorescence-based imaging system (*top*). Cell lysates (10% volume) were also run along side immune-complexes (*bottom*). **(B)** Recombinant proteins GST-NLRP1, GST-NLRP1ΔLRR, GST-Bfl-1, or GST (5 µg) were incubated with or without purified F1L (10 µg) in 20 mM HEPES-KOH, [pH 7.5], 10 mM KCl, 1 mM DTT in a final volume of 50 µl for 30 minutes on ice, followed by incubation overnight with Glutathione-Sepharose at 4°C. GST-purified complexes were isolated after centrifugation, analyzed by SDS-PAGE, and stained with Sypro Ruby. **(C)** HEK293T cells were transiently co-transfected with plasmids encoding myc-tagged NLRP1 and various GFP-tagged F1L constructs (GFP and GFP-tagged N1L served as negative controls). Cell lysates were normalized for protein content and co-IPs were performed as above. F1L binding was quantified by fluorescence-based imaging method measuring integrated intensity of bands. Data were normalized relative to wild-type F1L (= 1.0). All results are mean $\pm$ SD; n =3. **(D)** F1L inhibits NLRP1 activity in cells. HEK293T cells were transiently co-transfected in 12-well plates with plasmids encoding mouse proIL-1β (400 ng), pro-Caspase-1 (25 ng), ASC (20 ng), NLRP1 (200 ng), and various GFP-tagged F1L constructs (600 ng), maintaining a total DNA amount of 1 µg by addition of control (empty) plasmid. At 18 hr post-transfection, cells were stimulated with MDP (5 ug/ml) and ATP (5 mM) for 8 hr. Cell culture supernatants were analyzed by ELISA for secreted mIL-1β. As controls, we used pcDNA3-Myc, Bcl-B-Myc (negative), and Bcl-XL-Myc (positive). Specific NLRP1 inflammasome mIL-1β secretion was determined by substracting spontaneous secretion (unstimulated cells) from MDP-stimulated cells. Data were normalized relative to pcDNA3 control-transfected cells (= 1.0). All results are mean ± SD; n =3. Statistical significance was determined by unpaired t-tests in C and D. (With compliment to B. Faustin)

A

NLRP1-Myc	+	-	-	+	-	-
NOD2-Myc	-	+	-	-	+	-
IgG	-	-	+	-	-	+
F1L-GFP	+	+	+	-	-	-
N1L-GFP	-	-	-	+	+	+

B

GST-NLRP1	+	+	-	-	-	-	-
GST-NLRP1ΔLRR	-	-	+	-	-	-	-
GST-Bfl-1	-	-	-	+	+	-	-
GST	-	-	-	-	-	+	+
F1L	-	+	+	-	+	-	+
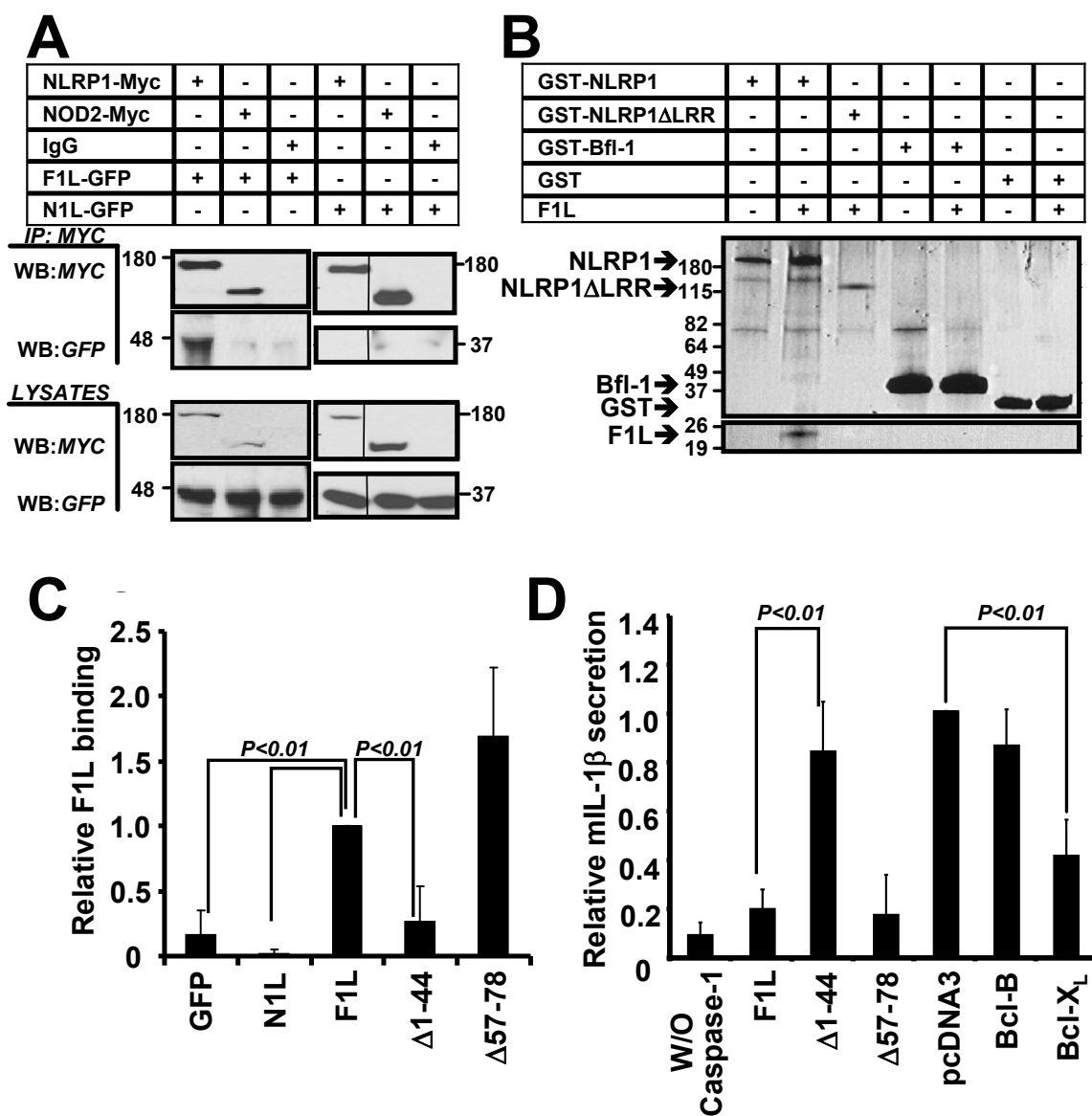
Figure 5-3. F1L binds NLRP1 and inhibits cellular NLRP1 inflammasome activity.

Figure 5-4. F1L residues 32-37 are necessary and sufficient to inhibit NLRP1 inflammasome. (A) In vitro reconstituted NLRP1 inflammasome was used to study F1L activity. Reactions contained His6-NLRP1 (8.5 nM), pro-caspase-1 (8.5 nM), 0.25 mM ATP, 0.5 mM Mg2+, 0.1 μg/ml MDP and 17 nM of GST-Bcl-2, N1L, or various GST-F1L constructs. Caspase-1 activity was measured after 60 minutes by hydrolysis of Ac-WEHD-AMC substrate (20 μM), reporting data as fold stimulation induced by MDP/ATP (mean + SD; n = 3) **(B)** HEK293T cells were transiently transfected with plasmid encoding Flag-tagged NLRP1 and lysates were prepare, to which were added various GST-F1L proteins as indicated. Samples were subjected to IP using Dynabeads proteinG pre-conjugated with anti-Flag. Immune-complexes were analyzed by SDS/PAGE/immunoblotting using anti-GST or anti-Flag antibodies (top). GST-tagged recombinant proteins (2 μg) were run directly in gels as a control for loading (bottom). **(C, D)** F1L peptides inhibit NLRP1. Various F1L peptides (F1Lp) or recombinant GST-F1L 1-47 protein (50 nM) were added to in vitro reconstituted NLRP1 inflammasome as above. Caspase-1 activity was measured (RFU/min), expressing data as mean ± SD, n=3. **(E)** F1L inhibits ATP binding to NLRP1. His6-NLRP1 (0.125 μM) was incubated for 5 min on ice in the presence of F1L 1-47 (2 μM), F1Lp 22-47 (0.5 or 2 μM), N1L, F1Lp 32-37, or Bcl-2p 41-60 (2 μM). The mixture was then incubated for additional 5 min with 1 μM MDP, FL-conjugated ATP analog (10 nM) and Mg^{2+} (0.5 mM) [19]. ATP binding was analyzed by fluorescence polarization (n = 3 milliPolars [mP]), and the percentage of inhibition was determined vs NLRP1 incubated only with MDP (mean + SD; n = 3). **(F)** Concentration-dependent suppression of NLRP1 by F1L. Various concentrations of F1Lp 32-37, F1Lp 22-37, or F1Lp 22-32 were added to in vitro reconstituted NLRP1 inflammasome. Caspase-1 activity was measured and IC50 values were calculated. **(G)** Alanine scanning substitution analysis of F1L peptides. Various F1Lp 32-37 peptides where specific residues were replaced by L-Ala (50 nM) were added to in vitro reconstituted NLRP1 inflammasome and analyzed as above. (H) Alanine substitution mutagenesis of F1L protein. Various recombinant GST-F1L mutants were produced and tested in the in vitro reconstituted NLRP1 inflammasome for inhibitory activity as above (mean + SD, n= 3). Data correlated with binding to NLRP1 (Figure 5-17). (With compliment to B. Faustin)
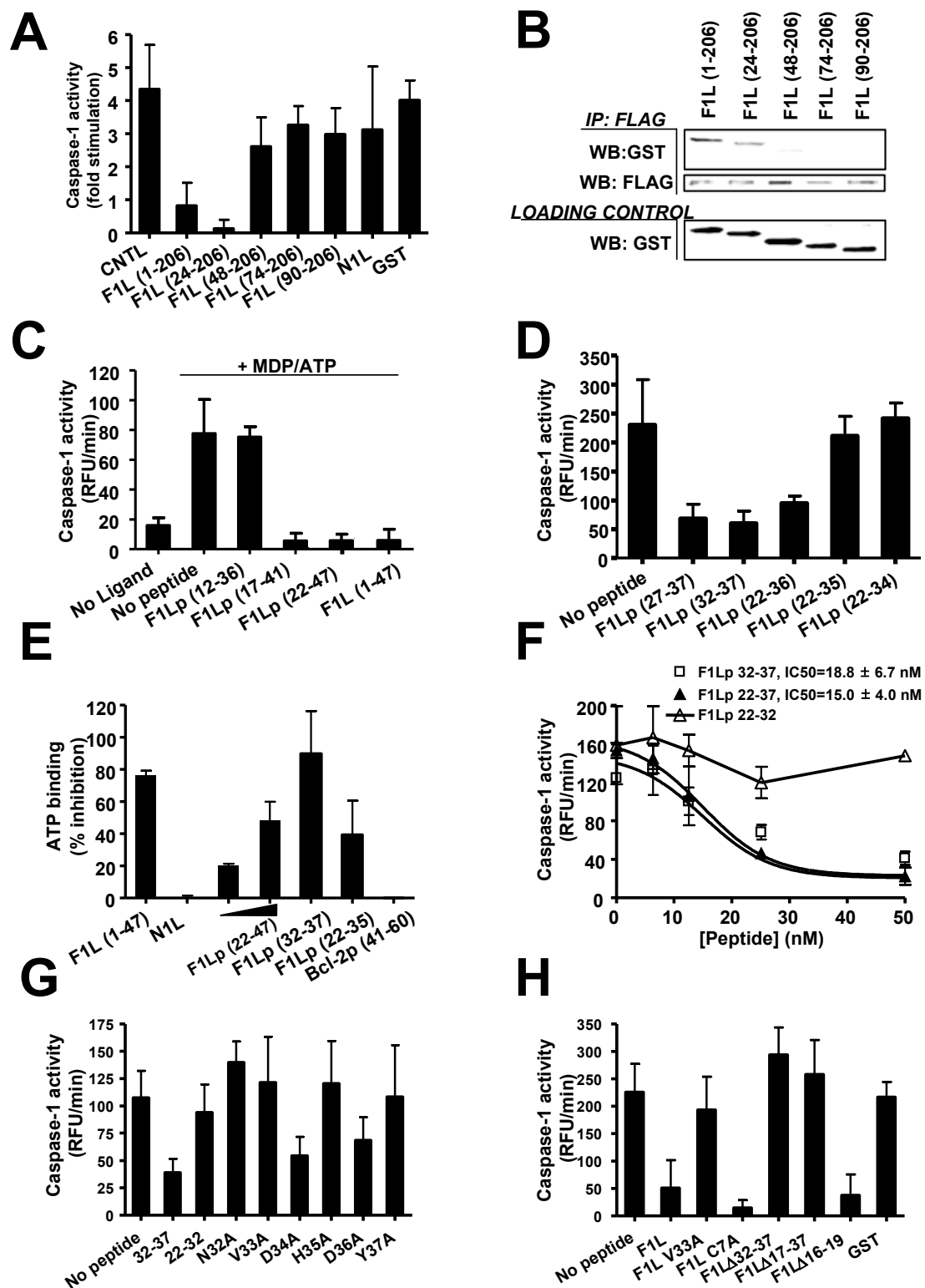
Figure 5-4. F1L residues 32-37 are necessary and sufficient to inhibit NLRP1 inflammasome.
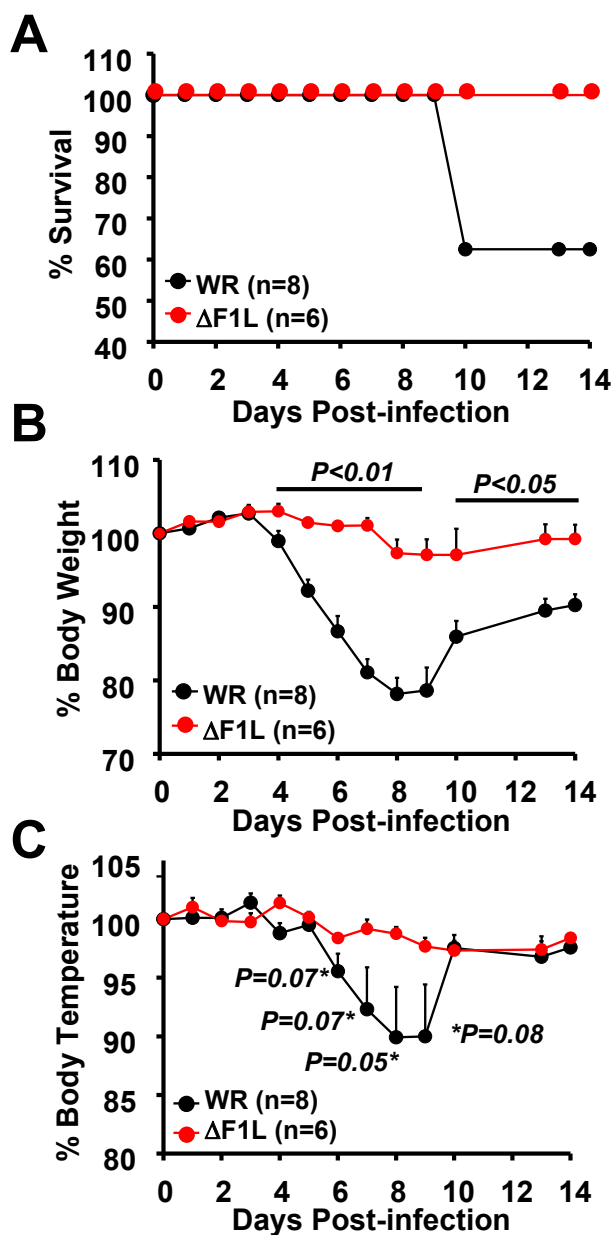
Figure 5-5. Virulence of Vaccinia virus F1L protein in a low dose murine intranasal infection model. In addition to the experimental data shown in the paper, mice were infected with a lower amount of viruses (10^4 PFU intranasal), with similar results. Groups of 6-8 female Balb/c mice were infected intranasally with 10^4 PFU of wild-type *vaccinia virus* Western Reserve (WR) (black circles) or F1L deleted virus (ΔF1L) (red circle), monitoring daily **(A)** survival (where mice that lost ≥ 30% of initial body weight were sacrificed and counted as dead), **(B)** body weight, and **(C)** rectal temperature All results are mean ± SEM. (With compliment to M. Gerlic)
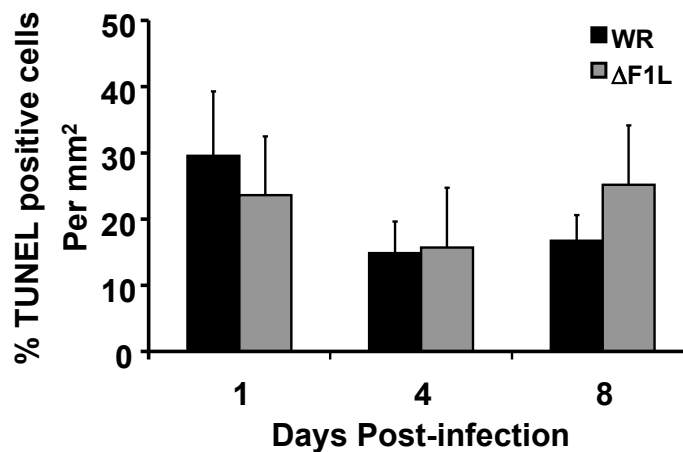
Figure 5-6. Apoptosis measured in lungs of Vaccinia virus-infected mice. Balb/c mice were infected intranasally with 10^5 PFU of wild-type *vaccinia virus* Western Reserve (WR) (*black bars*) or F1L deleted virus (ΔF1L) (*gray bars*). Lungs were harvested at various days post-infection. Deparaffinized 5 μm thick sections were stained by the TUNEL procedure, followed by hematoxylin and eosin counterstaining [31]. All slides were scanned at an absolute magnification of 400x (resolution of 0.25 μm/pixel) using the Aperio ScanScope CS system (Aperio Technologies, CA, US). The acquired digital images representing whole tissue sections were viewed and analyzed employing the ImageScope^TM viewer. TUNEL-positive nuclei in lung sections were quantified, analyzing a minimum of 1000 cells. Data represent mean $\pm$ SEM (n = 4). (With compliment to M. Gerlic)

Figure 5-7. Histology of lungs in Vaccinia virus murine intranasal model. Group of 14 Balb/c mice were infected intranasally with 10^5 PFU of wild-type *Vaccinia virus* (WR) or mutant virus (ΔF1L). Lungs were harvested on day 4 post-infection. Deparaffinized 5 μm thick sections were stained with hematoxylin and eosin for histopathological assessment. All slides were scanned at an absolute magnification of 400x (resolution of 0.25 μm/pixel) using the Aperio ScanScope CS system (Aperio Technologies, CA, US). The acquired digital images representing whole tissue sections were viewed and analyzed employing the ImageScope^{TM} viewer. Foci of inflammation in lung sections were quantified by selecting with the pen tool (green line), focal areas of peribronchial and perivascular inflammation. Pen tool annotations (green line) denote foci of inflammation of days 4 post-infection. Each scale bar corresponds to approximately 100 μm. (With compliment to M. Gerlic)
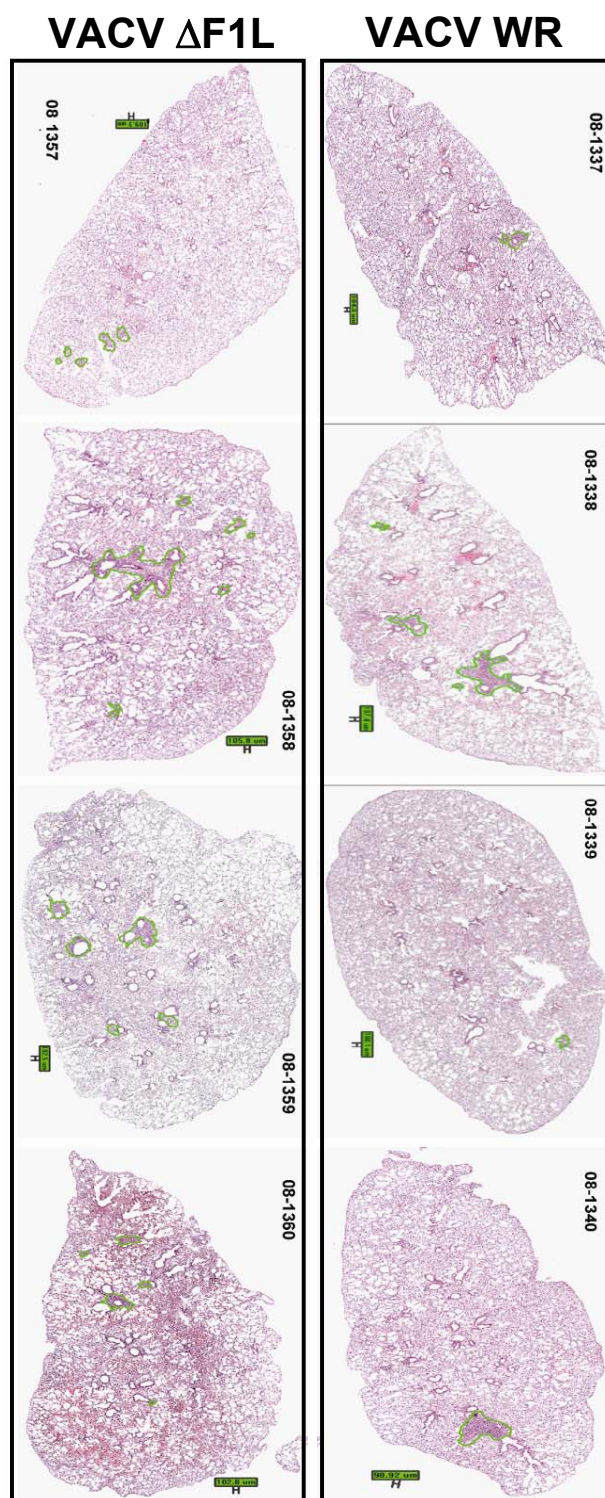
Figure 5-7 . Histology of lungs in Vaccinia virus murine intranasal model.
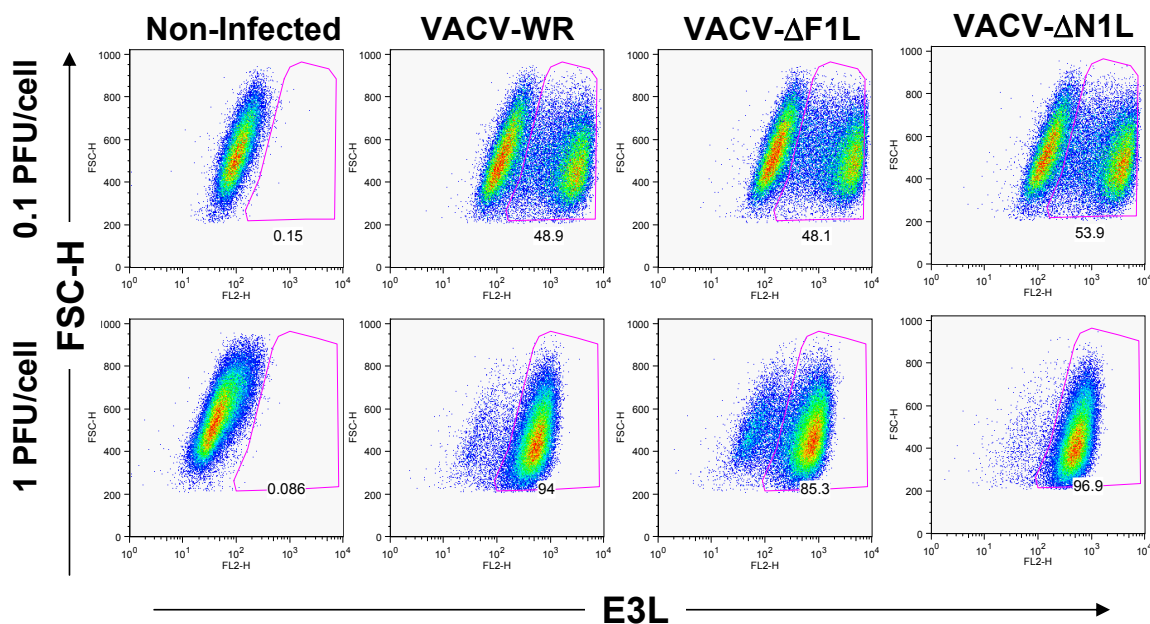
Figure 5-8. Deletion of F1L or N1L does not impair infection efficiency of Vaccinia virus in THP-1 cells. TPA-differentiated THP-1-Blue (InvivoGen) cells (10^6) were infected (MOI=0.1 and 1) with wild-type Vaccinia virus (VACV-WR), F1L deleted virus (ΔF1L), or N1L deleted virus (ΔN1L). Cells were collected, permeabilized, and stained using antibody recognizing the VACV early gene E3L, followed by Flow cytometry analysis. Data represent fluorescence intensity (x-axis) versus forward scatter (y-axis), where each cell analyzed appears as a dot and values are color-coded on the visible light spectrum to indicate low (blue) versus high (red) frequency values. The demarked areas represent immunopositive cells, where the percentage of E3L-expressing cells is provided in each panel. (With compliment to M. Gerlic)
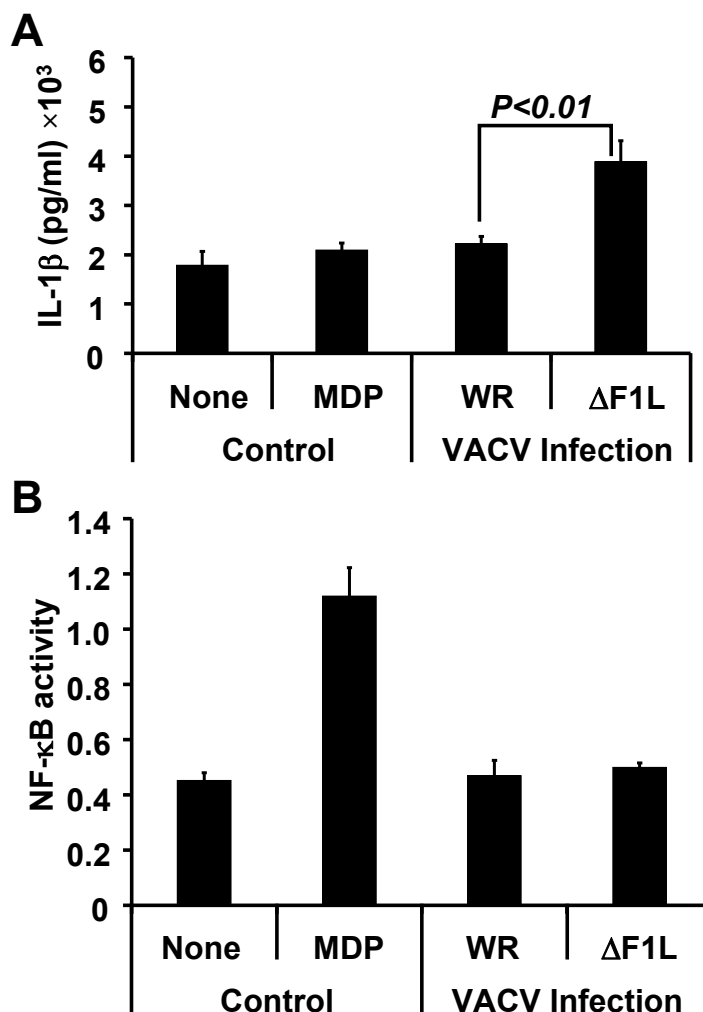
Figure 5-9. F1L inhibits IL-1β secretion by LPS-primed, Vaccinia-infected macrophages. TPA-differentiated THP-1-Blue (InvivoGen) cells (10^6) were stimulated with LPS (50 ng/ml) for 8 hours prior to infection (MOI=1) with wild-type Vaccinia virus (VACV-WR) or F1L deleted virus (ΔF1L). Supernatants were collected 18 hrs later for analysis of **(A)** IL-1β levels by ELISA or **(B)** NF-κB activity by measuring secreted Alkaline Phospatase activity in culture supernatants based on hydrolysis of QUANTI-Blue substrate (InvivoGen) for 180 minutes. As positive control, macrophages were stimulated for 18h with MDP (5 μg/ml). All results are mean ± SD; n = 3. (With compliment to M. Gerlic)

A

B
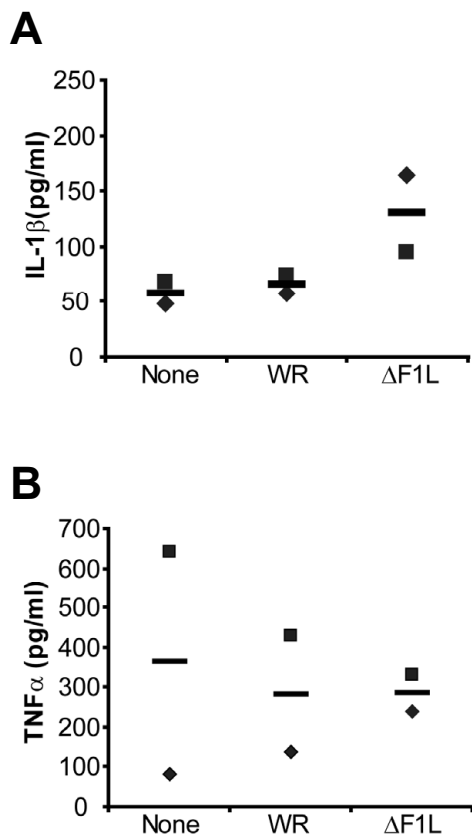
Figure 5-10. F1L inhibits IL-1β secretion by LPS-primed, Vaccinia virus-infected PBMC. PBMC were collected from two donors using Ficol and cultured over-night. PBMC were then primed with LPS (10 pg/ml) for 18 hrs prior to infection with wild-type Vaccinia virus (VACV-WR) or F1L deleted virus (ΔF1L) (MOI = 1). IL-1β and TNFα secretion were measured by ELISA (e-Bioscience) (n = 2). Hash marks indicate mean values. (With compliment to M. Gerlic)
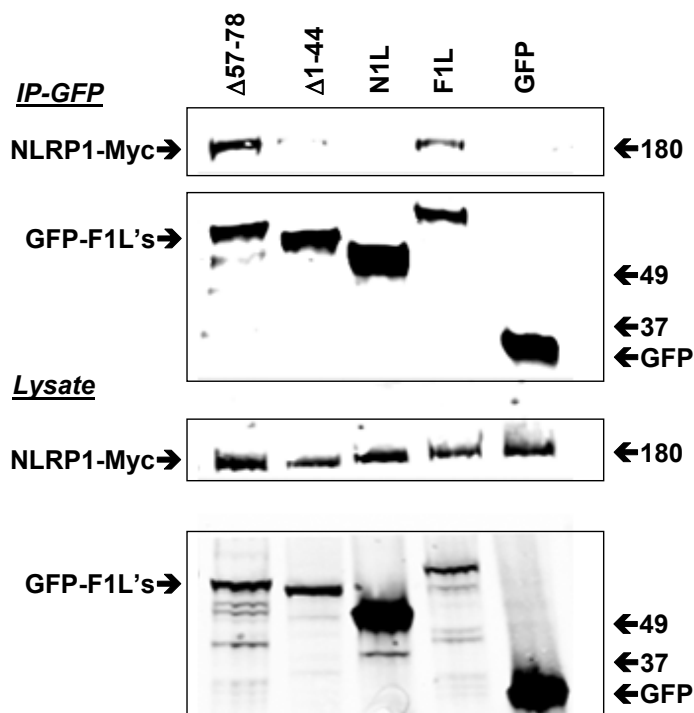
Figure 5-11. Representative of NLRP1/F1L constructs coIP experiment. HEK293T cells were transiently co-transfected with plasmid encoding myc-tagged NLRP1 together with plasmids encoding GFP or various GFP-fusion proteins including F1L (wild-type), F1L (Δ1-44), F1L (Δ57-78), and N1L. For co-immunoprecipitations (co-IPs), ~10^6 cells were lysed in isotonic, NP-40 lysis buffer (150 mM NaCl, 20 mM HEPES [pH 7.4], 0.2% NP-40, 5 mM MgCl$_2$, 2 mM EDTA, 2 mM DTT, 1 mM PMSF, and 1X protease inhibitor mix (Roche)). Clarified lysates were subjected to IP using Dynabeads proteinG (Invitrogen) conjugated anti-GFP (top). After overnight incubation at 4°C, immune-complexes were washed 3 times in lysis buffer, separated by SDS/PAGE and analyzed by immunoblotting using anti-myc (upper) or anti-GFP (lower) antibodies in conjunction with secondary IRDye 800/680CW conjugated antibodies (LI-COR Biosciences), followed by far-infrared imaging using Li-COR Odyssey v3.0 software. Cell lysates (10% volume) were also analyzed directly by SDS-PAGE/immunoblotting (bottom) to compare protein expression levels. (With compliment to M. Gerlic)
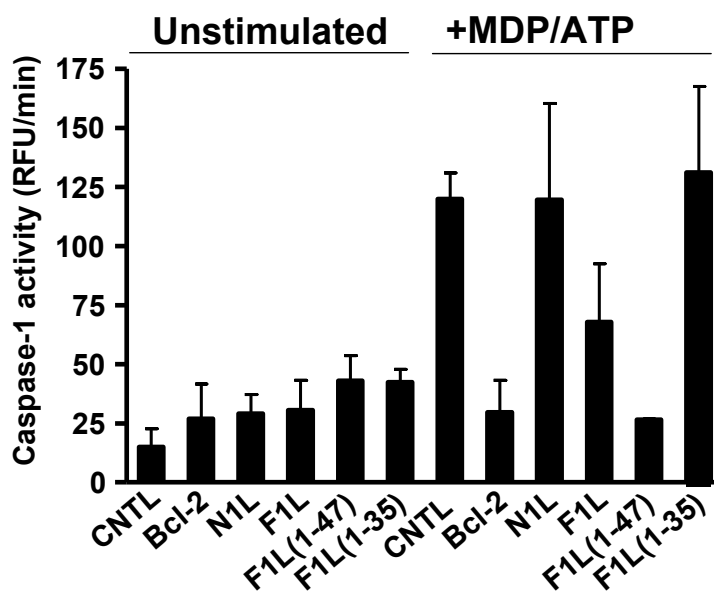
Figure 5-12. F1L residues 1-47 are sufficient to suppress the in vitro reconstituted NLRP1 inflammasome. Reactions contained His6-NLRP1 (8.5 nM), pro-caspase-1 (8.5 nM) and 17 nM of recombinant GST-Bcl-2, -N1L, or various GST-F1L proteins as indicated, with (right) or without (left) 0.25 mM ATP, 0.5 mM Mg^{2+} and 0.1µg/ml MDP. Caspase-1 activity was measured after 60 minutes by hydrolysis of Ac-WEHD-AMC substrate (20 µM), measuring relative fluorescence unit (RFU) generated per minute (mean + SD, n = 3). (With compliment to B. Faustin)
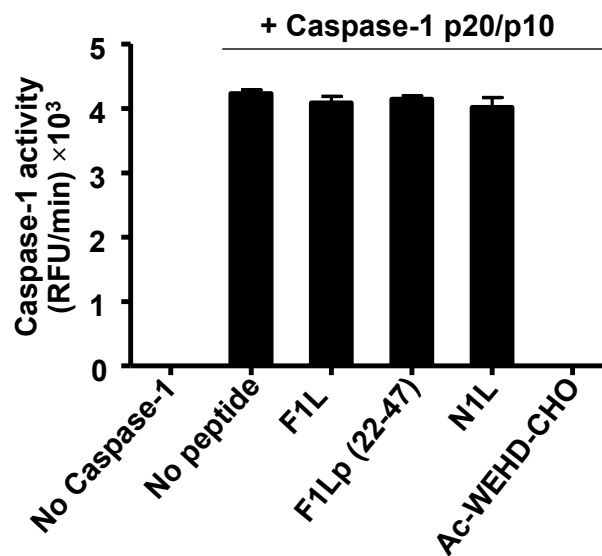
Figure 5-13. F1L peptide (22-47) does not inhibit active caspase-1. Recombinant, purified active (p10/p20 heterodimer) Caspase-1 (5 nM) was incubated with or without 50 nM of GST-F1L, F1Lp 22-47, or N1L, or with Ac-WEHD-CHO (10 nM). Caspase-1 activity was measured after 60 minutes by hydrolysis of Ac-WEHD-AMC substrate (20 µM), expressing data as mean ± SD, n=3. (With compliment to B. Faustin)

MDP+ATP	-	+	+	+	+	+	+
His-NLRP1	+	+	+	+	+	-	-
His-NLRP1ΔLRR	-	-	-	-	-	+	+
F1L(1-47)	-	-	-	+	-	-	-
F1Lp(22-47)	-	-	-	-	+	-	+
N1L	-	-	+	-	-	-	-

p10 →
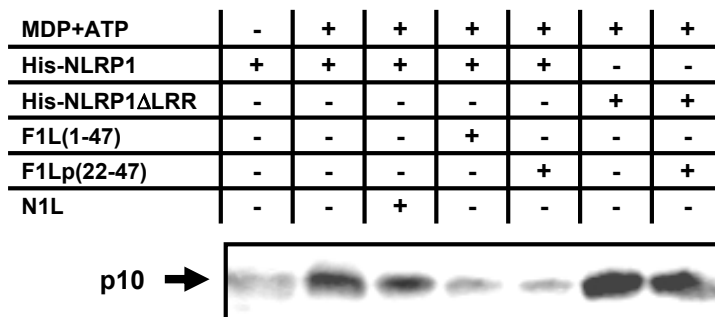
Figure 5-14. F1L peptide (22-47) suppresses NLRP1-induced proteolytic processing of pro-caspase-1 *in vitro*. Reactions contained His6-NLRP1 or GST-NLRP1ΔLRR (0.1 µM), pro-caspase-1 (0.1 µM), and 1 mM Mg2+, with (+) or without (-) 1 mM ATP and10 µg/ml MDP and with or without 0.4 µM of recombinant GST-F1L(1-47) or GST-N1L proteins or synthetic F1L(22-47) peptide (F1Lp). Following incubation for 30 min at 37°C, proteins were separated by SDS/PAGE and analyzed by immunoblotting using anti-p10 caspase-1 antibody. (With compliment to B. Faustin)
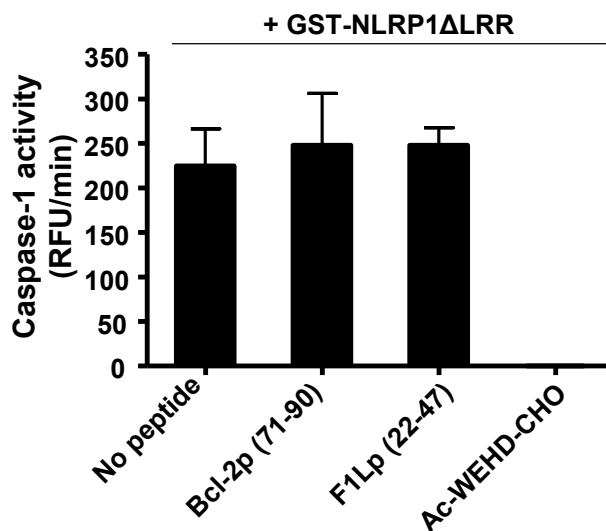
Figure 5-15. F1L peptide (22-47) does not inhibit NLRP1ΔLRR. Reactions contained GST-NLRP1ΔLRR (8.5 nM), pro-Caspase-1 (8.5 nM), 0.25 mM ATP, 0.5 mM Mg2+, with 0.1 µg/ml MDP, and with or without Bcl-2p 71-90, F1Lp 22-47 (50 nM), or Ac-WEHD-CHO (10 nM). Caspase-1 activity was measured after 60 minutes by hydrolysis of Ac-WEHD-AMC substrate (20 µM), expressing data as mean ± SD, n = 3. (With compliment to B. Faustin)
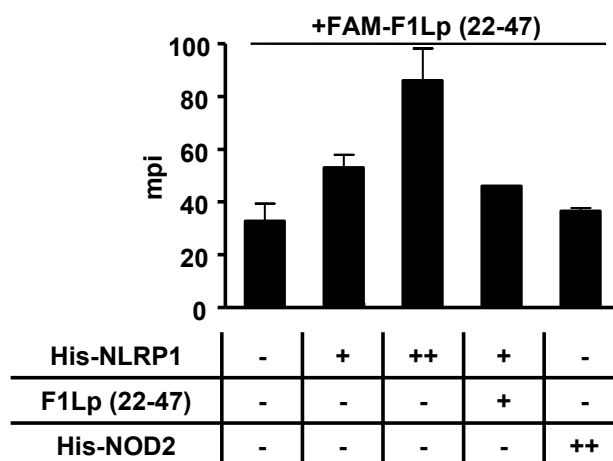
Figure 5-16. F1L peptide (22-47) binds NLRP1. His6-NLRP1 at 0.5 µM (+) or 2 µM (++) or His6-NOD2 at 2 µM (++) was incubated for 5 min on ice with (+) or without (-) unlabeled F1Lp 22-47 peptide. Then, fluorochrome(FAM)-conjugated F1Lp 22-47 peptide (0.1 µM) was added for 5 min at 4 °C. Binding of fluorochrome-labeled peptide was analyzed by FPA, measuring milliPolars [mP], mean ± SD (n = 3). (With compliment to B. Faustin)
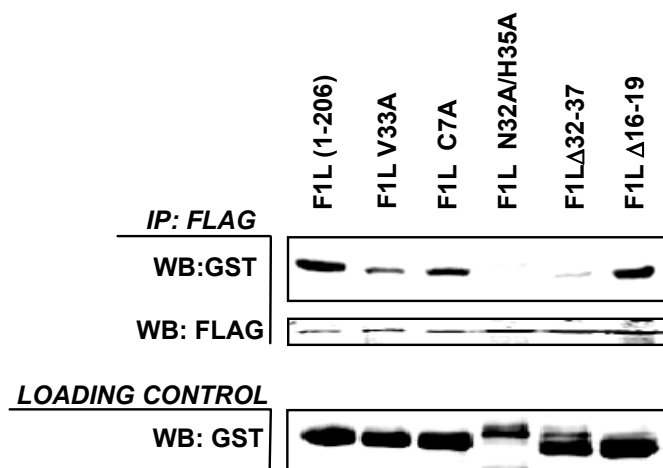
Figure 5-17. F1L residues 32-37 are necessary for binding NLRP1. (Top) HEK293T cells were transiently transfected with plasmid encoding Flag-tagged NLRP1. Cells were lysed in isotonic, NP-40 lysis buffer (150 mM NaCl, 20 mM HEPES [pH 7.4], 0.2% NP-40, 5mM MgCl2, 2 mM EDTA, 2 mM DTT, 1 mM PMSF, and 1X protease inhibitor mix (Roche)). Clarified lysates were aliquoted and incubated with various recombinant GST-fusion proteins, including F1L(1-206) or F1L V33A, F1L C7A, F1L N32A/H35A, F1LΔ32-37, and F1LΔ16-19 for 30 min in ice. The lysates were then subjected to IP using Dynabeads proteinG (Invitrogen) conjugated anti-Flag. After overnight incubation at 4°C, immune-complexes were washed 3 times in lysis buffer and eluted by competition with Flag peptide. Eluted immune-complexes were concentrated, separated by SDS/PAGE, and analyzed by immunoblotting using anti-GST (upper) or anti-Flag (lower) antibodies in conjunction with secondary IRDye 800/680CW conjugated antibodies (LI-COR Biosciences). **(Bottom)** The recombinant GST-fusion proteins (2 µg) were analyzed by immunoblotting. (With compliment to M. Gerlic)

Figure 5-18. Vaccinia Virus Inhibition of IL-1β Cascade. Vaccinia Virus inhibits the IL-1β cascade at five different steps: (1) Direct inhibition of Caspase-1 by CrmA (B13R; SPI-2) protein [28], thus, inhibiting proIL-1β processing; (2) Neutralizing IL-1β by the viral soluble receptor for IL-1β (B15R) [28]; (3) competing with cellular ASC by the viral M13L (vPOP) proteins [30]; (4) Inhibiting NF-κB activation downstream of the IL-1β receptor cascade by direct binding of viral A46R to MyD88, viral A52R binding to the IL-1R associated protein kinase, IRAK, and N1L binding to IKK [14, 32]; and (5) binding of F1L to NLRs such as NLPR1. Among other host proteins such as AIM2, NLR family proteins were recently implicated in innate immune responses to DNA viruses [4, 6, 7, 33, 34]. (With compliment to M. Gerlic)
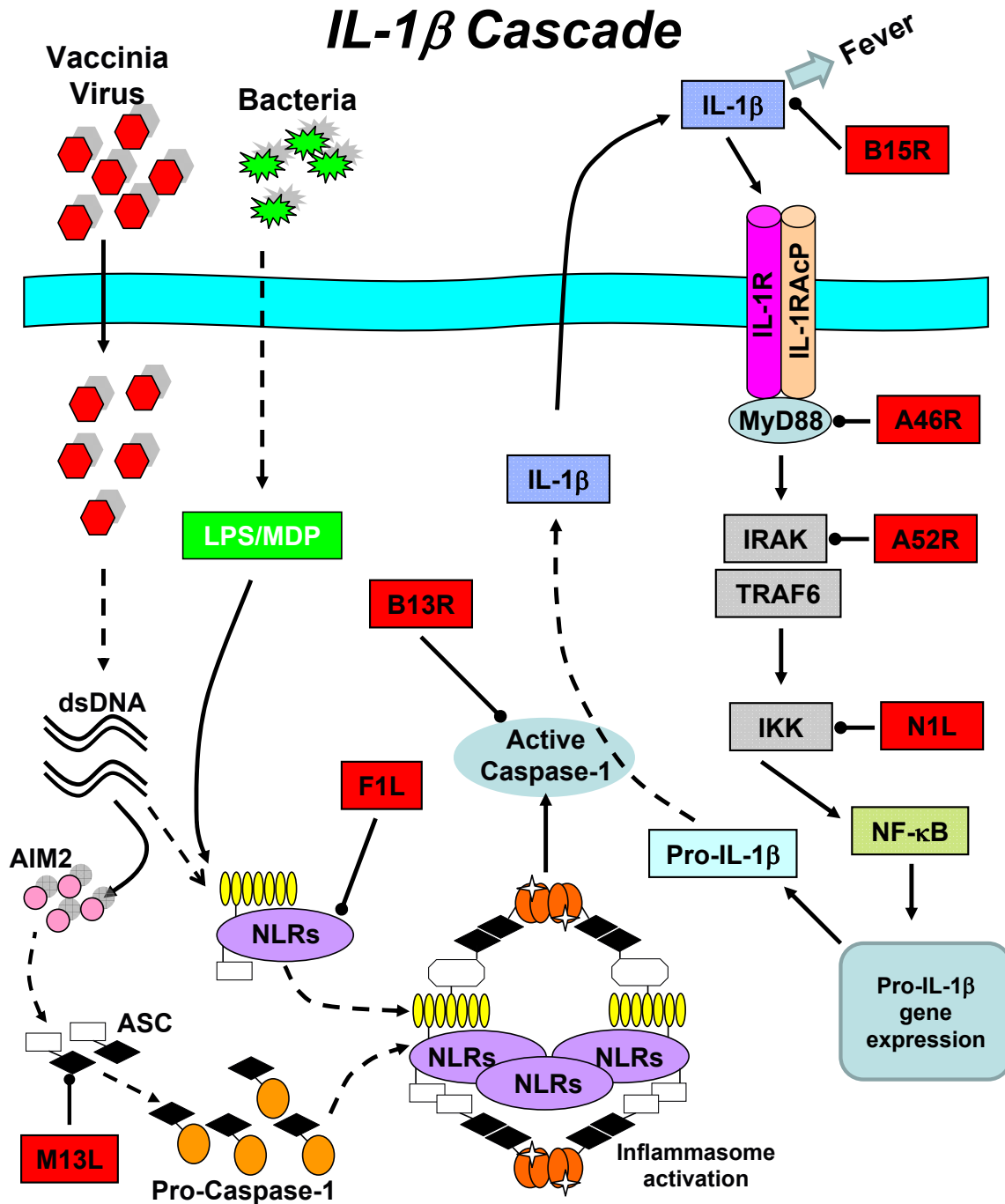
Figure 5-18. Vaccinia virus inhibition of IL-1β cascade.

Experimental procedures

Reagents, Chemicals, and Antibodies

Cell-culture supplies were obtained from GIBCO. The following antibodies were used for immunoblotting according to standard protocols: anti-Flag M2 (Sigma), anti-c-Myc (Roche), anti-human IL-1b (R&D Systems). The anti-GST, anti-GFP (B-2), anti-mouse caspase-1 p10 (M-20), anti-human caspase-1 p10 (C-20) and p20 (C-15) antibodies were purchased from Santa Cruz Biotech. Antibodies against the viral proteins F1L and N1L were produced in rabbits by immunization with peptides as previously described [9]. Muramyl dipeptide (MDP) was purchased from InvivoGen. Lipopolysaccharide (LPS) was obtained from Alexis and WEHD-AMC was obtained from Calbiochem.

Mice

The studies reported here conform to the animal Welfare Act and followed NIH guidelines for the care and use of animals in biomedical research. All experiments were performed in compliance with the regulations of the La Jolla Institute Animal care committee in accordance with the guidelines set by the Association for assessment and Accreditation of laboratory Animal Care. 8-12 wk-old female BALB/c mice were purchased from the Jackson Laboratory (Bar Harbor, ME).

Vaccinia virus intranasal challenge

Mice were anesthetized by inhalation of isoflurane and inoculated by the intranasal (i.n.) route with VACV, Western Reserve (VACV-WR), as well as a mutants

of WR in which only the F1L gene was deleted, VACV-F1L. Body weight and rectal temperature of mice were measured daily before and after infection. At various times post-infection, four mice from each group were sacrificed and lungs and BAL fluids were collected. Mice were euthanized when they lost 30% of their initial body weight.

Bronchoalveolar lavage (BAL)

Lungs were lavaged with 0.5 ml of PBS containing 2% BSA. The recovered BAL fluids were centrifuged to pellet cells. The superntants (500 ml) were concentrated 10x by using an Amicon Ultra (3 kDa cut-off). Proteins contained in elutes were mix with 5X Laemmli buffer, separated by SDS/PAGE and analyzed by immunoblotting using anti-mouse caspase-1 p10 (M-20) in conjunction with secondary IRDye 800/680CW-conjugated antibodies (LI-COR Biosciences). Results were imaged using Li-COR Odyssey v3.0 software, and quantified by the integrated fluorescence intensity.

Characterization of lung histology

Lungs were removed after sacrificing animals, fixed in 10% zinc-buffered formalin (Protocal; Fisher Diagnostics, Middletown, VA), and embedded in paraffin. Deparaffinized 5 μm thick sections were stained with hematoxylin and eosin for histopathological assessment. All slides were scanned at an absolute magnification of 400x (resolution of 0.25 μm/pixel) using the Aperio ScanScope CS system (Aperio Technologies, CA, US). The acquired digital images representing whole tissue sections were viewed and analyzed employing the ImageScopeTM viewer. To quantify foci of inflammation in lung sections, focal areas of peribronchial and perivascular inflammation were selected with the pen tool. Mean and SEM values for numbers of foci were

determined. Lung sections were analyzed by the terminal deoxynucleotidyl transferase end-labeling (TUNEL) method (Chemicon International; Temecula, CA) to identify the DNA fragmentation of apoptotic cells. The percentage of TUNEL-positive cells was evaluated by a morphometric method using an automated image analysis system (Aperio Technology, Vista, CA) and applying a nuclear scoring algorithm [31].

Vaccinia virus production

A Vaccinia virus (VACV) Western Reserve (WR) strain lacking only the F1L coding sequence (ΔF1L) was generated using a guanine phosphoribosyl transferase (gpt) cassette replacement strategy [9]. The resulting ΔF1L virus was verified by DNA sequencing and loss of expression of F1L was documented by immunoblot analysis of infected cells. Infections of HeLa cells with VACV and processing for immunoblot analysis were performed as described previously [9]. The VACV strains were grown in HeLa cells and titered on VeroE6 cells.

VACV-titer assay

Virus titers were determined as described previously [35]. Briefly, tissues from individual mice were homogenized, and sonicated for 0.5 minutes using an ultrasonic cleaner 1210 Branson (Danbury, CT). Serial dilutions were made and the virus titers were then determined by plaque assay on confluent VeroE6 cell cultures.

Plasmids

Plasmids encoding Flag-Caspase-1, ProIL-1b, Myc-ASC, Flag/Myc-NLRP1 and Myc-NOD2 GFP-F1L, -D44 and -D57-78 were described previously [9, 11]. Recombinant baculovirus transfer vectors encoding human NLRP1 or ASC, pro-Caspase-

1 (p45) or NALP1ΔLRR mutant (retains 1-723/1236-1473 amino acids) were described previously [19].

Cell culture

293T and HeLa cells were cultured in DMEM supplemented with 10% fetal bovine serum (FBS) and antibiotics. THP-1, THP-1-Blue and PBMC were cultured in complete RPMI 1640 medium 10% fetal bovine serum (FBS) and antibiotics. For differentiation, THP-1 cells were stimulated for 18 hr with 50 ng/ml phorbol-12-myristate-13-acetate (PMA). PBMC used in infection studies were obtained from healthy donors (San Diego Blood Bank) and isolated by density-gradient centrifugation using Ficol.

Vaccinia virus infection of cultured cells

TPA-differentiated THP-1 cells were infected at different MOI (0.1 to 1) with VACV-WR, N1L deleted virus (ΔN1L), or F1L deleted virus (ΔF1L). Culture supernatants were collected 18 hours post-infection.

Intracellular staining for E3L viral antigen

VACV infected THP-1 cells (as above) were collected 18 hours post-infection. Cells were fixed with cytofix-cytosperm (BD Biosciences) for 20 min at 4°C. Fixed cells were subjected to intracellular E3L staining in Perm/Wash buffer (BD Biosciences) for 30 min at 4°C. Anti-E3L Ab was kindly provided by Dr. Shane Crotty (La Jolla Institute for Allergy and Immunology) and used at a 1:100 v/v dilution. Cells were washed twice with BD Perm/Wash buffer and stained with goat anti-mouse IgG biotin conjugated antibody at 4°C followed by addition of PE-conjugated streptavidin (BD Biosiences).

Samples were analyzed for proportion of intracellular E3L staining after gating on live cells using a FACSCaliburTM flow cytometer with CellQuest (BD Biosciences) and FlowJo software (Tree Star, San Carlos, CA).

IL-1b secretion and caspase-1 activity assays.

TPA-differentiated THP-1-Blue (InvivoGen) cells (10^6) were infected (MOI=1) with VACV-WR, VACVΔF1L or VACVΔN1L. Supernatants were collected 18 hrs later for analysis. 10 µl of supernatant was incubated 30 min at 37°C in 96 well plate and Caspase-1 activity was measured for 60 minutes by hydrolysis of Ac-WEHD-RhoD112 substrate (20 μM), while IL-1β secretion was measured using ELISA (e-Biosciense). Where indicated, differentiated THP-1-Blue cells or PBMC were primed with LPS (50ng/ml for 12 hrs or 10 pg/ml for 18 hrs, respectively) prior to VACV infection.

NF-kB activation in THP-1-Blue cells

Using THP-1-Blue cells (ATCC; InvivoGen), NF-kB activation was evaluated by measuring Alkaline Phospatase activity in the supernatant for 180 minutes by hydrolysis of QUANTI-Blue substrate (InvivoGen). As positive control, THP-1 macrophages were stimulated for 18h with MDP (5 μg/ml). Reported results are mean $\pm$ SD; n = 3.

Immunoblot analysis.

Immunoblot analysis of cell extracts was performed by standard methods. For immunoblot analysis of culture supernatants, the recovered fluids were filtered using an Amicon Ultra (100 kDa cut-off). Proteins contained in eluates were precipitated by Trichloroacetic acid (TCA) and washed twice with acetone. Dry pellets were resuspended in 2X Laemmli buffer, normalized by the amount of total protein, separated

by SDS/PAGE and analyzed by immunoblotting using various antibodies in conjunction with secondary IRDye 800/680CW-conjugated antibodies (LI-COR Biosciences). Results were imaged using Li-COR Odyssey v3.0 software, and quantified by integrated fluorescence intensity.

Co-immunoprecipitations

HEK293T cells were transiently co-transfected with plasmids encoding myc or flag-tagged NLR full-length proteins and either GFP-tagged N1L or GFP-tagged F1L. For co-immunoprecipitations, $5x10^5$-$1x10^6$ cells were lysed in isotonic, NP-40-containing lysis buffer (150 mM NaCl, 20 mM HEPES [pH 7.4], 0.2% NP-40, 5 mM MgCl$_2$, 2 mM EDTA, 2 mM DTT, 1 mM PMSF, and 1X protease inhibitor mix (Roche)). Clarified lysates were subjected to immunoprecipitation (IP) using Dynabeads proteinG (Invitrogen) conjugated with anti-GFP, -myc, or -flag antibodies. After overnight incubation at 4°C, immune-complexes were washed 3 times in lysis buffer, separated by SDS/PAGE and analyzed by immunoblotting using various antibodies in conjunction with secondary IRDye 800/680CW-conjugated antibodies (LI-COR Biosciences). Results were imaged using Li-COR Odyssey v3.0 software, and quantified by integrated fluorescence intensity. Where indicated, cell lysates (10% volume) were run directly in SDS-gels.

GST pull-down

Recombinant proteins were produced by baculovirus infection of Sf9 insect cells (GST-NLRP1, GST-NLRP1ΔLRR) or in bacteria (GST-Bfl-1, or GST) and mixed (5 μg) with or without purified F1L protein (10 μg) in 20 mM HEPES-KOH, [pH 7.5], 10 mM

KCl, 1 mM DTT in a final volume of 50 μl for 30 minutes on ice, followed by incubation overnight with Glutathione-Sepharose at 4°C. GST-purified complexes were isolated after centrifugation, washed, and eluted with SDS-loading buffer, then analyzed by SDS-PAGE and stained by Sypro Ruby.

In vitro reconstituted NLRP1 inflammasome

The in vitro reconstitution of the NLRP1 inflammasome using proteins expressed in Sf9 cells from recombinant baculoviruses has been described [19]. Briefly, reactions contained His6-NLRP1 (8.5 nM), pro-caspase-1 (8.5 nM), 0.25 mM ATP, 0.5 mM MgCl$_2$, 0.1μg/ml MDP and GST-Bcl-2 or N1L, wild-type or various mutants of recombinant GST-F1L (17 nM), or various synthetic peptides. Caspase-1 activity was measured after 60 minutes by hydrolysis of Ac-WEHD-AMC substrate (20 μM), expressing data as mean ± SD, n=3.

Caspase-1 processing in the reconstituted NLRP1 inflammasome

Reactions contained His6-NLRP1 or GST-NLRP1ΔLRR (0.1 μM), pro-caspase-1 (0.1 μM), 1 mM ATP, 1 mM Mg2+, 10 μg/ml MDP and recombinant GST-F1L 1-47 protein or synthetic F1L 22-47 peptide (F1Lp), or recombinant N1L (0.4 μM) and were incubated 30 min at 37°C. Proteins were separated by SDS/PAGE and analyzed by immunoblotting using anti-p10 caspase-1 antibodies in conjunction with secondary IRDye 800/680CW-conjugated antibodies (LI-COR Biosciences). Results were imaged using Li-COR Odyssey v3.0 software.

Analysis of ATP binding to NLRP1 by FPA

His6-NLRP1 (0.125 μM) was incubated for 5 min on ice in the presence of F1L 1-47 (2 μM), F1Lp 22-47 (0.5 or 2 μM), N1L, F1Lp 32-37, or Bcl-2p 41-60 (2 μM). The mixture was then incubated for additional 5 min in ice with 1 μM MDP-LD, Fluorescein-conjugated ATP analog (10 nM) and Mg2+ (0.5 mM). ATP binding was analyzed by FPA (measuring milliPolars [mP]) using an Analyst AD Assay Detection System (LJL Biosystem), and the percentage of inhibition was determined versus NLRP1 incubated only with MDP-LD (mean ± SD).

Peptide synthesis and purification

F1L and Bcl-2 peptides were synthesized and purified essentially as described previously [23], and peptide mass was confirmed by MALDI-TOF mass spectometry.

Statistical Analysis.

In vivo data are presented as mean $\pm$ SEM. All other data were presented as the mean $\pm$ SD from at least 3 independent experiments. Statistical comparisons between different treatments were performed by Two-tailed Student's t-test, where $P \leq 0.05$ was considered statistically significant.

Acknowledgement

Liddington, Shahram Salek-Ardakani, John C. Reed (*Equal contribution). The dissertation author and Benjamin Faustin conceived the project, and designed the initial proof-of-concept experiments. The dissertation author also provided recombinant proteins and DNA constructs for experiments. Motti Gerlic and Benjamin Faustin designed and performed experiments, analyzed data, and wrote the initial draft of the manuscript.

References

1.   Martinon, F., A. Mayor, and J. Tschopp, *The inflammasomes: guardians of the body.* Annu Rev Immunol, 2009. **27**: p. 229-65.

2.   Franchi, L., et al., *The inflammasome: a caspase-1-activation platform that regulates immune responses and disease pathogenesis.* Nat Immunol, 2009. **10**(3): p. 241-7.

3.   Bergsbaken, T., S.L. Fink, and B.T. Cookson, *Pyroptosis: host cell death and inflammation.* Nat Rev Microbiol, 2009. **7**(2): p. 99-109.

4.   Schroder, K., D.A. Muruve, and J. Tschopp, *Innate immunity: cytoplasmic DNA sensing by the AIM2 inflammasome.* Curr Biol, 2009. **19**(6): p. R262-5.

5.   Roberts, T.L., et al., *HIN-200 proteins regulate caspase activation in response to foreign cytoplasmic DNA.* Science, 2009. **323**(5917): p. 1057-60.

6.   Hornung, V., et al., *AIM2 recognizes cytosolic dsDNA and forms a caspase-1-activating inflammasome with ASC.* Nature, 2009. **458**(7237): p. 514-8.

7.   Fernandes-Alnemri, T., et al., *AIM2 activates the inflammasome and cell death in response to cytoplasmic DNA.* Nature, 2009. **458**(7237): p. 509-13.

8.   Haga, I.R. and A.G. Bowie, *Evasion of innate immunity by vaccinia virus.* Parasitology, 2005. **130 Suppl**: p. S11-25.

9.   Postigo, A., et al., *Interaction of F1L with the BH3 domain of Bak is responsible for inhibiting vaccinia-induced apoptosis.* Cell Death Differ, 2006. **13**(10): p. 1651-62.

10. Kvansakul, M., et al., *Vaccinia virus anti-apoptotic F1L is a novel Bcl-2-like domain-swapped dimer that binds a highly selective subset of BH3-containing death ligands.* Cell Death Differ, 2008. **15**(10): p. 1564-71.

11. Bruey, J.M., et al., *Bcl-2 and Bcl-XL regulate proinflammatory caspase-1 activation by interaction with NALP1.* Cell, 2007. **129**(1): p. 45-56.

12. Wasilenko, S.T., et al., *Vaccinia virus encodes a previously uncharacterized mitochondrial-associated inhibitor of apoptosis.* Proc Natl Acad Sci U S A, 2003. **100**(24): p. 14345-50.

13. Aoyagi, M., et al., *Vaccinia virus N1L protein resembles a B cell lymphoma-2 (Bcl-2) family protein.* Protein Sci, 2007. **16**(1): p. 118-24.

14. Bartlett, N., et al., *The vaccinia virus N1L protein is an intracellular homodimer that promotes virulence.* J Gen Virol, 2002. **83**(Pt 8): p. 1965-1976.

15. Postigo, A. and P.E. Ferrer, *Viral inhibitors reveal overlapping themes in regulation of cell death and innate immunity.* Microbes Infect, 2009. **11**(13): p. 1071-8.

16. Alcami, A. and G.L. Smith, *A mechanism for the inhibition of fever by a virus.* Proc Natl Acad Sci U S A, 1996. **93**(20): p. 11029-34.

17. Reading, P.C. and G.L. Smith, *A kinetic analysis of immune mediators in the lungs of mice infected with vaccinia virus and comparison with intradermal infection.* J Gen Virol, 2003. **84**(Pt 8): p. 1973-83.

18. Martinon, F., et al., *Identification of bacterial muramyl dipeptide as activator of the NALP3/cryopyrin inflammasome.* Curr Biol, 2004. **14**: p. 1929-1934.

19. Faustin, B., et al., *Reconstituted NALP1 inflammasome reveals two-step mechanism of Caspase-1 activation.* Molecular Cell, 2007. **25**(5): p. 713-724.

20. McCullers, J.A. and B.K. English, *Improving therapeutic strategies for secondary bacterial pneumonia following influenza.* Future Microbiol, 2008. **3**: p. 397-404.

21. Warr, G.A. and G.J. Jakab, *Pulmonary inflammatory responses during viral pneumonia and secondary bacterial infection.* Inflammation, 1983. **7**(2): p. 93-104.

22. Moore, Z.S., J.F. Seward, and J.M. Lane, *Smallpox.* Lancet, 2006. **367**(9508): p. 425-35.

23. Faustin, B., et al., *Mechanism of Bcl-2 and Bcl-X(L) inhibition of NLRP1 inflammasome: loop domain-dependent suppression of ATP binding and oligomerization.* Proc Natl Acad Sci U S A, 2009. **106**(10): p. 3935-40.

24. Petros, A.M., E.T. Olejniczak, and S.W. Fesik, *Structural biology of the Bcl-2 family of proteins.* Biochim Biophys Acta, 2004. **1644**(2-3): p. 83-94.

25. Salvesen, G.S. and S.J. Riedl, *Caspase mechanisms.* Adv Exp Med Biol, 2008. **615**: p. 13-23.

26. Akira, S., *The role of IL-18 in innate immunity.* Curr Opin Immunol, 2000. **12**(1): p. 59-63.

27. Bowie, A., et al., *A46R and A52R from vaccinia virus are antagonists of host IL-1 and toll-like receptor signaling.* Proc Natl Acad Sci U S A, 2000. **97**: p. 10162-10167.

28. Kettle, S., et al., *Vaccinia virus serpin B13R (SPI-2) inhibits interleukin-1beta-converting enzyme and protects virus-infected cells from TNF- and Fas-mediated apoptosis, but does not prevent IL-1beta-induced fever.* J Gen Virol, 1997. **78 (Pt 3)**: p. 677-85.

29. Symons, J.A., et al., *The vaccinia virus C12L protein inhibits mouse IL-18 and promotes virus virulence in the murine intranasal model.* J Gen Virol, 2002. **83**(Pt 11): p. 2833-44.

30. Johnston, J.B., et al., *A poxvirus-encoded pyrin domain protein interacts with ASC-1 to inhibit host inflammatory and apoptotic responses to infection.* Immunity, 2005. **23**(6): p. 587-98.

31. Krajewska, M., et al., *Image Analysis Algorithms for Immunohistochemical Assessment of Cell Death Events and Fibrosis in Tissue Sections.* J Histochem Cytochem, 2009.

32. DiPerna, G., et al., *Poxvirus protein N1L targets the I-kappaB kinase complex, inhibits signaling to NF-kappaB by the tumor necrosis factor superfamily of receptors, and inhibits NF-kappaB and IRF3 signaling by toll-like receptors.* J Biol Chem, 2004. **279**(35): p. 36570-8.

33. Burckstummer, T., et al., *An orthogonal proteomic-genomic screen identifies AIM2 as a cytoplasmic DNA sensor for the inflammasome.* Nat Immunol, 2009. **10**(3): p. 266-72.

34. Delaloye, J., et al., *Innate immune sensing of modified vaccinia virus Ankara (MVA) is mediated by TLR2-TLR6, MDA-5 and the NALP3 inflammasome.* PLoS Pathog, 2009. **5**(6): p. e1000480.

35. Salek-Ardakani, S., et al., *OX40 drives protective vaccinia virus-specific CD8 T cells.* J Immunol, 2008. **181**(11): p. 7969-76.

Chapter 6

Conclusion and future directions

Conclusion

To cope with everyday challenges of pathogens, we need an economical strategy to defend against infections. When compared to the adaptive immunity, the non-specific innate immune system provides us immediate response against a tremendous diversity of pathogens. Importantly, the innate immunity detects invading pathogens and danger signals from damaged cells, and promotes secondary immune response to protect the host from infection. Programmed cell death (apoptosis) and caspase-1 activation in infected cells are examples of the vital mechanisms against viral infections in multi-cellular organisms. In this dissertation, we discovered that the vaccinia virus (VACV)-encoded Bcl-2 homologue, F1L, directly inhibits caspase-9, the apical protease in the mitochondrial cell death pathway, and NLRP1 (also known as NALP1), one of the inflammasome proteins that activates caspase-1.

Inhibition of apoptosome by F1L

With the notion that Bcl-XL may bind and inhibit Apaf-1, and thus the mitochondrial apoptosis pathway [1-4], we discovered that F1L, previously recognized as an anti-apoptotic protein that binds Bcl-2 family proteins, is also a caspase-9 inhibitor. We identified a conserved N-terminal motif of F1L that is necessary and sufficient for the interaction and inhibition of caspase-9. Moreover, we found that the C-terminal Bcl-2-like domain of F1L may also contribute to the interaction and/or inhibition of caspase-9

by binding to both inactive pro-enzyme and active form of caspase-9. Altogether, our evidence suggests that F1L suppresses caspase-9 by a unique mechanism that is different from other known caspase protein inhibitors.

Inhibition of inflammasome by F1L

It has been shown that the loop regions of Bcl-2 and Bcl-XL suppress caspase-1 activation by interacting with NLRP1 [5]. In addition to the caspase-9-inhibiting motif, we identified another conserved motif within the N-terminal extension preceding the Bcl-2-like domain of F1L that directly and selectively binds and inhibits NLRP1, and thus caspase-1 activation mediated by the NLRP1 inflammasome. Moreover, F1L is critical for suppression of caspase-1 activation and IL-1β secretion during VACV infection in macrophage cultures. In mice, we show that F1L is a prominent virulence factor that inhibits cytokine secretion upon VACV infection.

Collectively, in my dissertation research, we revealed two novel functions of F1L that are important for the virulence of VACV. Also, F1L is the first caspase-9 inhibitor that is a Bcl-2-like protein, and the first example of viral protein inhibitor of the NLRP family protein. In addition to these two functions described in this work, F1L also interacts with pro-apoptotic proteins, including Bak and Bim [6-9]. F1L is an addition to the numerous examples of viral proteins that possess multiple functions, thus showing once more the power of studying host-virus interactions. Since viruses have significantly smaller genome size than their host, they have evolved multi-tasking proteins to sabotage host's immunity. Therefore, studying how viruses modulate the host's signaling pathways could sometimes reveal surprising mechanisms of protein functions, like F1L in this case.

Figure 6-1. Schematic illustration of the functions of F1L. (A) Hypothetical model modified from the crystal structure of F1L (PBD 2VTY) showing the positions of the binding sites of BH3-only proteins, caspase-9 and NLRP1 on F1L. Note that the mitochondrial targeting sequence was not included in the crystal structure. **(B)** Schematic illustration of the roles of F1L in inhibition of the innate immunity. (1) F1L suppresses cytochrome c release and subsequent apoptosis by interacting with pro-apoptotic Bcl-2 family proteins such as Bak and Bim. (2) F1L inhibits apoptosis by inhibiting caspase-9 by interacting with both pro-caspase-9 and its activated form. (3) F1L represses NLRP1 inflammasome formation and thus subsequent cytokine secretion and inflammation.
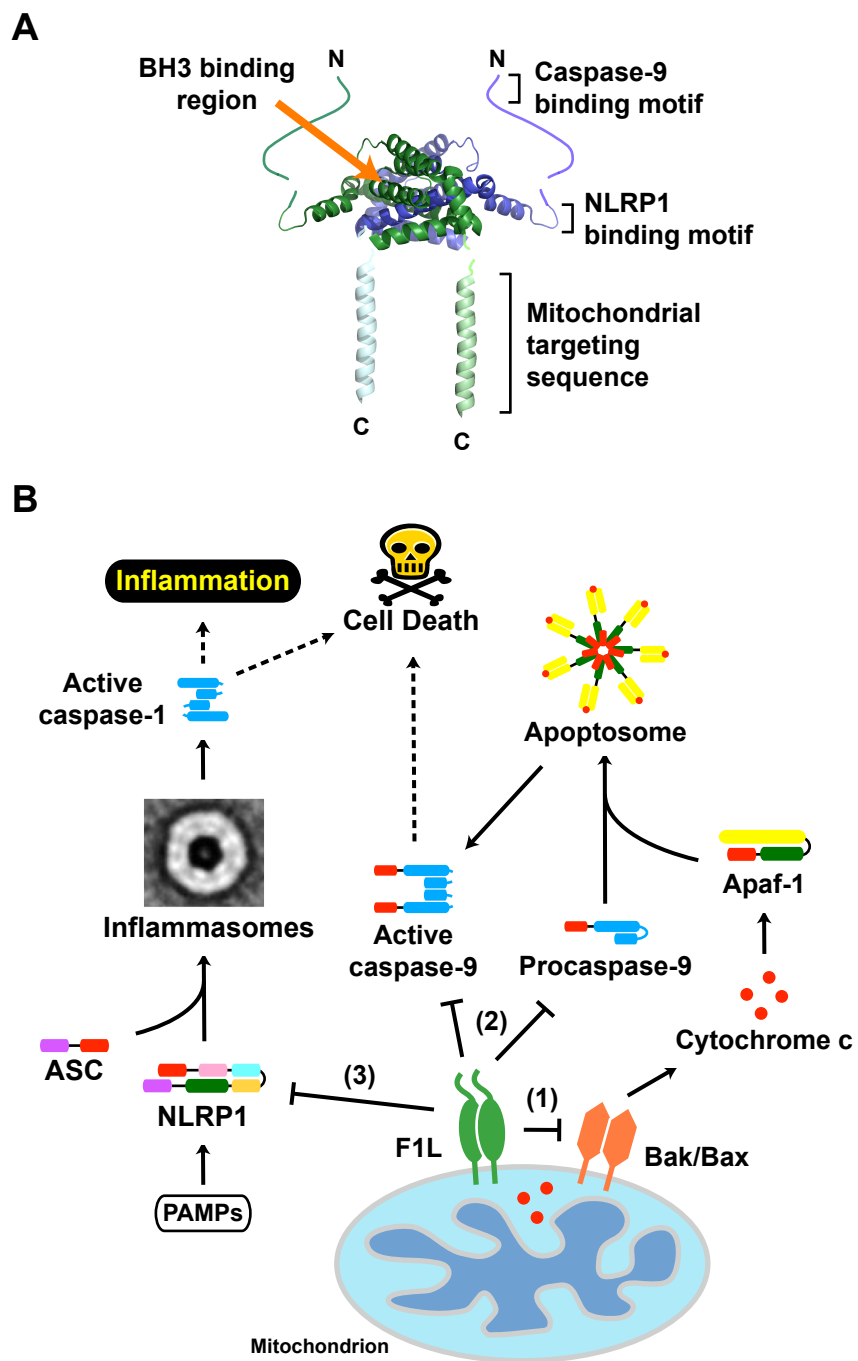
Figure 6-1. Schematic illustration of the functions of F1L.

Future directions

Previous studies and our work presented in this dissertation demonstrated that F1L possesses three functions: (i) Inhibition of pro-apoptotic Bcl-2 family proteins, (ii) Inhibition of caspase-9, and (iii) Inhibition of NLRP1. Even though F1L is critical for VACV virulence *in vivo* (Chapter 5), the precise roles of each of these functions of F1L during infection remain to be elucidated. Since different point mutations on F1L (C7A, N32A/H35A, M67P) have been shown to specifically disrupt each of these three interactions, mutant viruses containing either one of these point mutations can be generated to selectively knock out each of these functions of F1L. The significance of these interactions during infection could then be investigated by using these mutant viruses for infection studies in cell cultures and mouse model. Recently, AIM2 has been identified as a cytosolic DNA sensor that is responsible for caspase-1 activation during vaccinia viral infection. Since the physiology ligand of NLRP1 remains unknown, it is interesting to investigate what is the relationship between AIM2 and NLRP1 in innate immune response and, in particular, caspase-1 activation.

In this study, we identified two short peptides that are sufficient to inhibit caspase-9 (Chapter 4) and NLRP1 (Chapter 5), respectively. Notably, both peptides from F1L do not share any significant sequence homology with any protein sequence except to the immediate F1L orthologues in related poxviruses. Therefore, using these peptides for screening of small molecules may lead us to discovery of compounds that inhibit caspase-9 or NLRP1 by novel mechanisms. For screening of potential NLRP1 inhibitors, the fluorescence polarization assay (FPA) developed to study the interaction between the

F1L peptide and NLRP1 could be used for high throughput screening of chemical libraries. Unfortunately, due to the difficulties of synthesis of the caspase-9-inhibiting peptide derived from F1L, FPA is not suitable for screening of potential caspase-9 inhibitors. However, the information from the crystal structure of caspase-9, together with the peptide sequence from F1L can be used for in silica small molecules screening for putative caspase-9 inhibitors.

The sequence of F1L used in this study is from the VACV strain Western Reserve (VACV-WR). Although the motifs of F1L that are responsible for caspase-9 and NLRP1 inhibition are highly conserved among all the F1L orthologues in related poxviruses, there are some variations. In Chapter 5, mutagenesis study suggests that all the orthologues of F1L probably can bind and inhibit caspase-9. For the F1L motif that inhibits NLRP1, while the sequence used in this study (Asn-Val-Asp-His-Asp-Tyr[32-37]) is conserved among VACV strains, variola virus strains possess different sequence within this region (Asn-Asp-Asp-Asn-Asn-Tyr[32-37]). However, the activity of this peptide derived from variola virus strains on NLRP1 activity remains unexplored.

Finally, other than F1L and N1L tested in this study, it is intriguing to examine if other viral Bcl-2 proteins, including adenovirus E1B-19k, African swine fever virus A179L, cytomegalovirus vMIA, Epstein-Barr virus (EBV) BHRF1, fowlpox virus FPV039, Kaposi sarcoma-associated herpesvirus (KSHV) KSBcl-2, myxoma virus M11L, and Orf virus ORFV125 are able to bind and inhibit caspase-9 and/or NLRP1.

References

1. Yajima, H. and F. Suzuki, *Identification of a Bcl-XL binding region within the ATPase domain of Apaf-1.* Biochem Biophys Res Commun, 2003. **309**(3): p. 520-7.

2. Pan, G., K. O'Rourke, and V.M. Dixit, *Caspase-9, Bcl-XL, and Apaf-1 form a ternary complex.* J Biol Chem, 1998. **273**(10): p. 5841-5.

3. Hu, Y., et al., *Bcl-XL interacts with Apaf-1 and inhibits Apaf-1-dependent caspase-9 activation.* Proc Natl Acad Sci U S A, 1998. **95**(8): p. 4386-91.

4. Chinnaiyan, A.M., et al., *Interaction of CED-4 with CED-3 and CED-9: a molecular framework for cell death.* Science, 1997. **275**(5303): p. 1122-6.

5. Bruey, J.M., et al., *Bcl-2 and Bcl-XL regulate proinflammatory caspase-1 activation by interaction with NALP1.* Cell, 2007. **129**(1): p. 45-56.

6. Wasilenko, S.T., et al., *The vaccinia virus F1L protein interacts with the proapoptotic protein Bak and inhibits Bak activation.* J Virol, 2005. **79**(22): p. 14031-43.

7. Taylor, J.M., et al., *The vaccinia virus protein F1L interacts with Bim and inhibits activation of the pro-apoptotic protein Bax.* J Biol Chem, 2006. **281**(51): p. 39728-39.

8. Campbell, S., et al., *Vaccinia virus F1L interacts with Bak using highly divergent BCL-2 homology domains and replaces the function of Mcl-1.* J Biol Chem, 2009.

9. Postigo, A., et al., *Interaction of F1L with the BH3 domain of Bak is responsible for inhibiting vaccinia-induced apoptosis.* Cell Death Differ, 2006. **13**(10): p. 1651-62.